Assembly of Sensory-Motor Connectivity in the Spinal Cord of Mice

Inauguraldissertation

zur
Erlangung der Würde eines Doktors der Philosophie
vorgelegt der
Philosophisch-Naturwissenschaftlichen Fakultät
der Universität Basel

von

Eline Vrieseling
aus Wijns, die Niederlände

Basel, 2006

Genehmigt von der Philosophisch-Naturwissenschaftlichen Fakultät auf Antrag von

Prof. Dr. Silvia Arber
(Dissertationsleitung)

Prof. Dr. Andreas Lüthi
(Korreferat)

Prof. Dr. Markus Rüegg
(Vorsitzender)

Basel, den 06.11.2006

Prof. Dr. Hans-Jakob Wirz
(Dekan)

Die vorliegende Arbeit wurde unter der Leitung van Prof. Dr. Silvia Arber am Biozentrum der Universität Basel, Abteilung Zellbiologie sowie am Friedrich Miescher Institute (FMI) for Biomedical Research in Basel ausgeführt.

Fakultätsverantwortliche: Prof. Dr. Silvia Arber, Biozentrum,
Universität Basel
Korreferat: Prof. Dr. Andreas Lüthi, FMI, Basel

Table of Contents

Summary

Many features critical for proper functioning of an organism are under the control of neuronal circuits. The building blocks for these circuits are formed early during embryogenesis and are generated by the specification of distinct neuronal types. This process of neuronal specification is spatio-temporally regulated by extrinsic and intrinsic factors, defining the progenitor and subsequently postmitotic identity of neuronal subclasses. Postmitotic neurons migrate to specific locations in the central nervous system (CNS), send out axons to and innervate their targets, develop highly specific dendritic trees and form synaptic connections with a variety of inputs. All these processes are likely to be regulated by intriguing interactions of cell autonomous intrinsic and extrinsic factors. During the process of axonal pathfinding and dendrite patterning, activity-independent mechanisms, such as a variety of axon guidance molecules as well as neurotrophic factors are involved in the assembly of neuronal circuits. Although dendritic structures are of crucial importance for the function of neuronal circuits, not much is known about the molecular and cellular mechanisms underlying the formation of neuronal type-specific dendritic morphologies and this topic represented the main focus of my PhD thesis. Specifically, my thesis was centered on the monosynaptic stretch reflex circuit in the spinal cord, which offers a fairly accessible system for studying various aspects of neuronal circuit formation.

The main part of my thesis focused on 1) analyzing the correlation between motor neuron (MN) pool specific dendrite patterns and Ia proprioceptive afferent (IaPA)-MN connectivity; 2) determining cellular and molecular factors required for the formation of highly selective IaPA-MN connections. Our study (Vrieseling and Arber, Cell, *in press*) has demonstrated that there is a strong correlation between MN pool dendrite pattern and monosynaptic IaPA-MN connectivity. MN pools at cervical levels of the spinal cord projecting to Triceps (Tri) and Pectoralis major (Pec_{maj}) forelimb muscles occupy a dorso-medial cell body position in the ventral horn of the spinal cord and show radial dendrite patterns, extensively projecting into the central grey matter of the spinal cord. In contrast, two other MN pools found at the same rostro-caudal level of the cervical spinal

cord, projecting to the Cutaneous maximus (CM) and Latissimus dorsi (LD) forelimb muscles, occupy an extreme ventro-lateral position in the ventral spinal cord and project their dendrites along the grey-white matter border, almost completely avoiding the central grey matter. Using intracellular recording techniques, I showed that the MN pool selective dendrite patterns correlated strongly with monosynaptic IaPA-MN connectivity. Tri and $Pect_{maj}$ MNs both received monosynaptic inputs from homonymous IaPAs. However, almost none of the CM and LD MNs received monosynaptic IaPA input. To elucidate the cellular and molecular factors required for the formation of MN pool specific dendrite patterns and selective IaPA connectivity, we analyzed a mouse line mutant in the target-induced ETS transcription factor *Pea3*. In a previous study it was shown that *Pea3* is specifically expressed in CM and LD MN pools at cervical levels and that *Pea3* regulates MN cell body positioning (Livet et al., 2002). During my thesis, I showed that in the absence of the ETS transcription factor *Pea3*, CM and LD MN pools dramatically change their dendrite morphologies to a radial pattern resembling Tri and $Pect_{maj}$ dendrite patterns. Moreover, *Pea3* mutant CM and LD MNs received strong monosynaptic IaPA input from the Tri muscle nerve. Tri MNs do not express *Pea3*, hence *Pea3* mutation does not genetically change these MNs. Nevertheless, in *Pea3* mutants, Tri MNs occupy a different MN pool position due to the altered pool position of CM MNs. However, the change in Tri MN pool position did not dramatically change its dendrite pattern nor its monosynaptic IaPA connectivity. From these findings, we concluded that the target-induced transcription factor *Pea3* cell autonomously regulates MN pool position, dendrite pattern and Ia-MN connectivity.

The minor part of my thesis focused on the role of ETS signaling during late embryonic dorsal root ganglia (DRG) sensory neuron development (Hippenmeyer et al., 2005). We found that precocious ETS signaling in DRG sensory neurons dramatically changed the fate of these neurons. Precocious ETS signaling prevented normal development of DRG sensory neurons and instead led to abnormal axonal pathfinding, perturbation of expression of terminal differentiation markers and independence of neurotrophic support. These findings emphasize the importance for temporal regulation of factors during development for proper specification of neuronal identity.

Chapter I

Introduction

Assembly of spinal neural circuits

The ability of vertebrates to produce coordinated movements is partially accomplished by highly specific synaptic connections between different neuronal types within the spinal cord, resulting in the formation of spinal circuits. These circuits regulate muscle activity by converting onto the output neurons of the spinal cord, the MNs in the ventral horn. The axons of the MNs project out of the spinal cord via the ventral horn and make very selective connections with muscles in the periphery. Many studies on neuronal specification and circuit formation within the spinal cord, but also in other regions of the central nervous system (CNS) have shown that the high degree of specificity with which neural circuits are assembled is accomplished by intriguing interactions between temporally controlled genetic programs and activity patterns (Jessell, 2000), (Shirasaki and Pfaff, 2002), (Hanson and Landmesser, 2004), (McConnell, 1995).

Patterning of the spinal cord

The basis for neural circuit formation is the selective patterning of neural tissue. During this process, neuronal progenitor cells generate postmitotic neurons and acquire their unique neural properties that direct the formation of selective connections with appropriate target cells. In the spinal cord, progenitor cells are born in the ventricular zone. They migrate into the spinal cord where they encounter graded concentrations of inductive signals. They translate the specific concentration of these inductive signals into a patterned expression of basic-helix-loop-helix (bHLH) and homeodomain (HD) transcription factors, which in turn define the later properties of these progenitor cells (Edlund and Jessell, 1999; Gurdon and Bourillot, 2001). For example, in the dorsal horn progenitor cells are exposed to bone morphogenic proteins (BMPs) which are secreted from the surface ectoderm and the roof plate and induce the specification of dorsal cell types such as neural crest cells and dorsal sensory interneurons (Lee and Jessell, 1999). In contrast, progenitors in the ventral spinal cord encounter the signals Sonic Hedgehog (Shh) and Retinoic Acid (RA) signals which induce the specification of

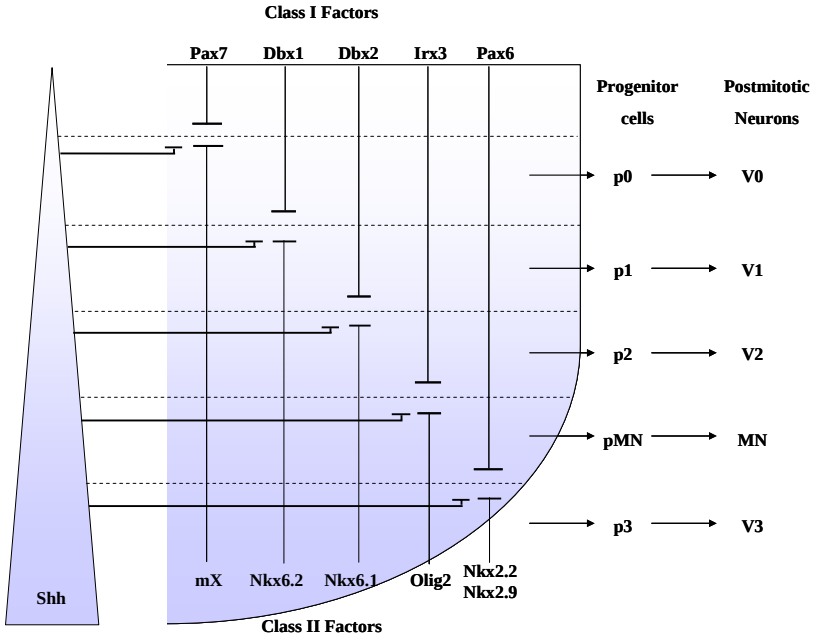

Figure 1: A combinatorial code of homeodomain and basic helix-loop-helix transcription factors specifies the identity of neuronal progenitor cells in the ventral neural tube. A gradient of Sonic Hedgehog (shh) signaling establishes the specification of different progenitors by inducing class II and repressing class I expression of transcription factors. Individual progenitor domains, termed p3 – p0, are further established by crossrepressive interactions between class I and class II transcription factors. Each progenitor domain gives rise to a specific class of postmitotic neurons. **mX** = unidentified class II transcription factor counteracting the activity of Pax7. (Adapted from Jessell, 2000; Shirasaki and Pfaff, 2002).

five different classes of progenitor and subsequently postmitotic neurons including MNs (Fig. 1). An early generic MN identity is defined by the expression of the LIM homeodomain (HD) transcription factor *Isl1* and the HD gene *Hb9* (Arber et al., 1999) (Thaler et al., 1999). However, different subtypes of MNs can be found in the spinal cord based on the specific expression of a combinatorial LIM-HD transcription factor code (Tsuchida et al., 1994), the topographic position in the ventral spinal cord and the innervation of a particular peripheral target (Landmesser, 1978a; Landmesser, 1978b). By these criteria, five subpopulations of MNs can be identified, belonging to three major

classes of MNs: the visceral autonomic preganglionic (PGC), the somatic axial, and limb innervating MNs. The different subpopulations of MNs are organized into longitudinally aligned columns within the spinal cord (Fig 2). MNs innervating the sympathetic ganglia are located in the preganglionic motor column (PMC) at thoracic levels of the spinal cord. Those innervating the trunk muscles are located in the medial motor column (MMC). The MMC can be subdivided into the medial MMC (MMCm) and the lateral MMC (MMCl). The MMCm extends across the whole longitudinal extend of the spinal cord and contains MNs innervating the axial muscles. In contrast, the MMCl is located at thoracic levels of the spinal cord and contains MNs innervating the ventral body wall musculature. Finally, MNs innervating the limb muscles are located in the lateral motor column (LMC) which is found at cervical and lumbar levels of the spinal cord. The LMC can also be subdivided into the medial LMC (LMCm) and the lateral LMC (LMCl). MNs in the LMCm innervate the ventral limb and MNs in the LMCl innervate the dorsal limb musculature. Such a grouping of neurons into a column is not restricted to the spinal cord, but instead is seen in many regions of the CNS. For example in the neocortex neurons with nearly identical receptive fields are grouped into columns which run perpendicular to the cortical surface (Mountcastle, 1997). In the cortical layer IV of the primary visual cortex neurons receiving input from either the left or the right eye are grouped together into ocular dominance columns ((Hubel et al., 1977)). Thus the columns link cell body position to neuronal function and in this way contribute to the establishment of topographic organization of neuronal maps.

Role of *Hox* genes during MN specification and spinal cord patterning

In the spinal cord MNs acquire their columnar identity across a temporal developmental time window. Studies in chick have shown that first MN progenitors and postmitotic MNs are exposed to graded concentrations of a node-derived source of fibroblast growth factor 8 (FGF8), with increasing concentration from rostral to caudal spinal cord levels. This results in a spatial expression pattern of members of the *Hox-c*

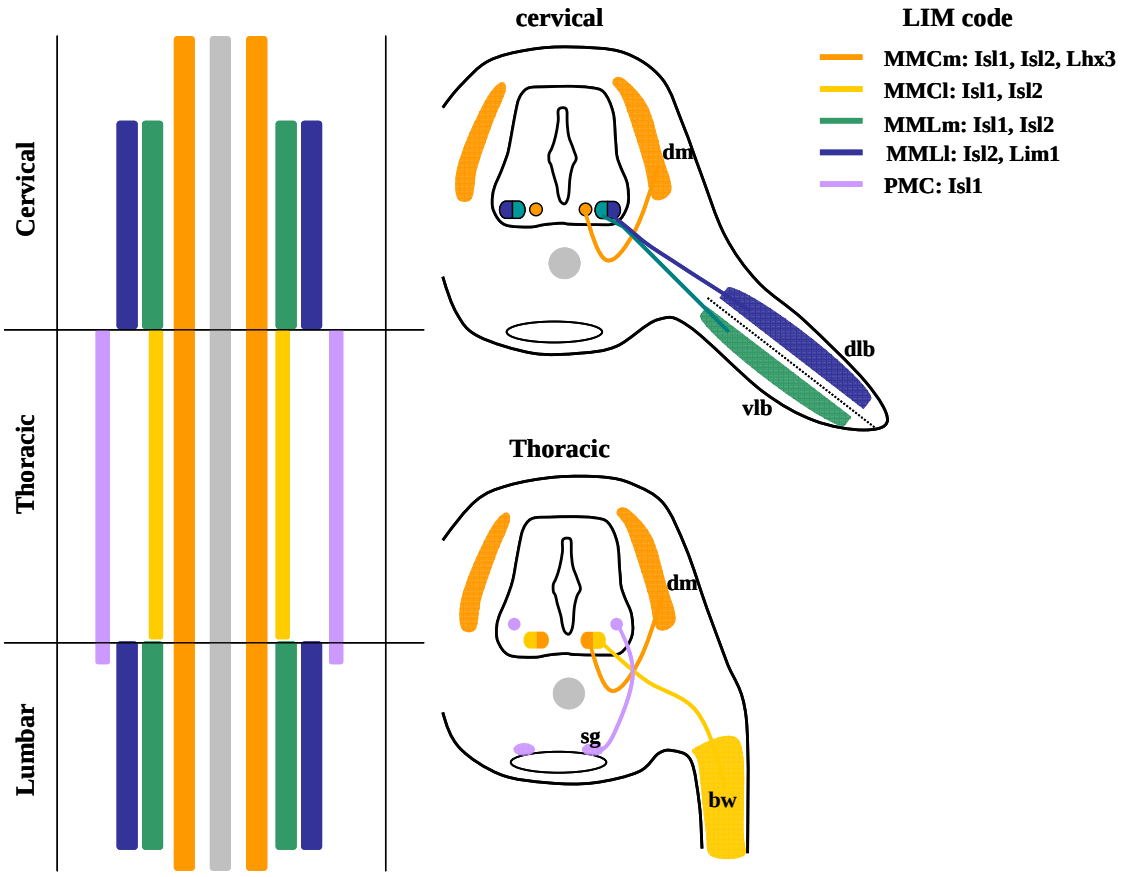

Figure 2: Columnar organization and target specificity of MN subtypes defined by a combinatorial LIM-HD transcription factor code in the chick spinal cord

MNs in the spinal cord are grouped into MN columns lining the longitudinal axis of the spinal cord shown in an open-book preparation of the spinal cord. The floor plate at the ventral midline is indicated in grey (left). The axonal projection pathways of MN subtypes are shown in a transverse section of the spinal cord at both brachial and lumbar levels (right). The LIM code for MN subtypes is shown by color coding (box top right). bw = body wall musculature; dlb = dorsal limb bud musculature; dm = dermomyotome; sg = neurons of the sympathetic ganglia; vlb = ventral limb bud musculature; LMCl = lateral lateral motor column (blue); LMCm = medial lateral motor column (green); MMCl = lateral medial motor column (yellow); MMCm = medial medial motor column (orange); PMC = preganglionic motor column (purple). (Adapted from Shirasaki and Pfaff, 2002).

homeodomain class of transcription factors, with Hoxc6 expressed in brachial MNs, Hoxc9 in thoracic MNs and Hoxc10 in lumbar MNs (Dasen et al., 2003). In addition the *Hoxa6* and *Hoxa9*, genes have been shown to have similar expression patterns and MN columnar specification activities. The expression of Hoxa6 and Hoxc6 by newly generated postmitotic MNs assigns brachial LMC columnar identity and this transcriptional profile directs the axons of LMC neurons to project into the limb. With the same mechanism, thoracic MNs expressing Hoxc9 and Hoxa9 direct their axons to the sympathetic ganglia.

The regionally restricted expression of the different *Hox-c* genes is obtained by mutual cross-repressive interactions between the different Hox-c classes of proteins. After MNs are subdivided into brachial, thoracic and lumbar columns, they become further specified to acquire a sub-columnar fate. This is achieved by the activator functions of the same *Hox-c* genes. At brachial levels, the Hoxc6 proteins induce expression of retinaldehyde dehydrogenase-2 (RALDH2), a key enzyme in retinoic acid (RA) synthesis in early-born LMCm MNs (Niederreither et al., 1997; Sockanathan and Jessell, 1998). The later-born LMC MNs migrate through the early-born LMCm MNs and become exposed to the non-cell-autonomous functioning RA signal. This signal induces the expression of Lim1 and represses the expression of Isl1 in this late-born LMC MNs, thus assigning LMCl identity.

In contrast, Hoxc9 proteins induce the expression of BMP5, inducing migration of these MNs to a more dorsal position and assign them to the PMC. Consequently, these early developmental inductive signals from the axial and paraxial mesoderm together with the MN subpopulation derived signals produce a variety of MN classes with a unique LIM-HD code. Such that LMCm MNs are characterized by the expression of Isl1 and Isl2, LMCl MNs by the expression of Isl2 and Lim1, MMCm MNs by the expression of Isl1, Isl2 and Lhx3, MMCl by the expression of Isl1 and Isl2 and PMC by the expression of Isl1.

The next developmental step towards the formation of precise spinal motor circuitry is the grouping of MNs projecting to the same muscle in the periphery into so

called MN pools. The existence of MN pools was first shown by Romanes (Romanes, 1964) in cat. Landmesser (Landmesser, 1978b) subsequently performed a thorough set of studies on the precise location of MN pools in the chick spinal cord. This study visualized MNs projecting to one particular muscle by utilizing the technique of retrograde transport of horseradish peroxidase (HRP) in late chick embryos. These studies revealed that all MNs projecting to a particular muscle were localized in stereotyped positions within the ventral spinal cord forming a pool. Similar studies revealed that the axons of MNs belonging to different pools were highly intermingled within proximal spinal nerves, but that they defasciculated at the base of the limb and regrouped into muscle-specific fascicles (Lance-Jones and Landmesser, 1981a). Later it was found that this was regulated by polysialic acid (PSA) on NCAM (Tang et al., 1994). An elegant set of surgical experiments in chick, initially designed by Victor Hamburger, showed that when MNs were displaced along the anterior-posterior axis of the spinal cord prior to MN genesis (Lance-Jones and Landmesser, 1980; Lance-Jones and Landmesser, 1981b) or when an entire limb bud was rotated around the dorsal-ventral axis (Ferguson, 1983), MNs were able to adapt their axonal trajectory in such a way that they could innervate their correct target muscle. The main conclusions from these early studies were that MNs must have intrinsic pool-specific identities at the time of initial axon outgrowth towards the target and that they have cell surface molecular differences that allow them to selectively fasciculate with like axons at the base of the limb and recognize limb derived guidance cues to pathfind to their appropriate muscle. The surgical experiments in addition suggest that the target derived guidance signals are diffusible chemoattractants.

After these initial, mainly anatomical findings, lots of progress has been made over the last few decades in unraveling the molecular mechanisms required for MN pool formation. It has been shown that also at this developmental step *Hox* genes play critical roles in the formation of muscle specific MN pools as they do in the formation of MN columns described above (Dasen et al., 2003; Dasen et al., 2005). A cell-autonomously acting *Hox* transcriptional program confers LMC neurons with pool specific identities that direct motor axons to individual muscle targets. This is accomplished by two sequential developmental steps. First a regulatory interaction between Hox5 and Hox8

proteins constrains MNs to a specific rostrocaudal level. Second, a sequential Hox regulatory network involving Hox4, Hox6, Hox7 and Meis1 (a Hox cofactor) directs MN diversification intrasegmentally (Fig.3). Consequently, the combinatorial expression of Hox genes within a particular MN can lead to the expression of either the runt domain transcription factor Runx1, the ETS transcription factor Pea3 or the POU domain transcription factor Scip. This together with the MN type specific LIM code separates MNs into MN pools and directs the MN axons to their specific muscle target.

The studies on Hox gene function during MN specification in vertebrates show that indeed MNs acquire already very early on cell intrinsic transcriptional programs that determine their later fate. Activity-manipulating experiments have shown that the specification of MNs and their consequent grouping into MN pools is mainly determined genetically. However, axonal pathfinding of MN axons to their selective muscle targets has been shown to depend on a combination of molecular and activity regulated processes (Hanson and Landmesser, 2004).

Formation of spinal circuits involved in locomotor behavior

The central pattern generator

Soon after MNs have acquired unique identities, they become integrated into spinal circuits. One of the earliest formed circuits are intrinsic spinal networks known as central pattern generators (CPGs), responsible for the generation of rhythmic behavior in the absence of sensory input. They control the timing and pattern of rhythmic muscle activity underlying locomotion. A good example of the behavioral output of this circuit is the asynchronous left-right movement of the limbs during walking. When this circuit is not

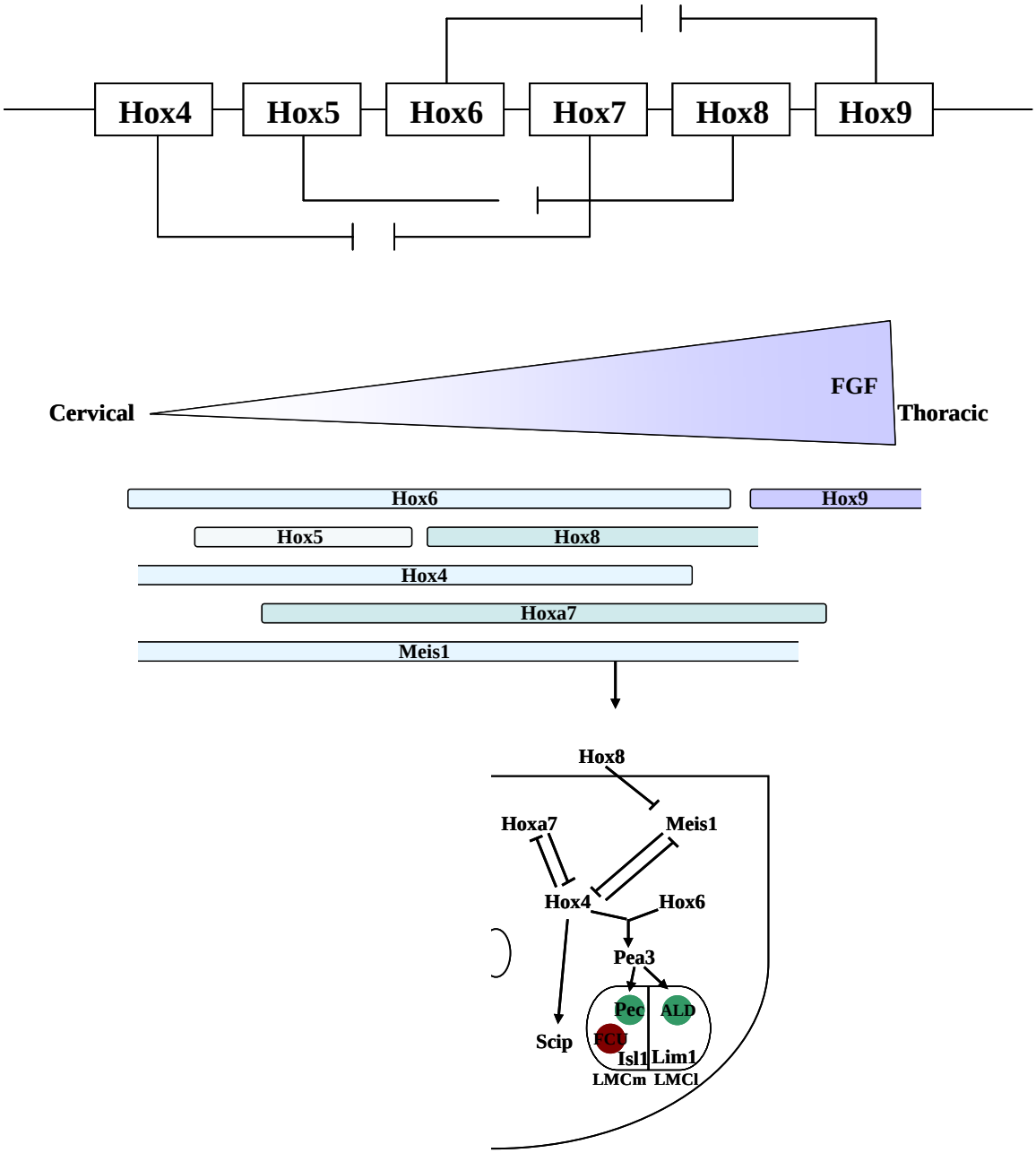

Figure 3: Hox regulatory network that specifies MN pool identity in chick.

(Top panel) Schematic arrangement of chromosomal Hox clusters showing the regulatory interactions that operate during the assignment of MN columnar and pool fates at brachial levels of the spinal cord. Hox genes that are separated by two other genes show selective repressive interactions. These repressive interactions direct MN columnar and MN pool identities. (lower panel) Sequential steps in the assignment of MN pool identity within the brachial LMC. Graded extrinsic FGF mediated signaling at early neural tube stages induces the patterned expression of Hox genes within MNs along the rostrocaudal axis of the spinal cord. The first set of Hox genes

(Hox6 and Hox9) directs the grouping of MNs into specific MN columns each of which is constrained to a particular rostral-caudal spinal cord level. This initial patterning event is followed by the expression of a second set of Hox genes (Hox5 and Hox8) which further subdivides the LMC into subcolumns also along the rostrocaudal extend of the spinal cord. A third set of Hox genes (Hox4, Hox6, Hoxa7 and Meis1) is then required for intrasegmental patterning of the spinal cord, directing the expression of Pea3 and Scip and in combination with LIM-HD proteins, specifies the identity of three MN pools that innervate the ALD, Pec and FCU muscles. ALD = anterior latissimus dorsi; Pec = pectoralis; FCU = flexor carpi ulnaris. (Adapted from Dasen et al., 2005).

functional the animal will display a hopping-like movement during walking (Kullander et al., 2003) like kangaroos. Although the CPG has lately been a major focus of many studies on circuit formation (Butt and Kiehn, 2003; Goulding and Pfaff, 2005; Kiehn and Butt, 2003; Lanuza et al., 2004), the mechanisms required for its assembly are still largely unknown. Lately, a combination of genetic and functional analysis using interneuron (IN) selective gene knock out approaches has been shown to be of key importance in dissecting local interneuronal functions (Gosgnach et al., 2006; Goulding and Pfaff, 2005; Lanuza et al., 2004). As shown in Fig.1, four types of ventral INs can be divided on the basis of their restricted expression of HD transcription factors. The V0 INs are found in lamina VIII of the spinal cord and derive from homeodomain transcription factor $Dbx1^{+}$ progenitor cells. V0 INs deriving from the ventral half of the Dbx1 progenitor domain transiently express Evx1 and are termed $V0_V$ (Moran-Rivard et al., 2001). $V0_D$ INs derive from the dorsal half of the Dbx1 progenitor domain and lack expression of Evx1 (Pierani et al., 2001). V0 INs are strictly commissural INs, projecting their axons rostrally to the contralateral side of the spinal cord and terminate on MNs. Around ~70% express the vesicular inhibitor amino acid transporter (VIAAT) that delineates both GABAergic and glycinergic neurons (Lanuza et al., 2004; Sagne et al., 1997). ~30% express the excitatory IN marker vesicular glutamate transporter 2 (VGlut2). Thus this suggest that the V0 INs are mainly required for inhibiting the activity of contralateral MNs. Studies in neonatal rat have shown that lamina VIII excitatory INs form connections with contralaterally located inhibitory INs which in turn synapse on

MNs (Butt and Kiehn, 2003). Thus the excitatory V0 population may inhibit contralateral located MNs via a disynaptic pathway. *Dbx1* knock out mice selectively lack V0 INs and show a clear decrease in the asynchronous left and right flexor or extensor MN bursting activity, required for the alternating left-right limb movement during walking (Lanuza et al., 2004). However, these experiments also show that this is not the only class of commissural INs involved in inducing asynchronous left-right MN activity, since hemisection of the spinal cord shows a complete switch from asynchronous to synchronous left-right MN bursting (Lanuza et al., 2004). Interestingly, the alternating ipsilateral flexor-extensor MN bursting activity is preserved after spinal cord hemisection (Gosgnach et al., 2006), suggesting that a so far unidentified IN population, most likely projecting onto ipsilateral MNs is responsible for regulating this activity.

Another by now well characterized ventral IN population is the V1 class, representing a local circuit inhibitory IN group. Renshaw cells (RC) and Ia inhibitory INs derive from this IN population. These INs are located in lamina IX, close to the MNs and project their axons locally to form monosynaptic connections with ipsilateral MNs. They are characterized by the expression of the transcription factor Engrailed1 (En1) and derive from transcription factor $Pax6^{+}$ progenitor cells. Functional analysis of two mouse models, *Pax6* knock out and $En1^{Cre}$;R26-$LacZ^{flox}$/DTA (En1-DTA) mice, lacking selectively the V1 class of INs showed that these INs are required for 'fast' motor bursting (Gosgnach et al., 2006). In the absence of V1 INs, selectively the duration of the extensor-flexor step-cycle was increased while the alternating extensor-flexor bursting pattern was preserved. Moreover, behavioral experiments with mice lacking the V1 IN population revealed a decrease in the time and speed (rounds per minute) that these mice could run on a rotarod compared to wild type mice (Gosgnach et al., 2006). This function is specific for V1 neurons, since ablation of V0 and V3 INs from the spinal cord does not markedly change the duration of extensor-flexor bursts (Gosgnach et al., 2006).

The role of V1 INs in determining the frequency of extensor-flexor bursting seems to be preserved in *Xenopus*. The mouse V1 homologue in *Xenopus* is the aIN. A strong correlation is found between aIN-derived inhibitory inputs to CPG neurons and the

frequency of swimming movements in *Xenopus* tadpoles (Li et al., 2004). Thus the V1 homologue in *Xenopus* may be involved in facilitating fast swimming movements and thus the aIN function may be evolutionary conserved in that, that its mammalian counterpart is required in much the same way to produce fast 'walking' movements.

The remaining two ventral IN populations V2 and V3 are so far less well described concerning their function during locomotion. V2 INs are located in lamina IX and project their axons intersegmentally in the ipsilateral spinal cord and they are marked by the transcription factor Chx10. The V3 class of ventral INs is located close to the floor plate in lamina VIII of the spinal cord and projects their axons contralaterally to form excitatory synapses on contralateral MNs (Goulding and Pfaff, 2005). They are marked by the selective expression of the transcription factor Sim1.

Studies on the spinal CPG have thus so far shown that different ventral IN classes play highly specific roles in regulating rhythmic locomotor behavior. Although the commissural V0 class of INs is required for left-right flexor or extensor alternation, they are dispensable for ipsilateral extensor-flexor alternation (Lanuza et al., 2004). Moreover the class V1 INs selectively influence the step-cycle duration of ipsilateral extensor-flexor MNs, while not at all affecting the asynchrony of the ipsilateral extensor-flexor bursting pattern (Gosgnach et al., 2006). The exact neuronal network responsible for producing highly selective rhythmic locomotor behaviors in mammals is still far from resolved, but with the growing powerful combination of genetic and functional techniques a big step forward has been made in identifying the contribution individual IN populations make to the CPG. A next step will be to understand the mechanisms via which MNs integrate the diverse pattern of CPG inputs to produce a precise locomotor behavior.

The monosynaptic stretch-reflex circuit

Another crucial input to MNs in the spinal cord to produce proper locomotion is the one derived from Ia proprioceptive sensory afferents (IaPA). Proprioception is the sense of relative position of neighboring parts of the body. It provides feedback solely on the

status of the body internally. In contrast to the CPG circuitry, the IaPA – motor connectivity and function is well understood. This is partially due to its fairly easy accessibility for tracing and functional studies.

After projecting into the spinal cord through dorsal roots, group IaPAs form two major termination zones: 1) in the intermediate spinal cord IaPA collaterals make extensive synapses onto INs of the Clarke's column (cc) which themselves project directly to granule cells of the cerebellum; 2) in the ventral spinal cord, IaPAs make direct excitatory connection to MNs as well as to INs (Brown, 1981b). Importantly, IaPAs represent the only population of dorsal root ganglion (DRG) neurons that make monosynaptic connections to alpha-MNs. IaPA-MN connections in the spinal cord are formed with a high degree of selectivity. IaPAs supplying a particular muscle make selective synapses with MNs innervating the same (homonymous) or a synergistic muscle, but rarely with MNs innervating an antagonistic or functionally unrelated muscle (Eccles et al., 1957; Frank and Westerfield, 1982; Lee and O'Donovan, 1991). These connections within the spinal cord and muscle form the basis for a neural circuit that is known as the simple monosynaptic stretch reflex (Fig.4). The monosynaptic stretch reflex circuit derives its name from its clearly described function. Peripherally, IaPAs innervate muscle stretch sensitive mechanoreceptors in the muscle called muscle spindles. Alpha-MNs innervate the extrafusal skeletal muscle fibers. Upon stretch of the muscle, IaPAs are activated and in turn monosynaptically excite alpha-MNs which consequently induce contraction of the muscle. The development of the monosynaptic stretch-reflex circuit includes the outgrowth of axons to their peripheral muscle targets (Tessier-Lavigne and Goodman, 1996), the selection of specific termination zones within the target regions (Sanes and Yamagata, 1999) and the formation of selective synapses in the spinal cord (Smith and Frank, 1988).

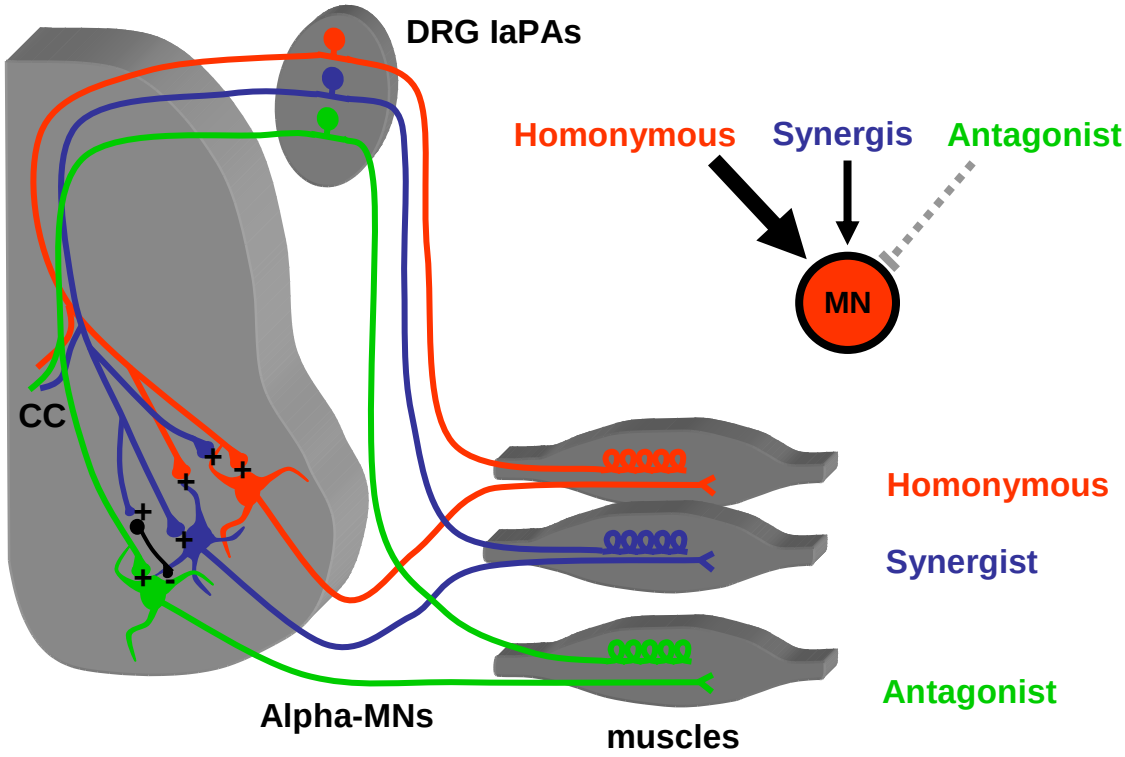

Figure 4: Schematic representation of monosynaptic stretch reflex circuit.

IaPAs innervate peripherally selective muscle targets and centrally they form two main termination zones: 1) in the intermediate spinal cord where they terminate on neurons belonging to the Clarke's column (CC); 2) in the ventral spinal cord where they terminate monosynaptically on alpha-MNs projecting to homonymous and / or synergistic muscles (blue and red IaPA-MN pair). In the ventral spinal cord they also terminate on IaPA inhibitory INs (black) which in turn terminate on alpha-MNs projecting to antagonistic muscles. The + indicates an excitatory glutamatergic input, while the – indicates an inhibitory GABA/glycinergic input. The arrows in the small scheme in the right top corner illustrate the strength of connections between homonymous and synergistic IaPAs and alpha-MNs. The dotted grey line illustrates a disynaptic inhibitory input from a IaPA to an antagonistic alpha-MN. (Adapted from David Ladle).

Early HRP tracing and intracellular electrophysiological studies in cat have delineated the high precision with which IaPA-MN connections are formed. The IaPA monosynaptic input a MN receives comprises 1 – 2 % of its total synaptic input. Each IaPA sends ~10 collaterals in the spinal cord along the longitudinal axis of the spinal cord. Every collateral makes 3-5 monosynaptic connections to a homonymous MN and 2-3 connections to a synergistic MN (Brown, 1981b). This is nicely reflected in intracellular recording studies where specific hindlimb muscle nerves were stimulated and intracellular excitatory postsynaptic potentials (EPSPs) were recorded from spinal MNs. This showed that stimulation of the homonymous muscle nerve elicited in general larger monosynaptic EPSP amplitudes than when a synergistic muscle nerve was stimulated (Eccles et al., 1957). Moreover, IaPA connections are generally found at restricted geometric distances (from somatic origin to termination) from the soma, namely between 40 and 800 μm from the soma. Since a MN dendrite in the cat is between 2-3 mm long, the contacts are made in the proximal geometric half of the dendritic tree. Each collateral makes all its contacts at similar geometric distances from the soma, but mainly on different dendrites. However, the contacts of different IaPAs on a single MN are found at different geometric distances from the soma so that the IaPA contacts are widespread across the dendritic tree (Brown, 1981b). This is again supported by electrophysiological data showing that single fiber IaPA EPSPs (induced by activation of a single IaPA) range from those with fast rise and decay times (indicative of proximal synaptic locations) to those with slow rise and decay times (indicative of distal locations) ((Jack et al., 1971; Mendell and Henneman, 1971). Yet another remarkable level of selectivity is seen in that a particular MN is contacted by only one of the 10 collaterals of a IaPA, although more collaterals of the same IaPA may run through the dendritic field of that particular MN (Brown, 1981b).

It has been shown that the peripheral target plays a crucial role in determining the specificity between IaPAs and spinal MNs (Frank and Westerfield, 1982; Smith and Frank, 1987; Wenner and Frank, 1995). Moreover, it has been suggested that the process of selective synapse formation is an activity-independent process, since the IaPA-MN connections are from the onset on correct (Frank and Jackson, 1997; Frank and

Westerfield, 1983; Wenner and Frank, 1995). In addition, experiments in chick embryos have demonstrated that when the normal pattern of activity is blocked by adding d-tubocurarine (dtc) chronically to chick embryos, during the period when sensory-motor connections are formed, no change in the specificity of monosynaptic IaPA-MN connections were observed (Mendelson and Frank, 1991). This mechanism could be explained by the fact that IaPAs and spinal MNs have already made peripheral projections to particular muscles before IaPA-MN connections are established. In addition, both pre- and postsynaptic neurons have already distinct molecular phenotypes (Dasen et al., 2005; Wenner and Frank, 1995). This system thus contrasts with the development of the visual system, where the correct pattern of synaptic connections cannot be predicted in advance, and thus in this system patterned activity is believed to play a crucial role in selective synapse formation (Wenner and Frank, 1995). The molecular mechanisms that underlie the formation of selective IaPA-MN connections is to date poorly understood.

Recently, it has been shown that the ETS transcription factor *Er81* plays an important role in the formation of functional connections between IaPA and MNs (Arber et al., 2000b). The *Er81* transcription factor belongs to the *Pea3* subfamily of ETS transcription factors, which consists of *Er81*, *Pea3* and *Erm*. These genes display ~95% identity within the DNA binding (ETS) domain and more then 85% identity within the N- and C- terminal transcription activation domains (Laget et al., 1996). From embryonic day (E) 12 onwards Er81 is expressed in distinct MN pools within the LMC, but its expression is excluded from MN pools within the MMC (Arber et al., 2000b). Moreover, the MN pools that express Er81 in the mouse appear to supply the functional homologs of chick muscles innervated by $Er81^{+}$ LMC MNs (Lance-Jones, 1979). Er81 is also expressed by all proprioceptive afferents (group Ia + Ib proprioceptive afferents) from E13 onwards.

In *Er81* mutant mice, it has been shown that elimination of the *Er81* gene leads to an absence of a ventral termination zone of IaPA in the spinal cord (Arber et al., 2000b). These mice exhibit motor deficits and an abnormal extensor-flexor posturing of their

limbs. In order to elucidate whether functional IaPA-MN connections are affected in these mice, extracellular recordings were performed from mice of postnatal day (P) 5 – 10. The monosynaptic output has been recorded from ventral roots after stimulation of the corresponding dorsal roots or muscle nerves. It was found that the monosynaptic input from IaPA to MNs is dramatically reduced in these mice. For some muscles, the monosynaptic input from IaPA to MNs is decreased to 25% of that detected in wild-type or heterozygous mice (Arber et al., 2000b). This indicates that the number of IaPA that form functional connections with MNs is drastically reduced in these mice.

Apart from the study described above on the role of the ETS transcription factor *Er81* in the formation of the monosynaptic stretch reflex circuit, the question of the molecular and cellular mechanisms underlying the formation of such a precise neural network has not been resolved.

Topic of this thesis

The major aim of this thesis was to begin to identify the cellular and molecular mechanisms required for selective synapse formation between muscle specific subpopulations of IaPAs and alpha-MNs in neonatal mice. It was known that ~95% of IaPA inputs are made on the dendrites of alpha-MNs and that there exist differences among dendritic tree morphology between individual spinal MNs ((Scheibel and Scheibel, 1969; Sterling and Kuypers, 1967). For this reason, I performed a first set of experiments on the dendritic morphologies of individual MN pools located at overlapping cervical levels of the spinal cord by retrograde labeling from five different forelimb muscle nerves in wild-type mice. The monosynaptic IaPA-MN connectivity pattern of individual MNs projecting to a specific muscle was assessed using intracellular recording techniques. This showed that there was a clear correlation between dendrite pattern and IaPA-MN connectivity. By using a binary genetic approach to tissue specifically ablate proprioceptive afferents I could demonstrate that IaPAs do not play a role in MN dendrite patterning. In previous studies (Haase et al., 2002; Livet et al., 2002) it was shown that

the ETS transcription factor *Pea3* induced by the peripheral signal GDNF, regulates cell body positioning of specific MN pools at cervical levels of the spinal cord. Furthermore it was found that *Pea3* is only expressed in selective cervical MN pools, while absent from others. Using *Pea3* mutant mice and comparing $Pea3^{+}$ with $Pea3^{-}$ MN pools, I addressed two questions in my thesis: 1) Does Pea3 play a role in dendrite patterning and IaPA-MN connectivity? 2) Does cell body positioning play a role in these developmental processes? My experiments revealed that Pea3 is of crucial importance not only for MN cell body positioning, but also to cell autonomously control MN dendrite pattern and monosynaptic IaPA-MN connectivity. Moreover, simply changing MN cell body position did not dramatically change dendrite pattern as well as monosynaptic IaPA-MN connectivity. Additional analysis showed that *GDNF* mutant mice exhibited a phenotype similar to *Pea3* mutant mice. Supporting the idea that a peripheral signal can retrogradely act via the activation of transcription factors, and therefore control the precise assembly of central neural circuits.

A minor part of this thesis was concerned with the identification of the role of ETS transcription factor signaling during postmitotic DRG sensory neuron development. *Er81* is expressed by all IaPA from about E13 onwards, indicating that it controls late steps during IaPA development. As shown in a previous study (Arber et al., 2000b) the elimination of *Er81* leads to premature termination of the IaPA in the intermediate spinal cord, resulting in a dramatic decrease in monosynaptic IaPA-MN connectivity. To elucidate whether the late onset of ETS signaling is of crucial importance for the proper development of postmitotic sensory DRG neurons, a genetic strategy was developed to precociously express ETS transcription factor signaling in postmitotic DRG neurons. These experiments revealed that DRG sensory neurons undergo a temporal developmental switch in response to ETS transcription factor signaling. Precocious expression of ETS transcription factor signaling prevented proper development of DRG sensory afferents as assayed by axonal pathfinding errors, perturbation of acquisition of terminal differentiation markers and independence of neurotrophic signaling.

Chapter 2

Target-regulated induction of ETS transcription factor Pea3 in specific motor neuron pools controls dendrite patterning and sensory-motor connectivity

Eline Vrieseling and Silvia Arber

Cell, *in press*

Summary

The apposition of axon terminals and dendrites is critical for the control of neuronal activation, but how distinct neuronal subpopulations establish selective dendrite patterns and acquire specific presynaptic inputs remains unclear. Spinal motor neuron (MN) pools project to specific target muscles and are activated by selective synaptic inputs from group Ia proprioceptive afferents (IaPAs). Here we show that MN pools with radially projecting dendrites respond to sensory stimulation with monosynaptic latency and are strikingly different from MN pools with dendrites avoiding the central grey matter, which are only activated through indirect connections. We provide genetic evidence that the induction of the ETS transcription factor *Pea3* by GDNF is essential in two cervical MN pools to control dendrite patterning and selectivity of IaPA connectivity. These findings suggest that target-induced transcriptional programs control MN dendrite orientation and play a crucial role in the establishment of sensory-motor connections in the spinal cord.

Introduction

Precisely interconnected neuronal circuits represent the cellular basis ultimately responsible for the control of animal behavior. Neuronal circuits gradually arise during development when individual neurons become specified to find their synaptic partners (Clandinin and Zipursky, 2002; Jessell, 2000; Salie et al., 2005). The close apposition of presynaptic axonal terminals and dendrites onto which synapses form is a crucial prerequisite for the precision with which neurons assemble into functional neuronal circuits (Wong and Ghosh, 2002). One important aspect in the control of neuronal differentiation therefore is the acquisition of unique architectural attributes, which manifest themselves in the formation of neuronal subpopulation-specific axonal and dendritic processes. Much progress has been made recently in understanding how axonal processes chose the correct route towards their targets. Axons are guided towards their target regions through the combinatorial activities of cell type specific expression of transcription factors and cell surface receptors that, in turn, enable axons to read localized extracellular guidance signals (Jessell, 2000; Salie et al., 2005; Yu and Bargmann, 2001). In contrast, much less is known about the mechanisms controlling the acquisition of dendritic architecture of distinct neuronal subpopulations (Jan and Jan, 2003), despite the fact that, historically, dendritic diversity represents one of the most important distinguishing features used in vertebrates to define a particular neuronal type (Hausser et al., 2000; Mel, 1994).

Dendritic morphology has fundamental consequences for neuronal function. Not only are dendritic branching patterns important for how synaptic inputs are integrated (Hausser et al., 2000; Rall, 1962), but also the size and orientation of dendritic trees determines the number and type of potential presynaptic partners that can be sampled by a neuron (Wong and Ghosh, 2002). Neocortical pyramidal neurons receive distinct presynaptic inputs to apical and basal dendrites and this dendritic segregation is at least in part controlled by Sema3A signaling (Polleux et al., 2000). Dendrite projection patterns can however also differ between functionally distinct subtypes of one neuronal class. The precision of selective ON or OFF responses of vertebrate retinal ganglion cells correlates

with dendritic stratification in defined sublayers of the inner plexiform layer (Wong and Ghosh, 2002), suggesting morphological segregation as a cellular mechanism to achieve selective connectivity. Nevertheless, the molecular mechanisms controlling dendritic segregation of functionally distinct subclasses of one neuronal type in the vertebrate CNS are only just beginning to be explored.

Spinal motor neurons (MNs) have taken center stage in the elucidation of genetic programs delineating distinct subpopulations during development as well as in functional and anatomical studies (Jessell, 2000; Shirasaki and Pfaff, 2002). MN cell bodies projecting to specific skeletal muscles cluster into MN pools and their positions are conserved between individual animals of one species (Landmesser, 1978b; Romanes, 1951; Ryan et al., 1998). MN pools receive a selective set of presynaptic inputs, the combinatorial activation of which predicts the coordinated and temporally appropriate activity of a particular MN pool during movement. In the spinal monosynaptic reflex circuit, inputs from group Ia (Ia) proprioceptive afferent (PA) dorsal root ganglion (DRG) sensory neurons to MNs have been particularly well studied. IaPAs respond to rapid changes in muscle stretch and convey this information centrally to MNs through mono- and polysynaptic connections (Brown, 1981a; Eccles et al., 1957). IaPAs make preferential connections with MN pools innervating the same muscle whereas they avoid making direct synapses to MNs innervating functionally antagonistic muscles (Baldissera et al., 1981; Eccles et al., 1957; Frank et al., 1988; Mears and Frank, 1997), raising the question of the mechanisms mediating this selectivity of connections. Extensive dendritic trees elaborated by MNs represent the targets for most presynaptic inputs (Brown, 1981a; Mel, 1994; Rall et al., 1967), but experiments in the frog suggest that the pattern of MN dendrites may not explain the observed difference in sensory-motor connectivity (Lichtman and Frank, 1984; Lichtman et al., 1984). Nevertheless, striking differences in the morphology of MN dendrites have been observed in several species (Landgraf et al., 2003; Okado et al., 1990; Szekely et al., 1980). These studies have, however, not explored a potential link between dendrite orientation and connectivity.

MNs acquire several important aspects of their unique identities before their axons reach the target (Jessell, 2000; Shirasaki and Pfaff, 2002). A combinatorial regulatory network of Hox transcription factors determines MN pool identity and coordinately controls the choice of a particular target muscle (Dasen et al., 2005). Several members of the ETS transcription factor family are expressed in specific MN pools only after axons project to the periphery (Arber et al., 2000a; Hippenmeyer et al., 2004; Lin et al., 1998b; Livet et al., 2002). The ETS transcription factor *Pea3* marks several MN pools and its expression is induced by the peripherally localized glial cell line-derived neurotrophic factor (GDNF) (Haase et al., 2002; Lin et al., 1998b; Livet et al., 2002). Consistent with the relatively late onset of Pea3 expression, *Pea3* mutant mice are not affected in the establishment of the initial motor axonal projections but exhibit selective defects in MN pool clustering (Livet et al., 2002). How these defects in MN pool clustering influence the functional integration of $Pea3^{+}$ MN pools into spinal circuits, has remained obscure.

Using anatomical, physiological and genetic strategies in the mouse, we addressed whether there is a link between MN dendrite orientation and connectivity, and also examined transcriptional programs regulating these processes. We show that different MN pools in the cervical spinal cord establish highly selective dendrite patterns correlating with observed responses elicited by sensory stimulation. We found that the expression of the ETS transcription factor *Pea3* in two cervical MN pools is essential to control dendritic patterning and sensory-motor connectivity. Our findings therefore suggest that the orientation of dendrites and the choice of presynaptic inputs to spinal MNs are tightly regulated by neuronal subpopulation specific transcriptional programs.

Results

MN pools exhibit striking differences in dendrite patterns

To study whether MN pools innervating distinct target muscles differ in their pattern of dendrites, we performed retrograde tracing experiments from identified muscles in

neonatal mice at the forelimb level, by application of fluorescent dextran to isolated muscle nerves (Fig 1A). We first examined the cell body position of distinct MN pools. We found that MN cell bodies innervating the triceps brachii (Tri) muscle were positioned in a tight, dorso-medial cluster at cervical (C) level C7-C8 (Fig 1B, F-M). MN cell bodies innervating the pectoralis major (Pec_{maj}) muscle were located at C6-C7 in a similar dorso-ventral medio-lateral position as Tri MNs (Fig 1B, F, I, J). At C7, where Tri and Pec_{maj} MN pools overlap rostro-caudally over a short distance, Pec_{maj} MN cell bodies were clustered medially to Tri MNs (Fig 1B, F). Cutaneous maximus (CM) and latissimus dorsi (LD) MN pools were clustered in a position ventral to Tri and Pec_{maj} MN pools (Fig 1B, F-M). The CM MN pool extended from C7 to anterior T1 in an extreme ventral position (Fig 1B, F-M), consistent with previous observations (Baulac and Meininger, 1981; Livet et al., 2002). LD MN cell bodies were also clustered ventro-laterally at C7, but in a position consistently dorsal to CM MNs (Fig 1B, G-I). Finally, the cell bodies of MNs innervating the biceps brachii longus (Bic) muscle were found in a dorso-lateral position at segmental levels C5-C6 (Fig 1B, D, E). At C6 where Bic and Pec_{maj} MN pools overlap rostro-caudally, Bic MNs were located dorso-lateral to Pec_{maj} MNs (Fig 1B, D, E). Together, these findings delineate the cell body positions of five MN pools in the cervical spinal cord of the mouse and define the segmental level C7 with maximal rostro-caudal overlap between these MN pools as the focus for further analysis.

We next examined the dendrite patterns of cervical MN pools in relation to their specific cell body positions. Retrograde labeling of the Tri MN pool revealed a radial dendrite pattern with extensive invasion into the central grey matter of the ventral spinal cord (Fig 2A, C, F, H, I). Similar to Tri MNs, Pec_{maj} MNs exhibited a radial dendrite pattern and at C7, dendrites between these two MN pools were highly intermingled (Fig 2B, C, H, I). In contrast, CM MN dendrites exhibited a pattern strikingly distinct from Tri and Pec_{maj} MN pools. Most CM MN dendrites were clustered at the borders of the ventral horn displaying pronounced avoidance of the central grey matter territory (Fig 2D, F, H, I). Similar to CM MNs, very few dendrites of the LD MN pool extended into the central grey matter and the majority of dendrites was confined to the lateral edges of the spinal cord (Fig 2E, H, I). We observed considerable overlap between the dendrites of CM and

LD MNs, but the majority of Tri and Pec_{maj} dendrites was separate from CM and LD MN dendrites (Fig 2A-F, Fig 6A-D, I). Finally, Bic MNs extended the majority of their dendrites ventrally and dorsally, whereas the density of dendrites reaching into the ventral part of the central grey matter was much lower (Fig 2G).

Together, these findings show that at caudal cervical levels, MN pools with a dorso-medial cell body position (Tri, Pec_{maj}) exhibit radial dendrite patterns invading the central grey matter extensively, but dendrites of MN pools with ventro-lateral cell body position (CM, LD) are confined to the lateral edges of the spinal cord. These findings raise the question of whether MNs with different dendritic patterns represent synaptic targets for distinct classes of presynaptic sensory inputs.

Distinct MN dendrite patterns correlate with differences in sensory evoked responses

To begin to examine whether the observed variation in MN dendrite patterns between MN pools might be paralleled by differences in response to sensory stimulation, we used electrophysiological recording techniques. We first measured synaptic inputs to defined MNs by intracellular recordings elicited by stimulation of sensory afferents (SA) innervating the same muscle peripherally (homonymous inputs), since monosynaptic connections between homonymous pairs of IaPAs and MNs are known to form preferentially (Baldissera et al., 1981; Eccles et al., 1957; Frank et al., 1988; Mears and Frank, 1997). Stimulation of Tri muscle nerves elicited an early onset, short latency response in Tri MNs in intracellular recording experiments (Fig 3C, F, Table 1). We used two-step cluster and jitter analysis as two independent methods to define the percentage of Tri MNs responding to Tri SA stimulation with monosynaptic latency (Experimental Procedures and Suppl Fig 1, 3L). This definition resulted in a monosynaptic latency window of 2.8$\pm$0.8ms, consistent with previous studies in the mouse (Arber et al., 2000a; Mears and Frank, 1997). We found that 95% of all Tri MNs received monosynaptic sensory connections with a mean latency of 3.3$\pm$0.2ms (21 of 22; Fig 3F, G). In contrast, when we recorded intracellularly from CM MNs, sensory stimulation of the CM muscle nerve evoked a response with a mean latency of 8.8$\pm$1.9ms in CM neurons (n=13),

clearly outside the window defined for monosynaptic inputs (Fig 3E, F, Suppl Fig 1A). These findings therefore demonstrate that most Tri MNs receive direct synaptic input from Tri SAs, whereas CM MNs do not receive any direct connections from CM SAs.

MNs have been described to receive the strongest monosynaptic inputs from homonymous IaPAs (Baldissera et al., 1981; Eccles et al., 1957; Mears and Frank, 1997). However, to determine whether CM MNs receive direct connections from IaPAs other than their own, we next stimulated individual DRs at C6-C8 (Suppl Fig 2A). Stimulation of DR SAs at C6-C8 elicited an early onset, short latency potential in Tri MNs (2.3$\pm$0.1ms; n=5; Suppl Fig 2B), but not in CM MNs (5.5$\pm$0.6ms; n=11; Suppl Fig 2C), demonstrating that SAs at C6-C8 form direct synaptic connections to Tri but not to CM MNs.

We next determined whether the variation in the onset of synaptic responses between Tri and CM MNs could be due to differences in the functionality or differentiation of IaPAs innervating these muscles. To determine peripheral conduction time, we stimulated Tri or CM muscle nerves and recorded the response at DR C7, but found no significant difference (Tri: 0.8$\pm$0.1ms; CM: 0.8$\pm$0.1ms; n$\geq$2). We next determined the existence of PV^+ IaPA terminals innervating muscle spindles in the CM muscle. To visualize PV^+ IaPAs, we used a conditional genetic approach to express membrane-bound eGFP selectively in these DRG neurons (Arber et al., 2000a; Hippenmeyer et al., 2005) and detected 35$\pm$2.52 muscle spindles in CM muscles (Fig 4A, B; n=3). We also found that intrafusal muscle fibers in CM muscles express the ETS transcription factor *Er81* (Fig 4C) (Arber et al., 2000a). Finally, to determine whether CM IaPAs elaborate a characteristic central projection pattern, we performed transganglionic retrograde labeling experiments from the CM muscle by cutting C6-T1 ventral roots to avoid interference with CM MN derived tracing signals. We found that both Tri and CM IaPAs terminated in the ventral horn in a pattern characteristic for IaPAs in a position close to MNs (Brown and Fyffe, 1978) (Fig 4G, H) and CM IaPA terminals were marked by the vesicular glutamate transporter vGlut1 (Fig 4J), which is enriched in axonal terminals of DRG neurons of early postnatal mice (Oliveira et al.,

2003). Together, these findings suggest that the differences in onset latency observed in Tri and CM MNs in response to sensory stimulation can most likely not be explained by distinct IaPA properties.

We next examined whether other MN pools at the same segmental levels showed similar distinctions in response to SA stimulation. Stimulation of the Pec_{maj} muscle nerve elicited a monosynaptic response in all Pec_{maj} MNs (3.2±0.1ms; n=3; Fig 3F, G, Table 1). In contrast, only one of six LD MNs showed monosynaptic responses to stimulation of the LD muscle nerve (Fig 3F, G, Table 1). Moreover, we detected 15±1.2 (n=3) muscle spindles in LD muscles (Fig 4D-F) and central trajectories of LD IaPAs extended into the ventral spinal cord (Fig 4I).

Together, these findings suggest that dendritic orientation of a MN pool correlates with the intracellular responses that can be elicited by sensory stimulation. Whereas MN pools with radially organized dendrites extending into the central grey matter receive pronounced monosynaptic input upon SA stimulation (Tri, Pec_{maj}), the sensory input to MN pools with dendrites not projecting into the central grey matter of the spinal cord is mainly mediated through di-and/or polysynaptic connections (CM, LD).

PAs do not contribute to selectivity of MN dendrite patterns

The observed correlation in the differences between distinct MN pool dendrite patterns and responses to sensory stimulation raised the possibility that IaPAs influence the establishment of dendritic projection patterns during development. We used a binary genetic approach in the mouse to selectively ablate PAs by Cre recombinase-mediated activation of diphtheria toxin A expression in PV^+ PAs ($Isl2^{DTA}/PV^{Cre}$) (Hippenmeyer et al., 2005; Yang et al., 2001). $Isl2^{DTA}/PV^{Cre}$ mice analyzed at P0 showed an absence of PV^+ DRG neurons, whereas $TrkA^+$ and $TrkB^+$ DRG neurons were still present in these mice (Suppl Fig 3A, D, data not shown). Analysis of the central trajectory of DRG axons by visualization of PV^+ or $TrkA^+$ SAs or by analysis of $vGlut1^+$ terminals revealed a selective absence of DRG axons invading the ventral horn of the spinal cord in

Isl2^{DTA}/*PV*^{Cre} mice while no differences in the innervation of the dorsal spinal cord were detected (Suppl Fig 3B, C, E, F).

How does the absence of PAs influence the establishment of MN pool specific dendrite patterns? We found that Tri and Pec_{maj} MN pool dendrites in the absence of PAs still exhibited a radial projection pattern with extensive invasion of the grey matter (Suppl Fig 3I-K), whereas CM and LD MN dendrites were still confined to the lateral edges of the spinal cord (Suppl Fig 3G-I). Moreover, to circumvent the possiblity that ablation of PAs might be too slow in *Isl2*^{DTA}/*PV*^{Cre} mice, we also confirmed these data by analysis of MN dendrite patterns in *TrkC* mutant mice at P0 in which PAs die at early developmental stages (Suppl Fig 3M-O) (Liebl et al., 1997). Together, these findings suggest that the presence of PAs does not play a major role in the initial shaping of MN pool specific dendrites, but do not exclude later roles for PAs in dendrite growth and branching.

The availability of mice lacking PAs also allowed us to examine the effect on MN activation in response to sensory stimulation under these experimental conditions. Recording intracellularly from Tri MNs of *Isl2*^{DTA}/*PV*^{Cre} mice upon DR stimulation showed a pronounced shift in the onset latency of sensory evoked potentials, outside the defined monosynaptic window (wild-type: 2.3$\pm$0.1ms; n=5; *Isl2*^{DTA}/*PV*^{Cre}: 5.1$\pm$0.6ms; n=3; Suppl Fig 3L). In contrast, elimination of PAs did not affect the onset latency detected in CM MNs in response to DR stimulation (wild-type: 5.5$\pm$0.6ms; n=11; *Isl2*^{DTA}/*PV*^{Cre}: 5.7$\pm$0.4ms; n=11; Suppl Fig 3L). While these findings do not rule out that PAs normally do contribute to di- or polysynaptic connectivity to CM MNs, they clearly provide further evidence that PAs do not contact CM MNs monosynaptically.

Altered dendrite pattern in *Pea3* mutant CM and LD MN pools

To examine the genetic programs involved in the regulation of MN pool specific dendrite patterns, we next analyzed a mouse mutant in the ETS class transcription factor *Pea3* (Livet et al., 2002). At cervical levels, the expression of *Pea3* in spinal MNs is restricted to a few MN pools and *Pea3* mutation results in selective defects in MN migration and

settling within the LMC (Livet et al., 2002). These findings allowed us to investigate the consequences of defects in MN cell body positioning on the establishment of MN pool specific dendrite patterning and sensory-motor connectivity, both in $Pea3^+$ and $Pea3^-$ MN pools at C6-C8.

We first assessed the molecular identity of the MN pools analyzed in this study by a combination of retrograde tracing experiments and immunocytochemistry. We found that Tri and $Pect_{maj}$ MNs did not express Pea3 and also did not express the LIM homeodomain transcription factor Isl1 (Fig 5A, B, F, G). In contrast, both CM and LD MNs expressed Pea3 (Fig 5C, D), as observed previously (Livet et al., 2002), but only CM MNs coexpressed Isl1 (Fig 5H, I). Bic MNs at C5-C6 were $Isl1^+$ but $Pea3^-$ (Fig 5E, J, N).

Since previous studies have not addressed the position of MNs in *Pea3* mutant mice at the level of individual MN pools (Livet et al., 2002), we next compared the cell body positions of MN pools between wild-type and *Pea3* mutant mice. We found that CM MNs in *Pea3* mutant mice were located in a dorso-medial position characteristic for Tri MNs in wild-type mice as previously shown (Livet et al., 2002). In contrast, Tri MNs in *Pea3* mutant mice took over the extreme ventro-lateral position of wild-type CM MNs (Fig 5O, T, S, X). $Pect_{maj}$ MNs in *Pea3* mutant mice were found completely segregated from Tri MNs in a position dorsal to Tri MNs, but were intermingled with CM MNs (Fig 5Q-S, V-X). LD MNs in *Pea3* mutant mice were intermingled with Tri MNs, in a position ventral to CM MNs (Fig 5P, S, U, X). Together with previous observations (Livet et al., 2002), these findings provide evidence for selective mispositioning of MN pools in the caudal cervical spinal cord of *Pea3* mutant mice, both in MN pools normally expressing or lacking Pea3 expression.

Does the absence of *Pea3* and the concomitant defects in cell body positioning in MNs affect the elaboration of MN dendrites? We first examined the dendrite pattern of CM and LD MN pools, normally expressing Pea3. *Pea3* mutant CM MNs showed a striking transformation in dendritic projections when compared to wild-type CM MN

dendrites. Instead of avoiding the central grey matter, *Pea3* mutant CM MN dendrites displayed a radial dendrite pattern highly reminiscent of the pattern normally observed for Tri MNs (Fig 6A, E, L, M, Q). Quantitative analysis of dendrite extension in the diagonal axis indeed revealed no significant difference between *Pea3* mutant CM MN dendrites and wild-type Tri MNs, but highly significant differences between CM MNs in *Pea3* mutants and wild-type mice (Fig 6Q). Moreover, *Pea3* mutant LD MNs also projected dendrites into the central grey matter, overlapping extensively with the dendritic field of *Pea3* mutant CM MNs (Fig 6F, L, Q). In contrast to the dramatic changes observed for CM and LD MNs, Tri MNs in *Pea3* mutant mice whose cell bodies took over the position normally characteristic for CM MNs, did not display CM-like dendrite projections but instead still projected many dendrites into the central grey matter territory overlapping with dendrites of CM, LD and Pec_{maj} MNs (Fig 6G, M, Q). Finally, we did not observe any alterations in Bic MN dendrites in *Pea3* mutant mice (Fig 6K, N). Taken together, these findings suggest that the expression of *Pea3* in CM and LD MNs plays a major role in shaping MN pool specific dendrite patterns. In contrast, our analysis of Tri MN dendrites in *Pea3* mutant mice suggests that the position of MN pools in the ventral horn does not represent a primary determinant of the overall dendritic pattern.

Previous experiments have demonstrated that GDNF is required for the induction of *Pea3* expression in most CM MNs (Haase et al., 2002), raising the question of whether GDNF also represents an upstream regulator in shaping MN dendrite patterns or whether this signaling pathway through *Pea3* is obscured by other GDNF activities. To directly address this question, we analyzed CM dendrites in E17.5 *GDNF* mutant embryos circumventing neonatal lethality of these mice due to kidney defects (Haase et al., 2002; Moore et al., 1996). In *GDNF* mutant embryos, CM MN dendrites extended into the central grey matter area similar to the phenotype observed in *Pea3* mutant mice (Fig 6E, P). These centrally projecting dendrites in *GDNF* mutant embryos were derived from CM MNs with a cell body position dorsal to Tri MNs. We also observed a fraction of CM MNs with a cell body position ventral to Tri MNs in *GDNF* mutants, most likely corresponding to MNs still expressing *Pea3* (Haase et al., 2002) and these MNs did not seem to be affected in their dendrite pattern (data not shown). In contrast, Tri MNs in

GDNF mutant embryos still projected towards the central grey matter area (data not shown). Taken together, these findings support the idea that peripheral GDNF acts through the induction of *Pea3* in CM but not Tri MNs to control the elaboration of a MN pool specific dendrite pattern.

Pea3 mutant CM MNs show specific defects in response to sensory stimulation

To examine whether the observed alterations in MN dendrite patterning in *Pea3* mutant mice influence sensory-motor connectivity, we performed intracellular recordings of identified MNs. Since in *Pea3* mutants, CM MNs displayed dramatic alterations in dendrite trajectory, we first studied connectivity to *Pea3* mutant CM MNs. We found that stimulation of DR SAs at C6-C8 elicited an early potential in *Pea3* mutant CM MNs (2.0$\pm$0.1ms; n=3; Fig 7B, C), in contrast to the much longer latency observed for wild-type CM MNs (5.5$\pm$0.6ms; n=11; Fig 7A, C).

To address the selectivity of direct sensory inputs to CM MNs in *Pea3* mutant mice, we stimulated specific peripheral muscle nerves. We first determined whether CM MNs in *Pea3* mutant mice received monosynaptic connections from homonymous IaPAs. We found that stimulation of CM SAs in *Pea3* mutants did not reveal the presence of any inputs of monosynaptic latency to CM MNs (n=18; Fig 7D, E; Table 1). In contrast, stimulation of Tri SAs evoked a pronounced short latency response in 94% of all *Pea3* mutant CM MNs analyzed (2.9$\pm$0.1ms; n=16; Fig 7F, G, H, I, Suppl Fig 4A, Table 1). Latency and jitter analysis of CM MNs in response to Tri SA stimulation between wild-type and *Pea3* mutants showed a clear shift from di- or polysynaptic to monosynaptic activation (wild-type: 6.1$\pm$1.8ms (n=12); *Pea3* mutants: 2.8$\pm$0.8ms (n=32); Suppl Fig 4). Furthermore, the excitatory postsynaptic potential (EPSP) amplitude of this response in CM MNs was not significantly different from the response detected in Tri MNs of either wild-type or *Pea3* mutant mice upon stimulation of Tri SAs (Fig 7L, Table 1). We confirmed these intracellular recording results by recording extracellular responses from CM muscle nerves upon stimulation of Tri SAs (Fig 7M).

Similar changes in sensory-motor connectivity were also examined when we recorded from *Pea3* mutant LD MNs in which stimulation of Tri SAs induced a short latency response in 85% of *Pea3* mutant LD MNs (2.7±0.1ms; n=11; Table 1). In contrast, LD SAs did not make any direct connections to *Pea3* mutant LD MNs (n=13; Table 1). Together, these findings show that *Pea3* mutant CM and LD MNs display extensive changes in sensory-motor connectivity and received monosynaptic inputs from SAs normally contacting MNs with similar dendrite patterns (Tri, Pec_{maj}).

Tri MNs in *Pea3* mutants exhibit subtle changes in connectivity

To examine whether the observed changes in connectivity in *Pea3* mutant mice are primarily a consequence of changes in MN cell body position or can be attributed to the absence of *Pea3* in CM and LD MNs, we next analyzed sensory connections to *Pea3* mutant Tri MNs. In *Pea3* mutant mice, Tri MNs undergo a pronounced ventro-lateral shift in MN cell body position but since these MNs normally do not express Pea3, they should not primarily be affected by cell-intrinsic *Pea3* loss. We found that 75% of all Tri MNs analyzed in *Pea3* mutant mice received short latency inputs from Tri SAs (n=44; 11 of 44 MNs did not receive monosynaptic inputs; Fig 7F, K). In contrast, none of the *Pea3* mutant Tri MNs received monosynaptic connections from CM SAs (Table 1). These findings suggest that the majority of Tri MNs in *Pea3* mutant mice are still activated by sensory stimulation of Tri but not CM SAs, but that the reliability of functional Tri SA connections to Tri MNs in *Pea3* mutant mice is reduced when compared to wild-type.

Discussion

The appropriate temporal activation of individual MN pools depends on the distribution of presynaptic inputs on MN dendrites. IaPAs make highly selective connections to MNs but whether and how MN specification contributes to the establishment of this selectivity, is currently unknown. In this study, we provide evidence that the strategies used to excite MNs are strikingly different between individual MN pools and that this observed diversity in sensory-induced MN activation correlates with the elaboration of specific dendritic trees (Fig 8). Furthermore, our findings suggest that transcriptional programs

induced by target-derived signals play an important role in the establishment of these MN pool specific characteristics. We discuss the implications of our findings in the context of different cellular and molecular strategies used to elaborate distinct dendritic shapes and to acquire selective presynaptic inputs.

Dendrite orientation as strategy to control presynaptic connectivity in MNs

MNs receive highly selective sensory inputs (Baldissera et al., 1981; Eccles et al., 1957; Frank et al., 1988), raising the question of how matching between pre- and postsynaptic partners is achieved. The number of MN pools in a higher vertebrate lateral motor column is estimated at approximately 50 (Dasen et al., 2005; Landmesser, 1978b; Romanes, 1951) and this number is matched by an equal number of distinct IaPA populations growing into the spinal cord in search for postsynaptic partners. Even the existence of only a few distinct dendrite patterns could help to dramatically reduce the molecular complexity required to resolve selectivity of connections in this system. In support of such a model, we found that distinct MN pools in the wild-type mouse orient their dendrites to avoid or invade particular territories of the spinal cord, and we observe these orientations to correlate with connectivity patterns (Fig 8). Our data are also supported by a study in the rat lumbar spinal cord, where dendrites of functionally unidentified MNs have been described to exhibit different morphologies strikingly similar to the ones observed in our study (Szekely et al., 1980). Nevertheless, IaPA derived inputs only represent a minor fraction of all presynaptic inputs to MNs and other classes of presynaptic inputs to MNs may therefore also be differentially distributed correlating with MN dendrite patterns. For example, distinct classes of interneurons participating in central pattern generator circuits settle in highly specific positions (Goulding and Pfaff, 2005), and could therefore target MN dendrites differentially. Moreover, cutaneous afferents activating MNs through di- or polysynaptic pathways and supraspinal connections could also be influenced by differential positioning of MN dendrites. From an evolutionary point of view, it is tempting to speculate that observed changes in MN dendrite patterning in different species could have contributed to the acquisition of altered muscle functions, through the acquisition of novel presynaptic inputs contributing to altered activation patterns during locomotion.

Nevertheless, dendritic orientation certainly does not represent the only parameter involved in the acquisition of presynaptic inputs. While the elaboration of CM and LD MN dendrites in *Pea3* mutants correlates with the IaPA input normally observed for MNs with similar dendrite patterns, we cannot exclude the possiblity that these MNs have acquired some molecular traits normally required to attract Tri SAs to make synaptic connections. Conclusive answers to these questions will await the identification and functional analysis of downstream genes regulated by *Pea3* in MNs. Moreover, molecular distinctions between MN pools with similar dendrite patterns are clearly required to explain the complexity of selective sensory-motor connectivity. Tri and Pec_{maj} MN pool dendrites both show radial dendrites in mice, yet Pec_{maj} SAs contact their own MNs at a much higher frequency than Tri MNs. These findings are consistent with previous work in the frog spinal cord concluding that MN dendrite orientation does not explain selectivity of sensory-motor connectivity for three MN pools including Tri and Pec MN pools (Lichtman and Frank, 1984; Lichtman et al., 1984). Together, these findings suggest that sensory-motor connectivity is likely to be controlled by a combination of MN dendrite arborization and selective recognition between IaPAs and MN pools.

Cellular and molecular pathways regulating specificity of connectivity

The diversity in dendrite patterns and differences in sensory-motor connectivity observed for distinct MN pools raises the question of the cellular and molecular pathways controlling the emergence of these divergent properties. Ingrowth of afferents into the target region exhibits a pronounced influence on the elaboration of dendritic trees of postsynaptic neurons in several neuronal circuits. For example, the elaboration of cerebellar Purkinje cell dendrites depends on interactions with granule cell axons establishing synaptic connections through parallel fibers (Wong and Ghosh, 2002). Surprisingly, we found that the ingrowth of IaPAs into the ventral horn of the spinal cord does not contribute to the process of initial shaping of MN pool specific dendrite orientation. These findings do however not exclude a later role of these IaPAs in

anatomical maturation of MNs as has been suggested to occur during the first postnatal month (Kalb, 1994).

We found that *Pea3* expression plays a critical role both in the elaboration of CM and LD MN dendrites and the establishment of selective sensory inputs to these MNs. In chick embryos, coordinate expression of *Pea3* in interconnected MN pools and PAs in the lumbar spinal cord was observed (Lin et al., 1998b), raising the question of whether the expression of Pea3 in DRG sensory neurons in the mouse might contribute to the observed phenotypes in *Pea3* mutants. In the mouse, we found that the expression of Pea3 in DRG neurons at late embryonic stages was almost exclusively restricted to a subpopulation of $TrkA^+$ neurons, but not in $TrkC^+$ PAs and expression was restricted to MNs within ventral spinal neurons (Vrieseling and Arber, unpublished observation). While we cannot exclude an earlier role for Pea3 in PAs influencing selective sensory-motor connectivity at late embryonic stages, we favor a model in which *Pea3* activity is required cell-autonomously in expressing MNs and indirectly influences the migratory behavior of neighboring MNs such as Tri.

Our findings also raise the question of whether altered MN cell body position in *Pea3* mutant mice is the primary cause of the dendrite and connectivity defects observed in these mutants or whether an active role of *Pea3* in the control of these latter events occurs. Indirect evidence for an active role of *Pea3* in dendrite patterning and control of sensory input to MNs comes from the analysis of Tri MNs in *Pea3* mutant mice. Tri MNs do not express *Pea3*, yet their cell body position in *Pea3* mutant mice is altered to adopt the position of CM MNs observed in wild-type mice. The consequence of this change in cell body position for dendrite patterning and sensory-motor connectivity is much less dramatic than the one observed for CM and LD MN pools, and the majority of Tri MNs in *Pea3* mutants still receive inputs from the appropriate SAs. However, we found that 25% of Tri MNs in *Pea3* mutant mice do not receive monosynaptic input anymore from Tri SAs, raising the possibility that at the level of individual Tri MNs there might still be a causal link between the establishment of a particular dendrite pattern and observed sensory inputs.

The expression of *Pea3* in defined MN pools of the cervical spinal cord is induced by GDNF (Haase et al., 2002). Together with our current work, these findings suggest that peripheral signals represent key regulators in the control of MN dendrite patterning and regulation of selective sensory-motor connectivity in vertebrates, the latter of which has already been suggested by a series of embryological studies (Frank and Wenner, 1993; Wenner and Frank, 1995). In support, we also observed alterations in MN dendrite patterning of CM MNs in *GDNF* mutant mice, which were reminiscent of the changes detected in *Pea3* mutants. A similar mechanism of retrograde modulation of dendritic geometry by target-derived signals has been proposed to occur in the developing chick embryo, where neurons of the isthmo-optic nucleus are dependent on the presence of the retina to acquire a polarized dendritic morphology (Blaser et al., 1990). In a more general context, our findings therefore raise the possibility that target-derived signals may represent a powerful way to retrogradely regulate the elaboration of neuronal subpopulation-specific dendritic trees and the assembly of selective presynaptic inputs.

How does the function of Pea3 link to other programs of MN specification and differentiation? Recent work has provided strong evidence that a regulatory network of Hox transcription factors acts to coordinately control acquisition of MN pool identity and target muscle innervation (Dasen et al., 2005). This work has also demonstrated that the pool-specific pattern of Pea3 expression is determined by a combinatorial Hox transcription factor code (Dasen et al., 2005). Together, these findings suggest that the appropriate combination of Hox transcription factors endows MNs with the competence to respond to peripheral signals by induction of *Pea3*. Consistent with the idea of a permissive peripheral signal acting on predetermined MNs, *in vitro* spinal cord explant experiments showed that GDNF induces *Pea3* expression in many fewer MNs than express GDNF receptors (Haase et al., 2002). Taken together with our current results, such a signaling pathway would then act to trigger MN dendrite orientation and acquisition of appropriate IaPA inputs. The induction of *Pea3* through GDNF therefore links early transcriptional programs in the spinal cord to the initiation of late events required for fine-tuning of neuronal circuit formation and function.

Experimental Procedures

Mouse genetics and immunocytochemistry

Pea3$^{+/-}$ (Livet et al., 2002), *Tau*$^{mGFP\text{-}INLA}$ (Hippenmeyer et al., 2005), *PV*^{Cre} (Hippenmeyer et al., 2005), *Isl2*^{DTA} (Yang et al., 2001), *Er81*^{nLacZ} (Arber et al., 2000a), *TrkC*$^{+/-}$ (Liebl et al., 1997) and *GDNF*$^{+/-}$ (Haase et al., 2002) mouse strains have been described previously. Sections for immunohistochemistry were essentially processed as described (Arber et al., 2000a) and quantification of dendrites performed using Image J 1.35f Software (NIH). Details are described in Suppl Material.

Electrophysiology and retrograde tracing experiments

Dissection of spinal cords for retrograde tracing and electrophysiology experiments. Postnatal (retrograde tracing: P0-P2; electrophysiology: P5-P7) or embryonic (E17.5 for *GDNF* mutants) mice were anesthetized on ice, perfused with artificial cerebral spinal fluid (ACSF), decapitated and transferred to a chamber containing ice-cold circulating oxygenated (95% O_2/ 5% CO_2) ACSF as described previously (Mears and Frank, 1997). Spinal cords were exposed by dorsal laminectomy and peripheral nerves up to individual identified muscles were dissected according to (Greene, 1935). For retrograde tracing of MN pools or transganglionic labeling of sensory afferents, fluorescein- or tetramethylrhodamine-labeled dextran (3000MW, Invitrogen) was applied to peripheral nerves using tightly fitting glass capillaries for overnight incubation at room temperature under continued oxygenation before fixation of the spinal cord in 4% paraformaldehyde. To reveal MN pools, dorsal roots of the preparation were cut, whereas for experiments to analyze sensory afferent projections, ventral roots were cut. For physiology experiments, spinal cords were hemisected, muscle nerves were placed in tightly fitting glass suction electrodes and the preparation was gradually warmed to 30°C. Muscle nerves were stimulated at 1.5 times the strength that evokes maximal monosynaptic response (0.4mA current pulses for 0.1ms at 0.5Hz) using a stimulus isolator unit (World Precision Instruments, A360).

Intracellular recordings. Sharp glass micropipettes with a resistance of 70 – 120 MΩ filled with 2M potassium acetate and 0.5% fast green were used for intracellular recording experiments from MNs (Figure 3A). MNs were identified by antidromic (AD) stimulation from peripheral muscle nerves. Only MNs with a resting potential below –45 mV were used for analysis. For each MN analyzed, 20 sequential traces were recorded (Axoclamp2B, Axon Instruments) digitally at 10kHz (LTP230D software) (Anderson and Collingridge, 2001) and averaged offline subsequently.

Extracellular recordings. Tightly fitting glass suction electrodes were placed either on the dorsal root or peripheral muscle nerve for recording of extracellular potentials evoked by muscle nerve stimulation. The alternating current (AC) coupled signal was first amplified (P55 AC-preamplifier, Grass) and then digitally acquired as for intracellular recordings.

Data analysis. Collected traces were analyzed with custom routines written in Matlab (Version 7.0.1.). In most intracellular recording experiments, monosynaptic EPSPs were contaminated by AD responses (Figure 3A). In order to correctly measure the monosynaptic EPSP onset latency, hyperpolarizing current was injected to let the AD response fail (Figure 3A). In instances in which this protocol was not successful, the stimulation strength was turned down to dispose of the AD response. Using an algorithm in Matlab, the EPSP onset was detected as an inflection point which corresponds to a peak in the second derivative of the trace. EPSP onset latencies refer to the time delay between the stimulation artifact and the onset of the earliest arising EPSP. The time window for monosynaptic EPSP onset latencies was defined by first performing a TwoStep Cluster analysis (SPSS 13.0 for Windows) of all MNs recorded from upon stimulation of homonymous sensory afferents in this study, resulting in two clearly distinct datasets. These datasets and the total data set were then analyzed using both Kolmogorov-Smirnov and Shapiro-Wilk tests for normality and only the split data sets followed a normal distribution. The monosynaptic time window was therefore considered as the mean latency of the short latency dataset $\pm$ 2 SD (2.8$\pm$0.8ms). All other inputs were considered to be di- or polysynaptic (Supplemental Figure 1A). In addition, we

analyzed MNs with onset latencies below 8ms for the jitter in the onset of the EPSP in non-averaged, individual traces. Monosynaptic connectivity was characterized by highly consistent onset latencies, whereas di- or polysynaptic connections showed a higher degree of variance in the EPSP onset time (Supplemental Figure 1B) (Doyle and Andresen, 2001; Rose and Metherate, 2005). All data collected across P5–P7 animals were pooled in our analysis. Consistent with previous observations (Mears and Frank, 1997), monosynaptic EPSP onset latencies decreased slightly from P5–P7. Due to unequal distribution of age in some comparative datasets, these age differences resulted in significant differences between these datasets. Therefore, Student's t-tests were performed on age-matched data sets to exclude misinterpreting differences. Throughout the paper, mean latency refers to mean monosynaptic latency whenever monosynaptic input is present; otherwise it refers to mean EPSP onset latency of the earliest arising EPSP. Monosynaptic EPSP amplitudes were measured in the absence of AD response as described above. In the presence of an action potential, the EPSP amplitude was determined by an inflection point obtained from the second derivative of the trace from the time point the action potential is initiated. Monosynaptic latency window for intracellular recording experiments upon dorsal root stimulation was defined by subtraction of peripheral conduction time (0.8ms) from the latency window determined for homonymous inputs (2.0$\pm$0.8ms). Time is shown by indicating monosynaptic latency window for each trace (red dashed lines) and stimulation artifacts in traces are cut off, except for Figure 3A and 8M. To reveal the small extracellular potentials recorded from the muscle nerves, averaged traces recorded without muscle nerve stimulation were subtracted from traces recorded with muscle nerve stimulation. In all experiments, significance was determined performing a Student's t-test and defined as: * $p \leq 0.05$, ** $p \leq 0.01$ and *** $p \leq 0.001$.

Immunohistochemistry

Antibodies used in this study were: rabbit anti-tetramethylrhodamine (Invitrogen), rabbit anti-PV (Swant), rabbit anti-TrkA (gift from L.F. Reichardt), rabbit anti-LacZ (Arber et al., 2000a), rabbit anti-Pea3 (Livet et al., 2002), rabbit anti-GFP (Molecular Probes),

chick anti-TrkB (gift from L.F. Reichardt), guinea pig anti-fluorescein (generated against fluorescein coupled to blue carrier, Pierce), guinea pig anti-vGlut1 (Chemicon), guinea pig anti-Isl1 (Arber et al., 2000a). For the analysis of MN cell body position and dendrite patterns, spinal cords were embedded in gelatin before floating sections on a Leica vibratome at 100μm thickness were generated and incubated with antibodies. Cryostat sections were processed for immunohistochemistry as described (Arber et al., 2000a) using fluorophore-conjugated secondary antibodies (Invitrogen and Jackson Laboratories). Signal intensity of GFP expression in proprioceptive afferents innervating muscles in $PV^{Cre}/Tau^{Lox\text{-}Stop\text{-}Lox\text{-}mGFP}$ mice was amplified using an antibody to reconstruct the peripheral innervation pattern. LacZ whole-mount staining was performed as described (Livet et al., 2002). Images were collected on an Olympus confocal or dissection microscope. Quantification of dendrite projection patterns was performed using Image J 1.35f Software (NIH) to measure the extent of dendritic projections in three dimensions (comparative to 100% of the diagonal, medio-lateral or dorso-ventral dimension of outer borders of the hemisected spinal cord). Colocalization of dextran-filled afferents with $vGlut1^{+}$ terminals was analyzed using Imaris (Version 4.20; colocalization plugin) and colocalization was displayed in separate colors.

Figures, Table and Supplemental Figures

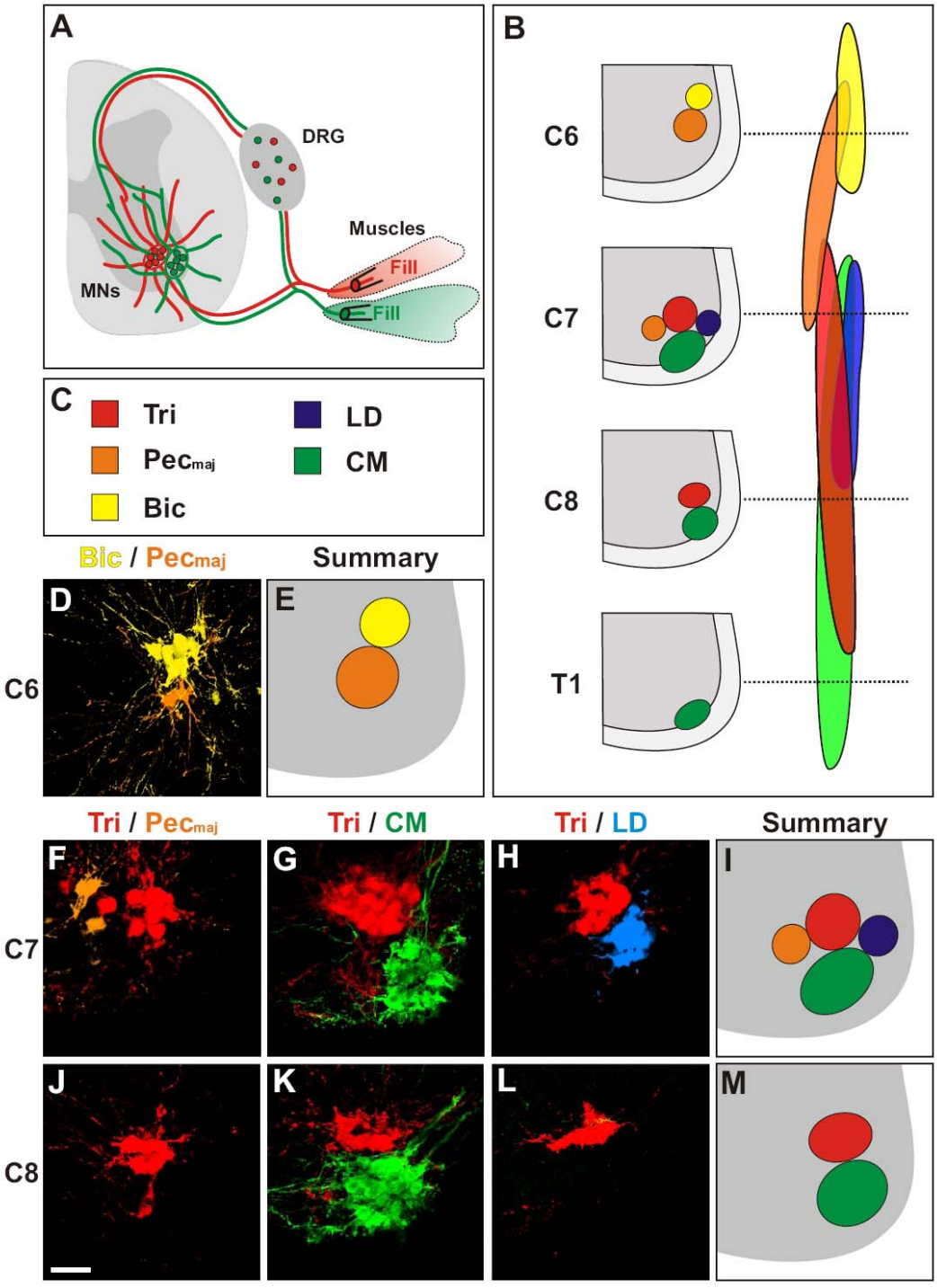

Figure 1. Cell body positions of cervical MN pools in the mouse spinal cord

(A) Schematic diagram depicting retrograde tracing technique used in this study. Fluorescently labeled dextran dyes were applied to the cut ends of individual muscle nerves in the periphery (fill) to trace MN cell bodies and dendrites.

(B, C) Schematic representation depicting transverse and top-down longitudinal view of MN pools at C6-T1 levels of the mouse spinal cord (rostral: top, caudal: bottom). MN pools are shown in colors (Tri: red; Pec_{maj}: orange; Bic: yellow; LD: blue; CM: green).
(D, E) Transverse sections of Bic and Pec_{maj} MN pools at C6 upon retrograde labeling (D) or as summary diagram (E).
(F-M) Transverse sections of MN pools at C7 (F-I) and C8 (J-M) shown upon retrograde labeling (F-H; J-L) or as summary diagrams (I, M).
Scale bar = 50μm.

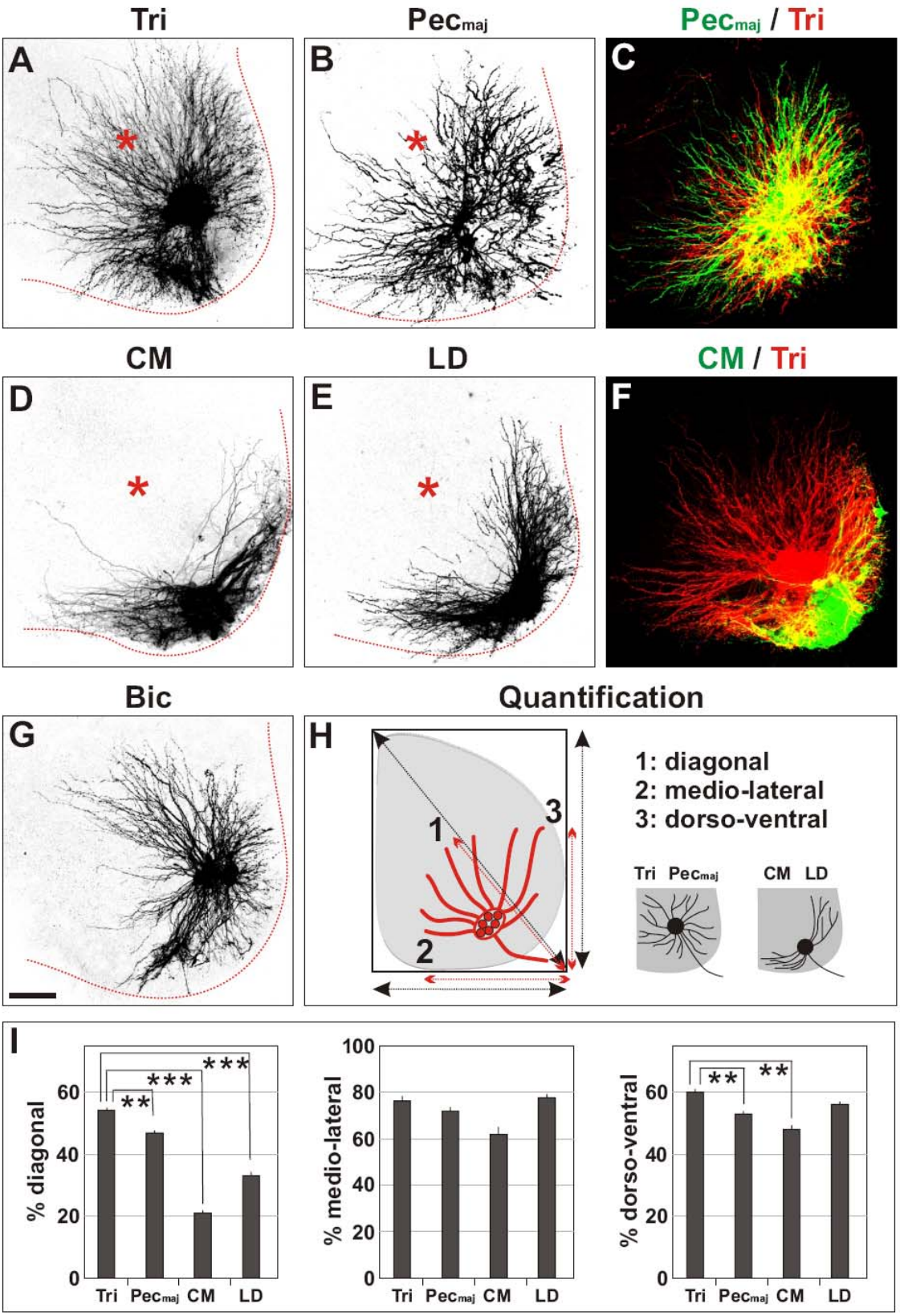
Tri
Pecmaj
Pecmaj / Tri
A
B
C
CM
LD
CM / Tri
D
E
F
Bic
Quantification
G
H
1: diagonal
2: medio-lateral
3: dorso-ventral
Tri Pecmaj
CM LD
I
% diagonal
% medio-lateral
% dorso-ventral
Tri Pecmaj CM LD

Figure 2. Correlation between MN pool cell body position and dendrite pattern

(A-G) Analysis of dendrite patterns of different MN pools in the neonatal mouse cervical spinal cord revealed by retrograde tracing from peripheral nerves. Note dendritic overlap (C: Pec_{maj}, green; Tri, red) or lack thereof (F: CM, green; Tri, red) between different MN pools (red dotted lines: ventral spinal cord, red asterisks: central grey matter).

(H, I) Quantification of elaboration of dendritic trees of different MN pools. Values are given as percentage of dimensions defined by outer borders of hemisected spinal cord (% of diagonal (1), medio-lateral (2) or dorso-ventral (3) dimension; ** $p \leq 0.01$, *** $p \leq 0.001$; error bars: SEM).

Scale bar = 100μm.

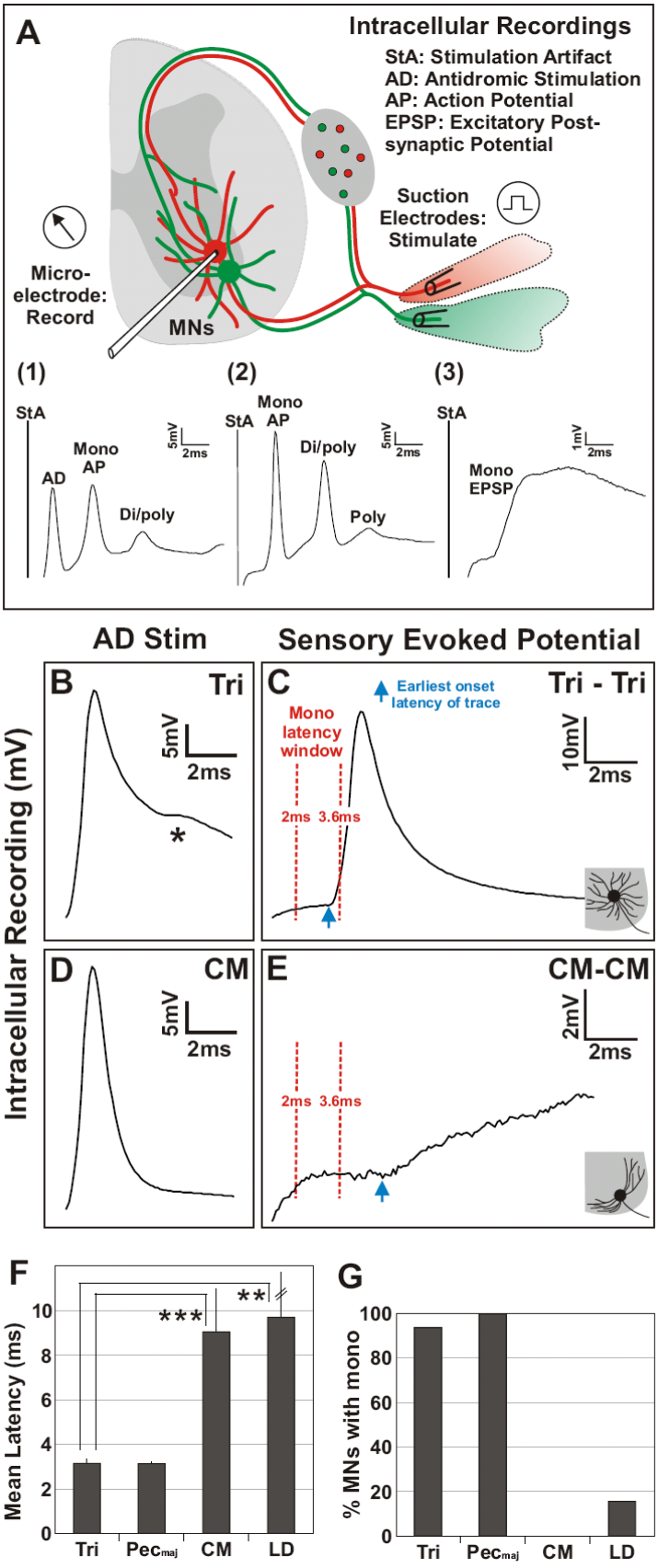
A
Intracellular Recordings
StA: Stimulation Artifact
AD: Antidromic Stimulation
AP: Action Potential
EPSP: Excitatory Post-synaptic Potential
Suction Electrodes: Stimulate
Micro-electrode: Record
MNs
(1)
(2)
(3)
StA
AD
Mono AP
Di/poly
Poly
Mono EPSP
5mV
2ms
1mV
AD Stim
Sensory Evoked Potential
Intracellular Recording (mV)
B
Tri
C
Earliest onset latency of trace
Tri - Tri
Mono latency window
2ms 3.6ms
10mV
D
CM
E
CM-CM
2mV
F
Mean Latency (ms)
***
**
Tri
Pecmaj
CM
LD
G
% MNs with mono

Figure 3. Correlation between MN pool dendrite patterns and IaPA connectivity

(A) Diagram of intracellular recording technique for analysis of sensory-motor connectivity. Three representative traces illustrate different responses recorded using this preparation: (1) MNs are identified on the basis of their peripheral projections using antidromic stimulation (AD response). (2) and (3) depict traces after failure of AD response (2), in the presence (2) or absence (3) of an action potential (AP), revealing a pure EPSP of monosynaptic latency. Stimulation artifact (StA) is present in all three traces, but is cut off in subsequent traces.

(B-E) Intracellular recording experiments from Tri or CM MN identified by antidromic stimulation and followed by sensory evoked responses upon Tri or CM nerve stimulation. Asterisk in (B) shows slow decay of potential due to the underlying sensory evoked response. Red dashed lines depicts expected monosynaptic latency window.

(F) Mean latency ($\pm$SEM) recorded from MN pools after homonymous muscle nerve stimulation (** $p \leq 0.01$, *** $p \leq 0.001$). SEM of LD-LD: mean latency exceeds the scale, indicated by double line in the graph (9.7 ± 5.2ms).

(G) % MNs within a particular MN pool receiving monosynaptic homonymous sensory evoked input.

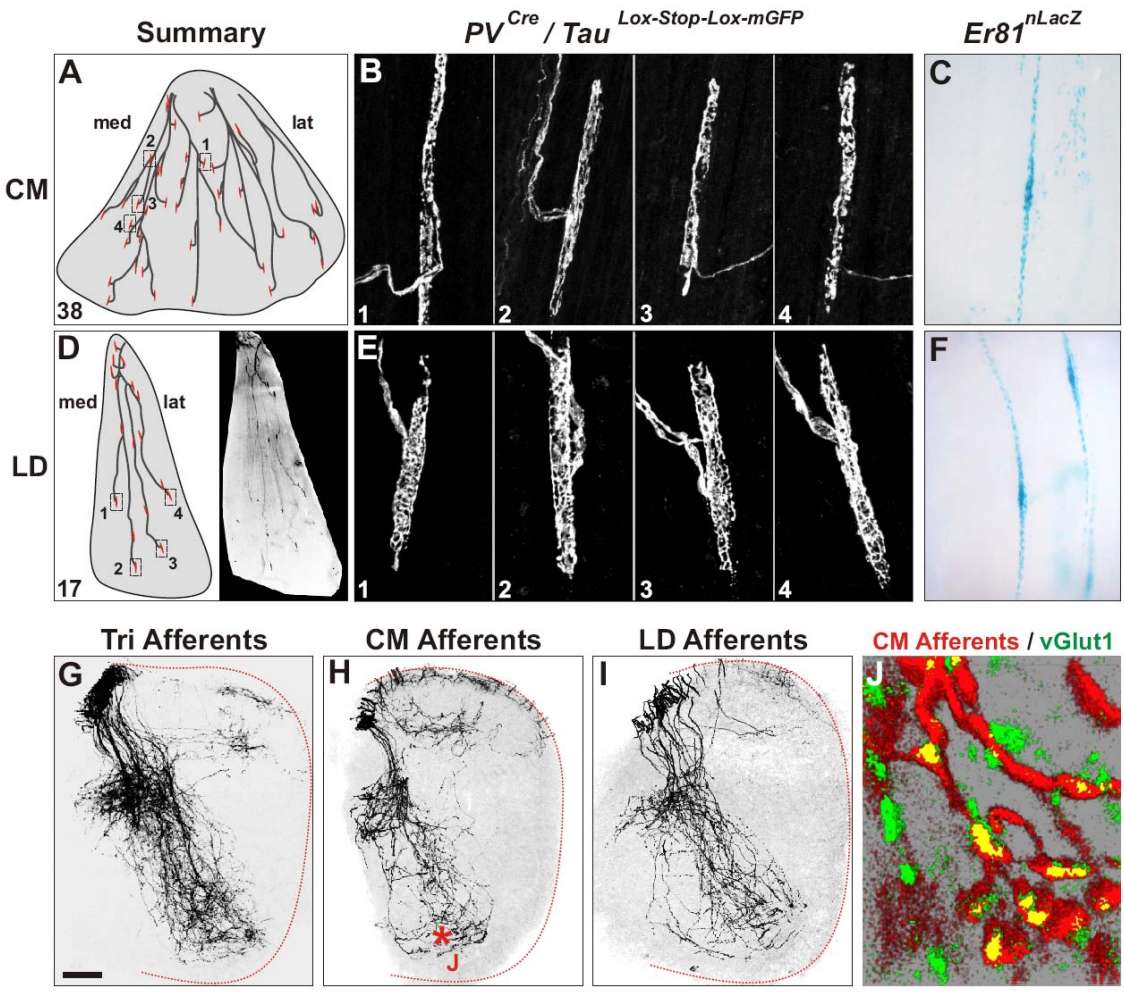

Figure 4. CM and LD IaPA projection patterns

(A-F) Analysis of innervation of CM and LD muscle spindles. Camera lucida drawing of innervation of representative CM (A: 38 muscle spindles) and LD (D: 17 muscle spindles; right depicts low power view of fluorescent primary data) muscle in $PV^{Cre}/Tau^{Lox\text{-}Stop\text{-}Lox\text{-}mGFP}$ mice. High power images of the innervation of four muscle spindles (1-4; boxes in A and D) are shown in (B, E) and *Er81* expression in intrafusal muscle fibers of CM and LD muscle spindles in $Er81^{nLacZ}$ mice is shown in (C, F).

(G-J) Visualization of central trajectory of SAs as revealed by transganglionic retrograde tracing from identified muscle nerves. (J) shows a high power image of labeled CM IaPAs (red) taken from the ventral spinal cord (see H) and colabeled with vGlut1 (green). (colocalization = yellow).

Scale bar: (B, E) =30µm; (C, F) = 75µm; (G-I) = 100µm; J=2.4µm.

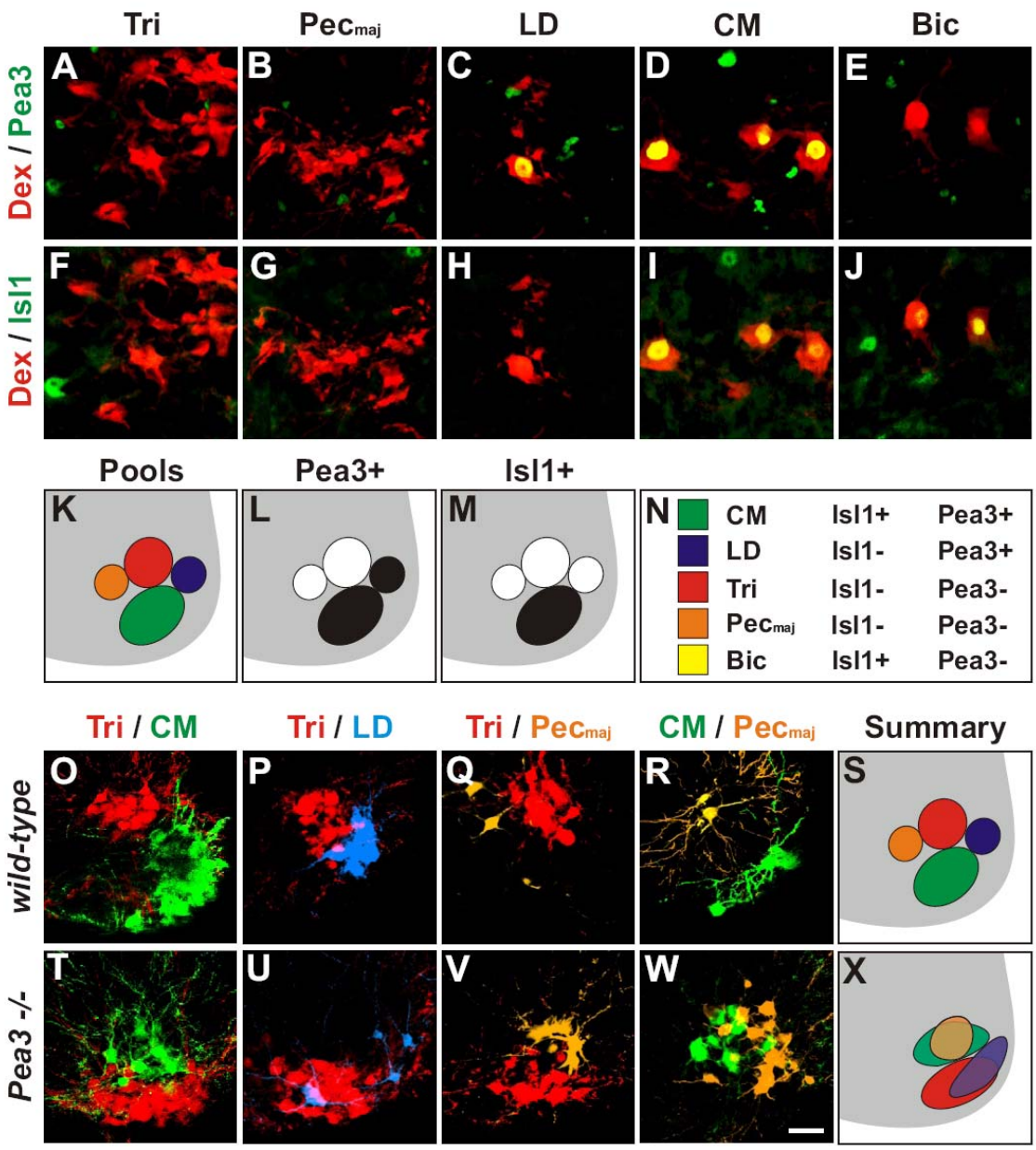

Figure 5. *Pea3* mutant mice exhibit selective defects in MN pool cell body positioning

(A-J) Analysis of *Pea3* by virtue of LacZ expression in *Pea3*$^{+/-}$ mice (A-E: green) and Isl1 (F-J: green) expression in neonatal MN pools by retrograde tracing (Dex: red).

(K-N) Summary diagrams depicting expression of Pea3 and Isl1 in different cervical MN pools. Note selective expression of Pea3 in CM and LD MN pools.

(O-X) Transverse sections of MN pools in wild-type (O-S) and *Pea3*$^{-/-}$ (T-X) mice shown upon retrograde labeling (O-R, T-W) or as summary diagrams (S, X). Note that in *Pea3*$^{-/-}$ mice, CM and Pec_{maj} (W) as well as Tri and LD (U) cell bodies are intermingled.
Scale bar: (A-J) = 20μm; (O-R, T-W) = 50μm.

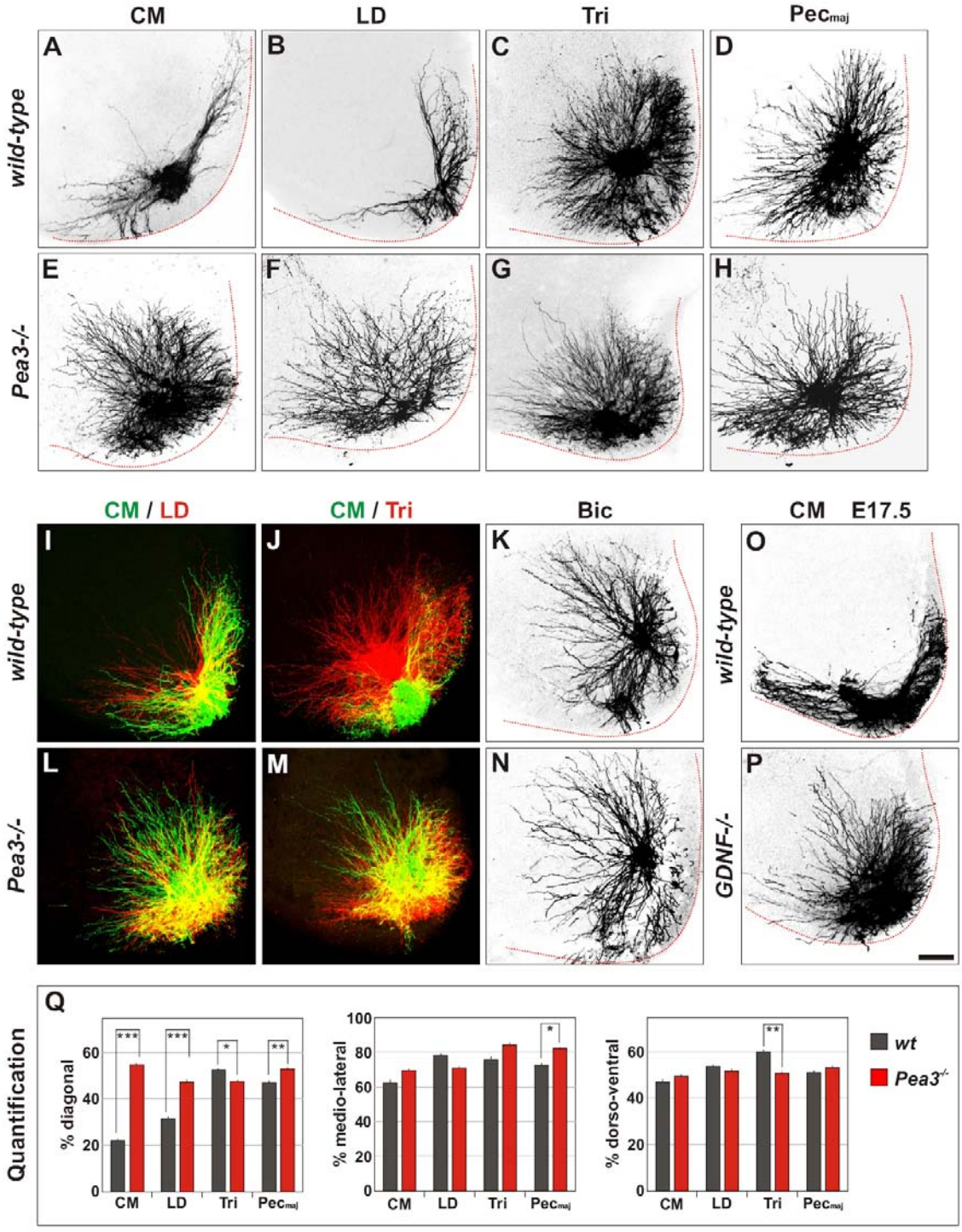

Figure 6. Alteration in MN pool specific dendrite patterning in *Pea3* mutant mice

(A-N) Dendrite patterns of different MN pools in neonatal wild-type (A-D, I-K) and *Pea3*$^{-/-}$ (E-H, L-N) mice.

(O, P) Comparison of CM MN pool dendrites in E17.5 wild-type and *GDNF* mutant mice.

(Q) Quantification of elaboration of dendritic trees of different MN pools (see Figure 2H; * $p \leq 0.05$, ** $p \leq 0.01$ and *** $p \leq 0.001$).

Scale bar = 100μm.

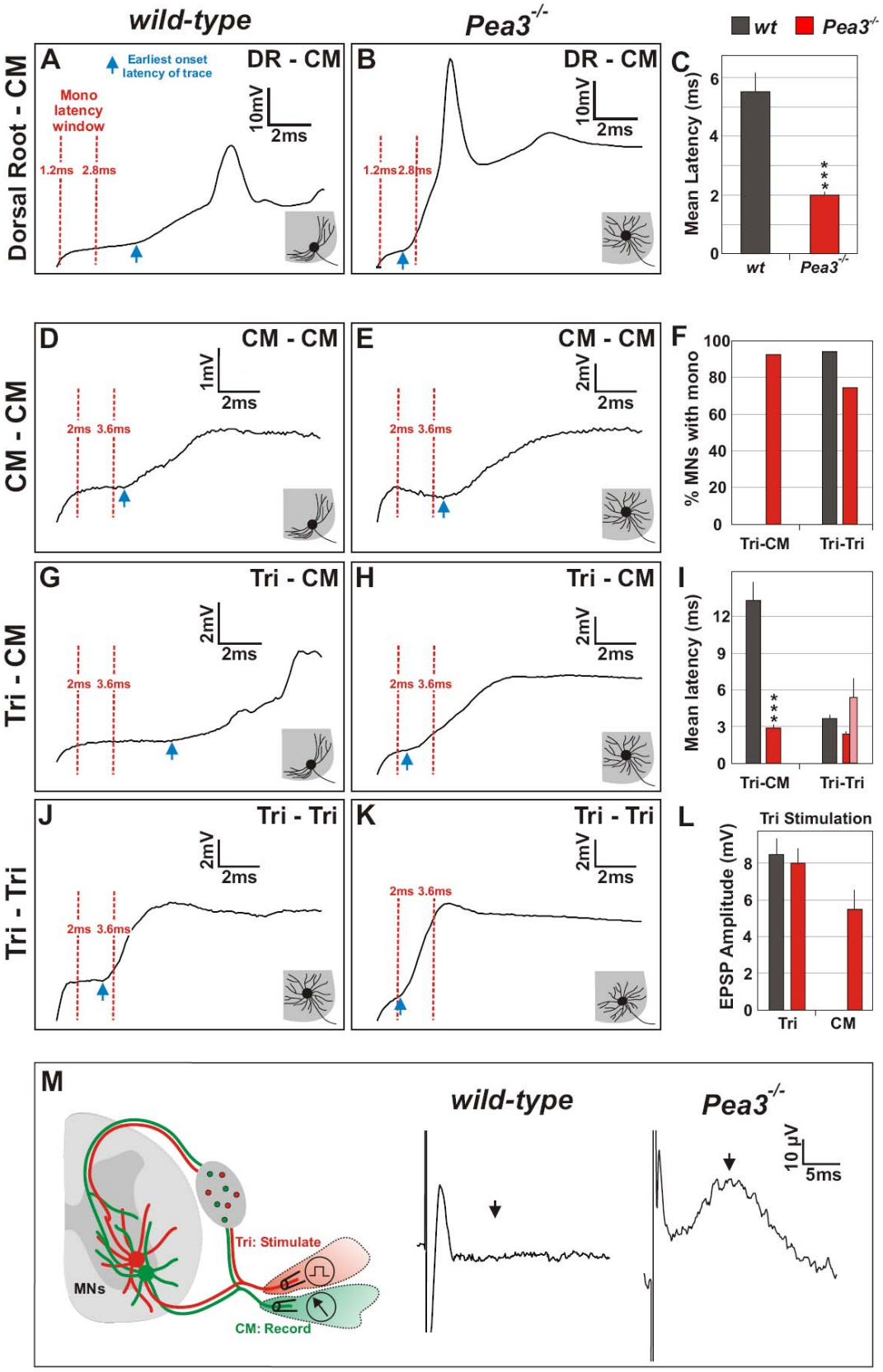
wild-type
Pea3-/-
wt
Pea3-/-
Dorsal Root - CM
A
Earliest onset latency of trace
Mono latency window
1.2ms 2.8ms
DR - CM
10mV
2ms
B
DR - CM
1.2ms 2.8ms
10mV
2ms
C
Mean Latency (ms)
0
2
4
6
***
wt
Pea3-/-
CM - CM
D
CM - CM
1mV
2ms
2ms 3.6ms
E
CM - CM
2mV
2ms
2ms 3.6ms
F
% MNs with mono
0
20
40
60
80
100
Tri-CM
Tri-Tri
Tri - CM
G
Tri - CM
2mV
2ms
2ms 3.6ms
H
Tri - CM
2mV
2ms
2ms 3.6ms
I
Mean latency (ms)
0
3
6
9
12
***
Tri-CM
Tri-Tri
Tri - Tri
J
Tri - Tri
2mV
2ms
2ms 3.6ms
K
Tri - Tri
2mV
2ms
2ms 3.6ms
L
Tri Stimulation
EPSP Amplitude (mV)
0
2
4
6
8
Tri
CM
M
MNs
Tri: Stimulate
CM: Record
wild-type
Pea3-/-
10 µV
5ms

Figure 7. Changes in dendrite pattern in *Pea3* mutant mice are paralleled by defects in sensory-motor connectivity

(A-C) CM MNs recorded intracellularly in wild-type or *Pea3*$^{-/-}$ mice upon DR stimulation and quantification of mean latency (±SEM; *** $p \leq 0.001$).

(D-L) Individual EPSP traces and quantification of intracellular recordings from CM and Tri MNs upon CM or Tri muscle nerve stimulation. (I) Tri MNs in *Pea3*$^{-/-}$ mice were divided into MNs with (red) or without (light red) monosynaptic input (±SEM; *** $p \leq 0.001$).

(M) Responses recorded extracellularly from CM muscle nerves upon stimulation of Tri muscle nerves in wild-type and *Pea3*$^{-/-}$ mice. Scheme depicting experimental setup (left) and representative traces recorded (right; arrows: peak of short latency responses).

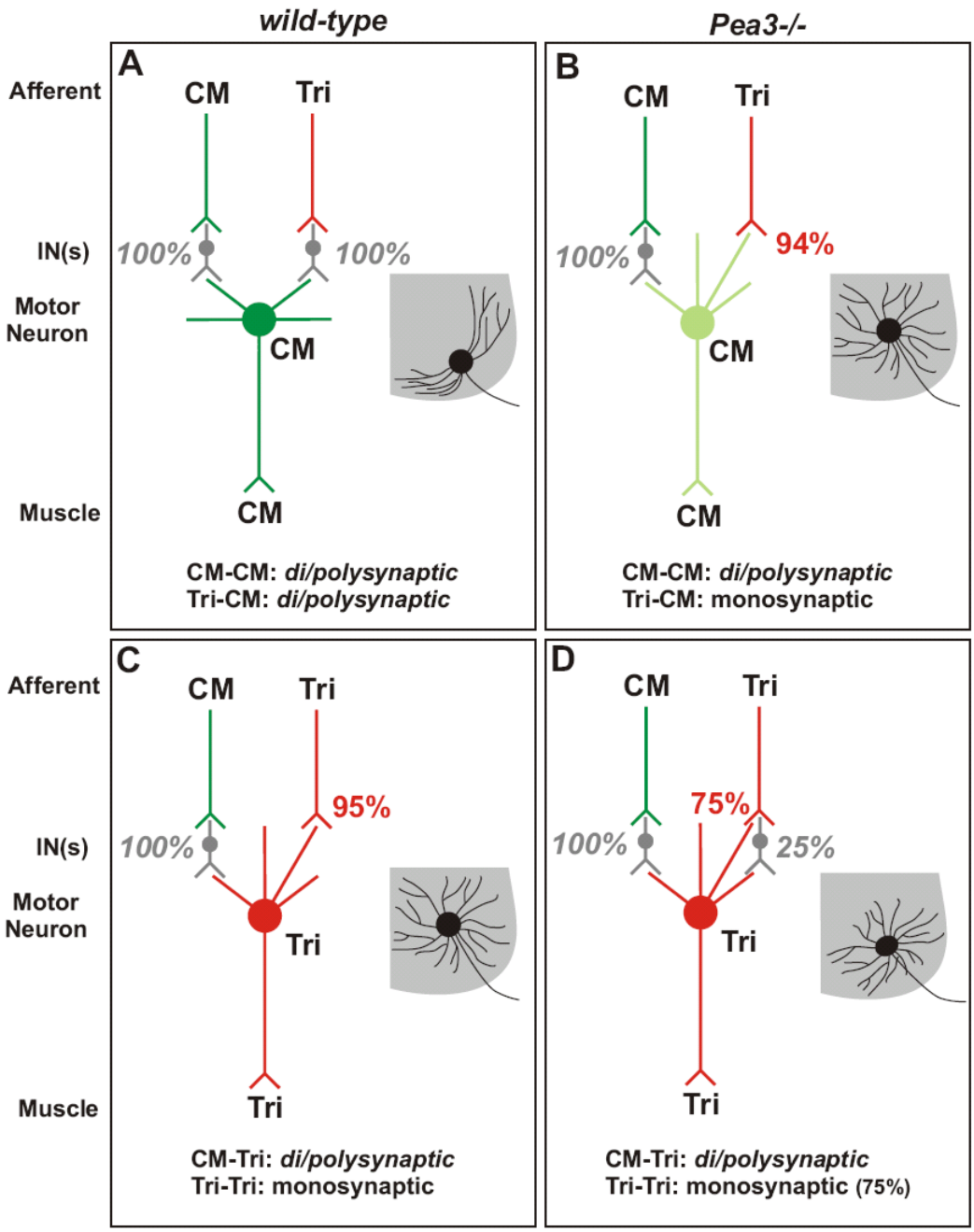

Figure 8. *Pea3* controls MN dendrite pattern and sensory-motor connectivity in defined MN pools

Diagrams depicting putative neuronal pathways leading to earliest onset latency EPSPs in CM and Tri MNs of wild-type and *Pea3*$^{-/-}$ mice (% of MNs responding with monosynaptic latency shown in red and MNs responding with di- or polysynaptic latency displayed in grey italics). Only MNs responding to sensory stimulation are shown. CM

IaPAs and MNs are shown in green, Tri IaPAs and MNs in red, MN dendrite patterns in schematic grey drawings and interneurons (IN) in grey.

(A, C) In wild-type mice, CM MNs display dendrites avoiding the central grey matter and respond to sensory stimulation with di- or polysynaptic latency (A). In contrast, Tri MNs exhibit radial dendrites and receive monosynaptic connections from Tri but not CM IaPAs (C).

(B, D) In *Pea3*$^{-/-}$ mice, CM MNs (light green) display a radial dendrite pattern similar to Tri MNs in wild-type and respond monosynaptically to sensory stimulation of Tri SAs but not CM SAs (B). In contrast, Tri MNs display radial dendrites despite the change in cell body position, and 75% of Tri MNs still receive monosynaptic connections from Tri SAs (D).

MN Recording		Triceps (Muscle Nerve Stimulated)			
		% MNs mono	Mono latency (ms)	Di/poly latency (ms)	Pamp (mV)
Triceps	*wt*	95% (22)	3.3±0.2 (21)	19.4 (1)	8.5±0.8
	Pea3$^{-/-}$	75% (44)	2.6±0.1 (33)	5.4±1.1 (8)	8.0±0.8
CM	*wt*	0% (21)	–	11.0±1.1 (20)	–
	Pea3$^{-/-}$	94% (17)	2.9±0.1 (16)	4.7 (1)	5.7±1.0
LD	*wt*	0% (3)	–	5.1±1.1 (2)	–
	Pea3$^{-/-}$	85% (13)	2.7±0.1 (11)	5.2±0.1 (2)	8.1±1.0

MN Recording		Pec_{maj} (Muscle Nerve Stimulated)			
		% MNs mono	Mono latency (ms)	Di/poly latency (ms)	Pamp (mV)
Triceps	*wt*	25% (4)	3.6 (1)	11.3±3.0 (3)	1.0
	Pea3$^{-/-}$	33% (12)	2.7±0.1 (4)	6.7±0.9 (6)	4.0±1.1
Pec_{maj}	*wt*	100% (3)	3.2±0.1 (3)	–	4.7±0.5
	Pea3$^{-/-}$	75% (4)	3.1±0.3 (3)	3.8 (1)	2.0±0.5
CM	*wt*	0% (4)	–	14.4±9.2 (2)	–
	Pea3$^{-/-}$	66% (3)	2.9±0.3 (2)	4.6 (1)	3.0

MN Recording		CM (Muscle Nerve Stimulated)			
		% MNs mono	Mono latency (ms)	Di/poly latency (ms)	Pamp (mV)
Triceps	*wt*	0% (6)	–	9.0±1.6 (4)	–
	Pea3$^{-/-}$	0% (22)	–	15.3±1.6 (9)	–
CM	*wt*	0% (25)	–	8.8±1.9 (13)	–
	Pea3$^{-/-}$	0% (18)	–	19.9±2.3 (9)	–
LD	*wt*	0% (2)	–	4.9±0.2 (2)	–
	Pea3$^{-/-}$	0% (9)	–	17.0±1.5 (6)	–

MN Recording		LD (Muscle Nerve Stimulated)			
		% MNs mono	Mono latency (ms)	Di/poly latency (ms)	Pamp (mV)
Triceps	*wt*	9% (11)	3.1 (1)	21.6±8.9 (9)	11.6
	Pea3$^{-/-}$	0% (16)	–	12.4±2.4 (9)	–
CM	*wt*	0% (15)	–	12.8±1.6 (11)	–
	Pea3$^{-/-}$	0% (11)	–	17.1±2.9 (7)	–
LD	*wt*	17% (6)	2.6 (1)	9.7±5.2 (3)	8.3
	Pea3$^{-/-}$	0% (13)	–	16.5±3.0 (6)	–

Table 1. Summary of intracellular physiology results

Table listing values from intracellular recordings of Tri, Pec_{maj}, CM and LD MNs in wild-type and *Pea3* mutant mice. Individual columns list percentages of MNs receiving

sensory input at monosynaptic latency, values for monosynaptic latency, values for di- or polysynaptic latency (for MNs not receiving inputs at monosynaptic latency), and peak amplitude for MNs receiving input at monosynaptic latency. Numbers in parentheses equal numbers of MNs recorded in each case.

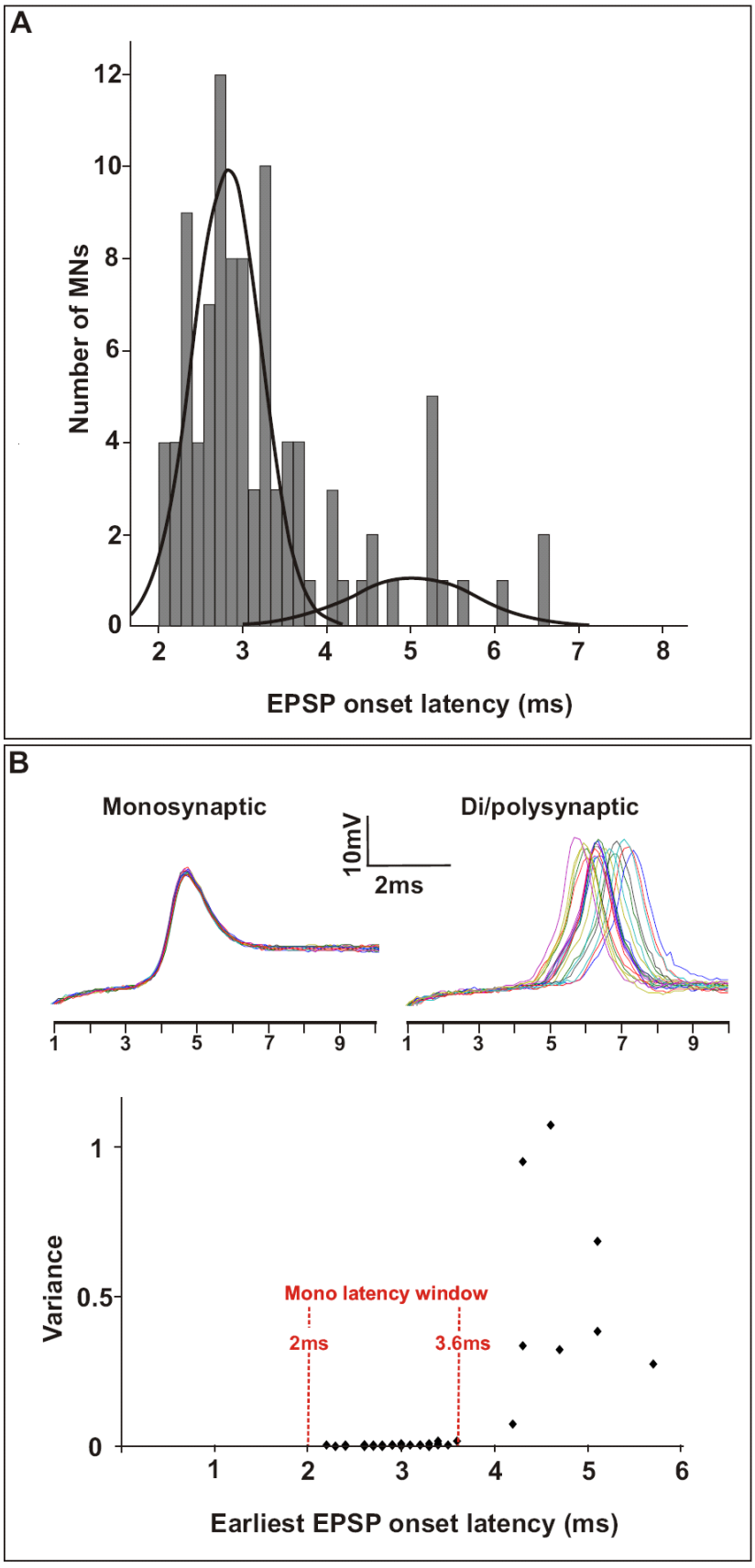
A
Number of MNs
EPSP onset latency (ms)
B
Monosynaptic
Di/polysynaptic
10mV
2ms
Variance
Mono latency window
2ms
3.6ms
Earliest EPSP onset latency (ms)

Supplemental Figure 1. Definition of monosynaptic latency for intracellular recordings

(A) Plot showing homonymous monosynaptic EPSP latencies recorded at cervical spinal cord levels in this study (number of MNs vs EPSP onset latency in ms is shown). Normalized distributions of two clustered datasets define MNs which receive inputs with monosynaptic latency (left) and MNs which receive inputs with di- or polysynaptic latency (right). The monosynaptic latency window is defined as mean latency of normalized distribution $\pm$2 SD (2.8$\pm$0.8ms). This plot only includes di- and polysynaptic inputs recorded with latencies shorter than 8ms.

(B) 20 individual traces depicted in different colors recorded upon muscle nerve stimulation from a representative MN receiving monosynaptic input (left) and a MN receiving only di- or polysynaptic input (right). Note jitter in the onset latency for traces of MN with di- or polysynaptic connections. Data points indicate variance of EPSP onset latencies recorded in individual MNs and defined monosynaptic latency window is indicated by red dotted lines.

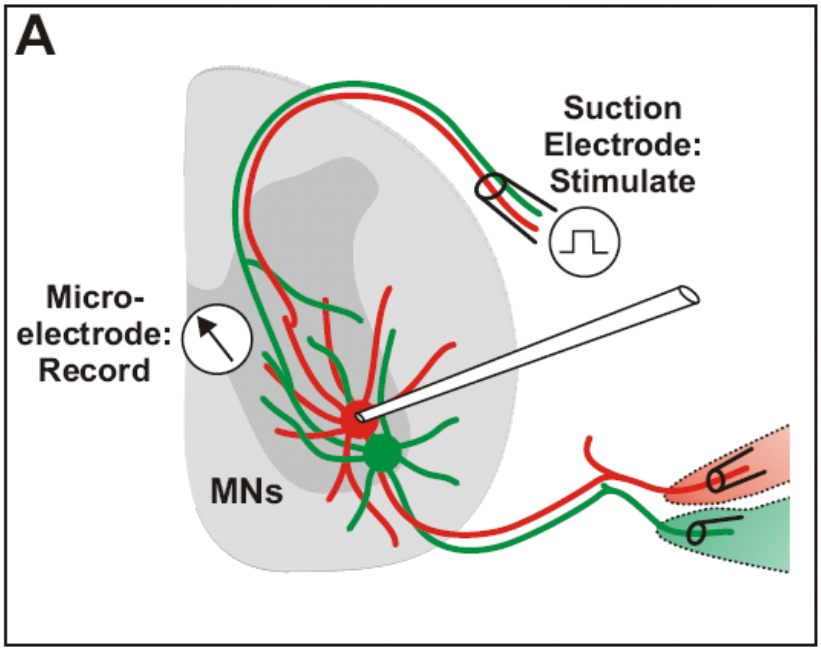

Dorsal Root Stimulation

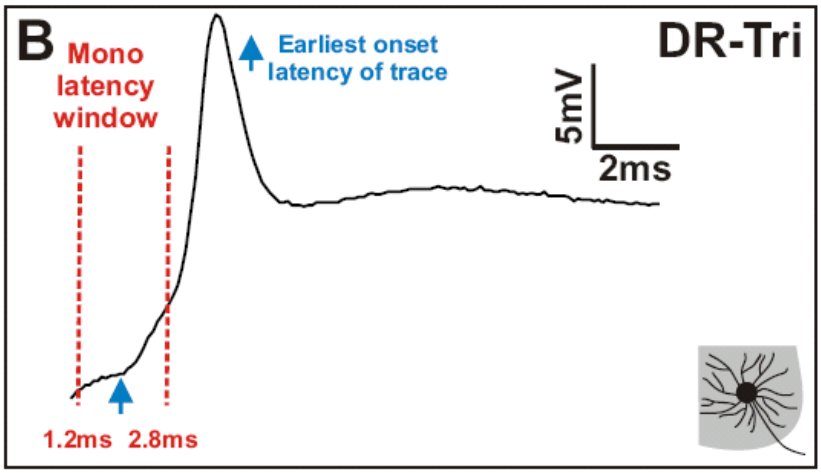

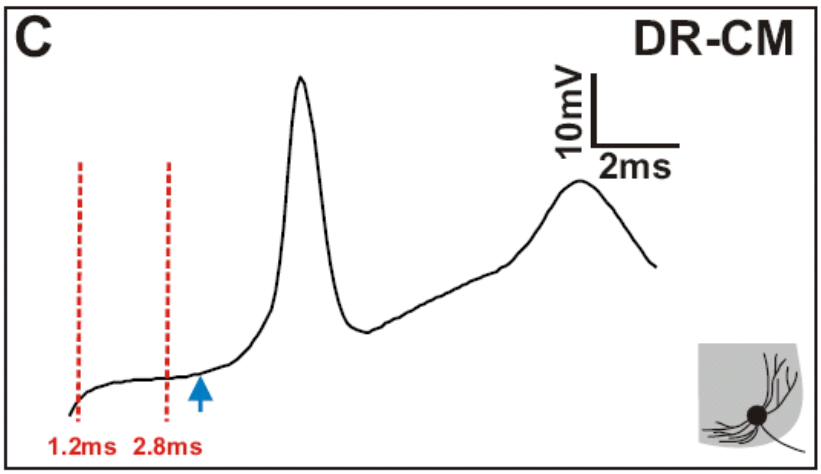

Supplemental Figure 2. Dorsal root stimulation does not elicit monosynaptic responses in CM MNs

(A) Schematic diagram depicting intracellular recording technique for analysis of sensory-motor connectivity upon dorsal root stimulation in an early postnatal mouse spinal cord preparation. Suction electrodes applied to dorsal roots are used as stimulation electrodes and microelectrodes within the ventral spinal cord to record intracellularly from MNs upon identification of peripheral muscle target by antidromic stimulation.

(B, C) Traces recorded during intracellular recording experiments from Tri (B) or CM (C) MN upon dorsal root (DR) stimulation (traces with action potential are shown). Red dashed lines depict expected monosynaptic latency window. Schematic drawing in bottom right corners illustrate dendrite pattern of corresponding MN pool as determined in Figure 2.

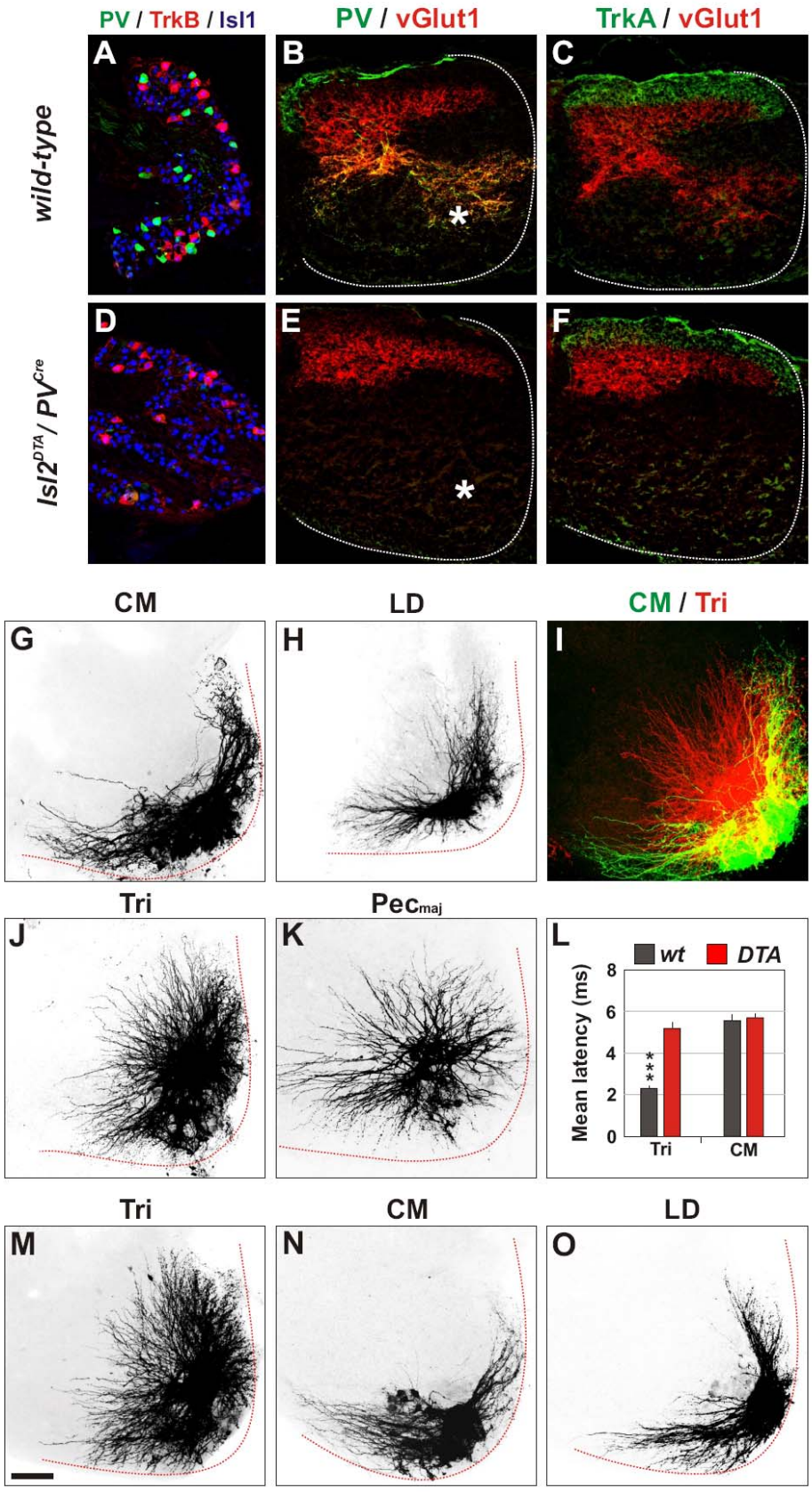
PV / TrkB / Isl1
PV / vGlut1
TrkA / vGlut1
wild-type
Isl2DTA / PVCre
A
B
C
D
E
F
CM
LD
CM / Tri
G
H
I
Tri
Pecmaj
J
K
L
wt
DTA
Mean latency (ms)
8
6
4
2
0
***
Tri
CM
Tri
CM
LD
M
N
O

Supplemental Figure 3. PAs are not involved in MN dendrite patterning

(A-F) Immunohistochemical analysis revealing the selective absence of PV^{+} DRG neurons (A, D) or central PA projections (B, C, E, F) in $Isl2^{DTA}/PV^{Cre}$ mice (D-F) when compared to wild-type (A-C) at P0. (A, D) shows DRG stained for PV (green), TrkB (red) and Isl1 (blue). (B, C, E, F) depicts DRG SA projections in the spinal cord (outlined by white dotted line) stained for vGlut1 (red), PV (B, E: green) and TrkA (C, F: green). Termination zone of PAs in the ventral spinal cord is absent in $Isl2^{DTA}/PV^{Cre}$ mice (white asterisk).

(G-K) Analysis of dendrite patterns of MN pools in $Isl2^{DTA}/PV^{Cre}$ mice revealed by retrograde tracing from peripheral nerves.

(L) Quantification of mean latency recorded from Tri and CM MNs upon dorsal root stimulation. In the absence of PAs (DTA, red), Tri MNs do not receive inputs at monosynaptic latency as they do in wild-type (wt, grey). In contrast, elimination of PAs does not influence the onset latency to CM MNs. Error bars represent standard error of the mean (SEM). Level of significance is indicated (*** $p \leq 0.001$).

(M-O) Analysis of dendrite patterns of MN pools in P0 $TrkC^{-/-}$ mice revealed by retrograde tracing from peripheral nerves.

Scale bar: (A, D) = 80μm; (B, C, E, F) = 160μm; (G-K) = 100μm.

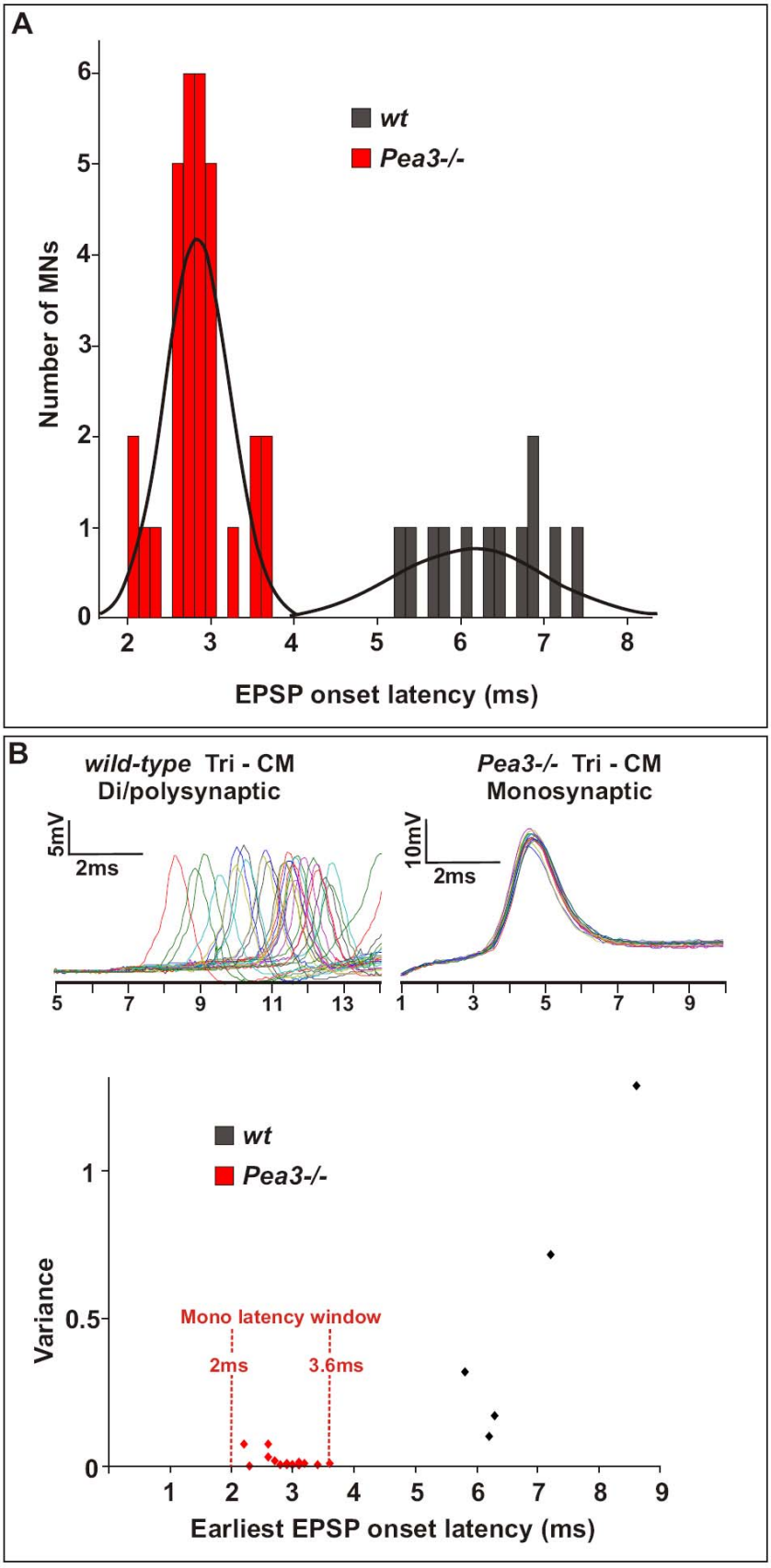
A
wt
Pea3-/-
Number of MNs
EPSP onset latency (ms)
B
wild-type Tri - CM
Di/polysynaptic
Pea3-/- Tri - CM
Monosynaptic
5mV
2ms
10mV
2ms
wt
Pea3-/-
Mono latency window
2ms
3.6ms
Variance
Earliest EPSP onset latency (ms)

Supplemental Figure 4. Latency analysis in *Pea3* mutant mice

(A) Plot depicting CM and LD MNs analyzed in *Pea3* mutant (red) and wild-type (grey) mice after either Tri or Pec_{maj} muscle nerve stimulation (number of MNs vs EPSP onset latency in ms is shown). Cluster analysis revealed the presence of two clusters precisely correlating with MNs recorded from in *Pea3* mutants (short latency inputs; latency window: 2.8±0.8ms; left) and wild-type (right). Normalized distribution of two clusters is shown. EPSPs with onset latencies longer then 8ms are excluded from this plot.

(B) 20 individual traces depicted in different colors recorded upon muscle nerve stimulation from a representative CM MN after Tri muscle nerve stimulation in wild-type (left) or *Pea3* mutant (right) mice. Data points indicate variance of EPSP onset latencies recorded in individual MNs and defined monosynaptic latency window is indicated by red dotted lines. Note that *Pea3* mutant CM MNs receive inputs at monosynaptic latencies and show essentially no variance in onset latency.

Chapter 3

A developmental switch in the response of DRG neurons to ETS transcription factor signaling

Simon Hippenmeyer, Eline Vrieseling, Markus Sigrist, Thomas Portmann, Celia Laengle, David R. Ladle, and Silvia Arber

PLoS Biol 3(5): e159, 2005

Abstract

Two ETS transcription factors of the Pea3 subfamily are induced in subpopulations of dorsal root ganglion (DRG) sensory and spinal motor neurons by target-derived factors. Their expression controls late aspects of neuronal differentiation such as target invasion and branching. Here, we show that the late onset of ETS gene expression is an essential requirement for normal sensory neuron differentiation. We provide genetic evidence in the mouse that precocious ETS expression in DRG sensory neurons perturbs axonal projections, the acquisition of terminal differentiation markers and their dependence on neurotrophic support. Together, our findings indicate that DRG sensory neurons exhibit a temporal developmental switch that can be revealed by distinct responses to ETS transcription factor signaling at sequential steps of neuronal maturation.

Introduction

Neuronal differentiation is a protracted process during which newly-generated neurons express distinct cellular and molecular programs at precise times during their maturation: long-distance axon outgrowth, subsequent terminal branching and finally synaptogenesis. Many important aspects of neuronal character appear to be acquired through the expression of transcription factors at progenitor cell stages, whereas others depend on expression immediately upon cell cycle exit (Edlund and Jessell, 1999). But whether the orderly expression and activity of transcriptional programs at much later developmental stages, well after cell cycle exit, is an essential step in the progression of neuronal differentiation and circuit assembly has yet to be resolved.

The differentiation of sensory neurons of the dorsal root ganglia (DRG) has been studied extensively with respect to inductive events that specify neuronal fate (Anderson et al., 1997; Knecht and Bronner-Fraser, 2002), as well as the involvement of late target-derived neurotrophic factors in the control of neuronal survival (Huang and Reichardt, 2001). Recent evidence has begun to emerge that target-derived factors are also involved in regulating later aspects of neuronal differentiation (Bibel and Barde, 2000; Markus et al., 2002a; Mendell et al., 2001). In particular, genetic experiments have addressed the survival-independent role of neurotrophic factors during development by exploiting strains of mice defective both in neurotrophin signaling and in the function of the proapoptotic gene *Bax* (Patel et al., 2000; Patel et al., 2003). These studies, for example, have revealed that neurotrophin signaling controls the acquisition of peptidergic traits in nociceptive DRG neurons and the control of target innervation (Patel et al., 2000; Patel et al., 2003).

The onset of some transcriptional programs in neurons, however, has also been shown to occur long after neurons exit the cell cycle. An emerging principle from work in Drosophila and vertebrates is that target-derived factors play a crucial role in the induction of these transcriptional programs (Hippenmeyer et al., 2004). In Drosophila, retrograde BMP signals from the target region control the terminal differentiation of a

subpopulation of peptidergic neurons expressing apterous and squeeze (Allan et al., 2003; Marques et al., 2003). In vertebrates, peripheral neurotrophic signals have been shown to direct the onset of expression of the ETS transcription factors Er81 and Pea3 in DRG sensory neurons and motor neuron pools several days after these neurons have become post-mitotic (Arber et al., 2000a; Haase et al., 2002; Lin et al., 1998a; Livet et al., 2002; Patel et al., 2003). Moreover, the induction of Er81 expression in proprioceptive afferents is known to be mediated by peripheral neurotrophin 3 (NT-3) (Patel et al., 2003). These two ETS proteins control late aspects of spinal monosynaptic circuit assembly: with Er81 directing proprioceptive sensory neuron, and Pea3 motor neuron pool differentiation, respectively (Arber et al., 2000a; Livet et al., 2002). In particular, in the absence of *Er81,* achieved by mutation in the gene or by deprivation of peripheral neurotrophin signaling, group Ia proprioceptive afferents fail to invade the ventral spinal cord and to make effective synaptic connections with motor neurons (Arber et al., 2000a; Patel et al., 2003).

The involvement of target-derived signals in induction of ETS transcription factor expression raises the question of the necessity for the observed delay in the onset of ETS signaling for neuronal maturation. Would precocious expression of ETS proteins in post-mitotic neurons also direct the appropriate sensory neuron developmental programs? In this study, we have used mouse genetics to test this general idea, by investigating whether the timing of onset of ETS transcription factor signaling is essential for normal sensory neuron development. We have assessed the biological effects of inducing ETS signaling either at the correct developmental time, or precociously. We find that within proprioceptive sensory neurons, the late onset of ETS signaling is essential for the establishment of normal sensory afferent projections in the spinal cord. Precocious initiation of ETS signaling in post-mitotic DRG neurons leads to abnormal DRG neuron differentiation characterized by neurotrophin-independent neurite outgrowth and inappropriate profiles of gene expression. Our findings reveal that target-triggered inductive signals provide an effective means of ensuring the late onset of expression of transcription factors, and thus an orderly temporal transcriptional sequence that is crucial for neuronal maturation and circuit assembly.

Results

To test the hypothesis that a temporal delay in the onset of transcriptional programs is crucial for the control of appropriate neuronal maturation, we studied the development of proprioceptive DRG neurons, since transcriptional effectors regulated by target-derived signals, as well as some of their downstream biological actions have been identified. Er81 controls proprioceptive afferent connectivity (Arber et al., 2000a), and we therefore sought to identify an ETS transcriptional regulator which when expressed over the normal time course of Er81 expression, is able to substitute for Er81 function within group Ia afferent sensory neurons. With this reference point, we then designed experiments to examine the effects of precocious post-mitotic expression of the same ETS transcription factor on sensory neuron differentiation.

EWS-Pea3 can replace *Er81* function in controlling Ia afferent projections

We first defined an ETS transcription regulator that is able to replace the function of Er81 within proprioceptive afferents to direct projections into the ventral spinal cord. Er81, Pea3 and Erm constitute the Pea3 subfamily of ETS transcription factors, show a high degree of amino acid identity and bind to very similar DNA target sequences (Bojovic and Hassell, 2001; de Launoit et al., 1997; Mo et al., 1998). Nevertheless, when introduced into the *Er81* locus in analogy to a previously used targeting strategy (data not shown; (Arber et al., 2000a)), neither *Pea3* nor *Erm* could rescue Ia proprioceptive afferent projections to extensively invade the ventral horn of the spinal cord (data not shown). These findings prompted us to analyze mice in which we integrated *EWS-Pea3*, a break-point fusion product between the amino-terminal domain of the Ewing sarcoma (EWS) gene and the Pea3 DNA binding domain (Arvand and Denny, 2001; Urano et al., 1996), into the *Er81* locus (Figure 1A, B). We found that in a luciferase enzyme-based cell culture transfection assay, EWS-Pea3 showed stronger transactivation activity than Er81 or Pea3 (Figure 1J; data not shown), in agreement with previous studies (de Alava and Gerald, 2000; May et al., 1993; Ohno et al., 1993). Moreover, transactivation by

EWS-Pea3 was abolished by mutation of ETS-binding sites in the reporter plasmid, demonstrating ETS-binding site dependence (data not shown).

Expression of Er81 in DRG neurons of embryos containing integration of *EWS-Pea3* in the *Er81* locus ($Er81^{EWS\text{-}Pea3/-}$) was abolished (Figure 1E) and the expression level of the calcium binding protein Parvalbumin (PV) in proprioceptive afferents which is decreased ~5- to 10-fold in *Er81* mutants (Arber et al., 2000a) was comparable to wild-type levels in $Er81^{EWS\text{-}Pea3/-}$ embryos (Figure 1F, G, H). To further define DRG neuron differentiation in the presence of *EWS-Pea3* in proprioceptive afferents *in vivo*, we assessed whether replacement of *Er81* by *EWS-Pea3* had an influence on neuronal survival or on the expression of proprioceptive afferent-specific genes. The number of proprioceptive afferent cell bodies within the DRG of L1 to L5, the expression of several genes normally expressed by proprioceptive afferents, or expression of genes not normally expressed in proprioceptive afferents was not changed in $Er81^{EWS\text{-}Pea3/-}$ mice when compared to wild-type (Supplemental Figure 1; data not shown). Together, these findings suggest that the expression of EWS-Pea3 from the normal time of onset mimics the function of Er81 as assessed by induction and maintenance of gene expression within proprioceptive afferents.

To determine the extent of rescue of Ia proprioceptive afferent projections into the ventral spinal cord of *Er81* mutant mice achieved by expression of *EWS-Pea3* we traced intraspinal afferent projections by axonal labeling of PV (Figure 2A-C). In addition, to analyze axon ingrowth independent of the level of PV expression in DRG neurons, we used anterograde labeling of afferent fibers by applying fluorescently labeled dextran to cut dorsal roots (Figure 2D-F). Using both assays, we found extensive rescue of the projections into the ventral horn of the spinal cord in $Er81^{EWS\text{-}Pea3/-}$ mice (Figure 2C, F, L). Within the ventral horn, Ia afferents in both wild-type and $Er81^{EWS\text{-}Pea3/-}$ mice formed $vGlut1^{+}$ terminals which were absent in *Er81* mutant mice (Figure 2G-I). To assess whether synapses between Ia afferents and motor neurons are functional in $Er81^{EWS\text{-}Pea3/-}$ mice, we performed intracellular recordings from identified quadriceps motor neurons after stimulation of nerves innervating the quadriceps muscle group. We found no

significant difference in the input amplitude to quadriceps motor neurons when comparing wild-type to *Er81*$^{EWS\text{-}Pea3/-}$ mice (Supplemental Figure 2; wild-type: 10.6±0.9mV, n=11; *Er81*$^{EWS\text{-}Pea3/-}$: 10.9±1mV, n=8). Together, these findings suggest that in the absence of *Er81*, *EWS-Pea3* can direct the complex biological process of correct laminar termination within the ventral spinal cord and the formation of synapses with motor neurons, thus identifying an ETS transcription factor suitable for heterochronic expression experiments in DRG neurons.

Precocious expression of *EWS-Pea3* in DRG neurons leads to axonal projection defects

To address the consequences of precocious ETS signaling for proprioceptive afferent differentiation, we next expressed EWS-Pea3 in DRG neurons as soon as they become post-mitotic. We used a binary mouse genetic system based on Cre recombinase-mediated excision of a transcriptional stop cassette flanked by *loxP* sites. Targeting cassettes were integrated into the *Tau* locus to generate two strains of mice conditionally expressing either *EWS-Pea3* or a membrane-targeted version of enhanced green fluorescent protein to trace axonal projections of DRG neurons (*mGFP*; Supplemental Figure 3; (De Paola et al., 2003)). Embryos positive for both *Isl1*$^{Cre/+}$ and *Tau*$^{EWS\text{-}Pea3/+}$ or *Tau*$^{mGFP/+}$ alleles showed efficient activation of the silent *Tau* allele in ≥95% of all DRG neurons, including proprioceptive afferents, at all segmental levels (Supplemental Figure 3).

We first assessed the influence of *EWS-Pea3* expression in early post-mitotic DRG neurons on the establishment of afferent projections into the spinal cord using the *Tau*$^{mGFP/+}$ allele or a *Thy1* promoter driven spGFP with an expression profile restricted to DRG sensory neurons at E13.5 (*Thy-1*^{spGFP}; (De Paola et al., 2003)). In contrast to wild-type proprioceptive afferent projections (Figure 3A-C), GFP^{+} sensory afferents in *Tau*$^{EWS\text{-}Pea3/+}$ *Isl1*$^{Cre/+}$ embryos failed to invade the spinal cord and instead were found in an extreme lateral position at the dorsal root entry zone, a phenotype observed at least up to E18.5 (Figure 3A-C, G-I, data not shown). We next visualized the path of sensory

afferent projections towards the dorsal root entry zone in $Tau^{EWS\text{-}Pea3/+}$ $Isl1^{Cre/+}$ embryos by injecting fluorescently-labeled dextran into an individual DRG (L3; n=3; Figure 3M-Q). Sensory afferents in E13.5 wild-type embryos bifurcated at their lateral spinal entry point, projected rostrally and caudally over ≥6 segmental levels while gradually approaching the midline (Figure 3M). Sensory afferents in $Tau^{EWS\text{-}Pea3/+}$ $Isl1^{Cre/+}$ embryos also bifurcated at the entry point, although ~5% of afferent fibers continued to grow towards the midline (Figure 3O, Q). While rostro-caudal projections were present in $Tau^{EWS\text{-}Pea3/+}$ $Isl1^{Cre/+}$ embryos, afferent fibers failed to approach the midline at distal segments and continued to occupy an extreme lateral position (Figure 3O), consistent with the analysis of transverse sections.

We next examined the establishment of peripheral projections upon precocious *EWS-Pea3* expression in DRG neurons. While sensory axons in $Tau^{EWS\text{-}Pea3/+}$ $Isl1^{Cre/+}$ embryos reached the skin and established major nerve trunks by E16.5, only rudimentary sensory axon branching was established within the skin (Figure 3D, J). In addition, there was a significant reduction in the number of muscle spindles in $Tau^{EWS\text{-}Pea3/+}$ $Isl1^{Cre/+}$ embryos (~25% of wild-type complement, n=3) as assessed by innervation and expression of genes specific for intrafusal muscle fibers such as *Egr3* (Figure 3E, F, K, L; (Hippenmeyer et al., 2002)). In summary, whereas isochronic expression of *EWS-Pea3* promoted the establishment of proprioceptive afferent projections into the ventral spinal cord, precocious expression of the same ETS signaling factor in DRG neurons interfered with establishment of projections into the spinal cord as well as to peripheral targets.

Precocious *EWS-Pea3* expression promotes neurotrophin-independent survival and neurite outgrowth

To begin to address the cellular and molecular mechanisms involved in the distinct biological actions of *EWS-Pea3* at different developmental stages, we first turned to *in vitro* culture experiments. These experiments permit assessment of whether precocious ETS transcription factor signaling influences neuronal survival and *in vitro* neurite

outgrowth of DRG neurons, two parameters prominently influenced by target-derived neurotrophic factors and their receptors.

We cultured E13.5 whole DRG explants from wild-type and $Tau^{EWS\text{-}Pea3/+}$ $Isl1^{Cre/+}$ embryos in the presence of NGF, NT-3 or in the absence of neurotrophins and analyzed neuronal survival and neurite outgrowth on matrigel substrate after 48 hours *in vitro*. Without neurotrophic support, very few wild-type DRG neurons survived (Figure 4A). In contrast, culturing wild-type DRG with neurotrophic factors led to neuronal survival and neurite outgrowth. Addition of NGF, which supports survival of cutaneous afferents, resulted in straight and unbranched neurite outgrowth (Figure 4B), while cultures grown in the presence of NT-3, which supports survival of proprioceptive afferents, resulted in a highly branched neurite outgrowth pattern after 48 hours *in vitro* (Figure 4C). Surprisingly, DRG neurons isolated from $Tau^{EWS\text{-}Pea3/+}$ $Isl1^{Cre/+}$ embryos and cultured without neurotrophic support survived after 48 hours *in vitro* and had established long and highly branched neurites (Figure 4D). Neither the pattern of neurite outgrowth nor neuronal survival changed significantly after application of either NGF or NT-3 (Figure 4E, F).

To directly compare neurotrophin-dependence between DRG neurons expressing *EWS-Pea3* from the *Tau* locus at precocious or isochronic time of onset, we generated a strain of mice in which *Cre* recombinase is expressed from the *Parvalbumin* (*PV*) locus (Supplemental Figure 4). The expression of GFP in $Tau^{mGFP/+}$ $PV^{Cre/+}$ was restricted to PV^{+} proprioceptive DRG neurons and mirrored the onset of expression of PV at ~E14 (Supplemental Figure 4; data not shown). We next cultured E14.5 whole DRG explants from $Tau^{EWS\text{-}Pea3/+}$ $PV^{Cre/+}$ and $Tau^{mGFP/+}$ $PV^{Cre/+}$ mice for 48 hours *in vitro* in the presence or absence of NT-3 (Figure 5). We found that DRG neurons from both genotypes survived and extended neurites only in the presence of NT-3, whereas they died in the absence of NT-3 (Figure 5). Together, these findings suggest that only precocious but not isochronic ETS signaling in DRG neurons is capable to uncouple survival and neurite outgrowth from a requirement for neurotrophin signaling normally observed in wild-type DRG.

To determine whether neuronal survival of DRG neurons from *Tau*$^{EWS\text{-}Pea3/+}$ *Isl1*$^{Cre/+}$ embryos in the absence of neurotrophic support is sufficient to explain the observed neuronal outgrowth, we analyzed DRG isolated from mice mutant in the proapoptotic gene *Bax* (White et al., 1998). Consistent with previous results, *Bax*$^{-/-}$ DRG neurons survived without neurotrophic support (Lentz et al., 1999). In contrast, neurite outgrowth of *Bax*$^{-/-}$ DRG neurons was significantly less (Figure 4G) than of either DRG from *Tau*$^{EWS\text{-}Pea3/+}$ *Isl1*$^{Cre/+}$ embryos cultured in the absence of neurotrophic support (Figure 4D) or *Bax*$^{-/-}$ DRG neurons cultured in the presence of neurotrophic support (Figure 4H, I). These findings suggest that in addition to mediating neurotrophin-independent neuronal survival, expression of *EWS-Pea3* in early post-mitotic neurons also promotes neurite outgrowth in a neurotrophin-independent manner.

To begin to assess at which step of the neurotrophin signaling cascade DRG neurons from *Tau*$^{EWS\text{-}Pea3/+}$ *Isl1*$^{Cre/+}$ embryos have become unresponsive to the addition of neurotrophins, we assayed the expression of neurotrophin receptors in *Tau*$^{EWS\text{-}Pea3/+}$ *Isl1*$^{Cre/+}$ embryos. Whereas expression of the neurotrophin receptors *TrkA*, *TrkB* and *TrkC* marks afferents of distinct sensory modalities in DRG of wild-type embryos (Figure 6A-C) (Huang and Reichardt, 2001; Huang and Reichardt, 2003), *Tau*$^{EWS\text{-}Pea3/+}$ *Isl1*$^{Cre/+}$ embryos showed complete absence of expression of *TrkA*, *TrkB* and *TrkC* in DRG neurons at E16.5 (Figure 6G-I). Thus this absence of Trk receptor expression in DRG of *Tau*$^{EWS\text{-}Pea3/+}$ *Isl1*$^{Cre/+}$ embryos provides a likely explanation for the lack of responsiveness of these neurons to the addition of neurotrophic factors.

We next assayed whether the complete absence of *Trk* receptor expression in *Tau*$^{EWS\text{-}Pea3/+}$ *Isl1*$^{Cre/+}$ embryos had an influence on naturally occurring cell death *in vivo* using TUNEL on DRG sections. Surprisingly, we found that apoptosis was decreased by ~50% (n=3 embryos, average of $\geq$50 sections) in DRG of *Tau*$^{EWS\text{-}Pea3/+}$ *Isl1*$^{Cre/+}$ embryos in comparison to wild-type (Figure 6D, J, M). Quantitative analysis of the number of neurons in lumbar DRG of *Tau*$^{EWS\text{-}Pea3/+}$ *Isl1*$^{Cre/+}$ embryos revealed a significant increase to ~170% of wild-type levels (Figure 6E, K, N). Moreover, BrdU pulse-chase

experiments ruled out the possibility that DRG neurons in *Tau*$^{EWS\text{-}Pea3/+}$ *Isl1*$^{Cre/+}$ embryos re-enter the cell cycle (no BrdU^{+}/LacZ^{+} cells, n=3 embryos, analysis of $\geq$50 sections each; Figure 6F, L). Together with the *in vitro* culture experiments, these findings suggest that DRG neurons from *Tau*$^{EWS\text{-}Pea3/+}$ *Isl1*$^{Cre/+}$ embryos remain post-mitotic but fail to become sensitive to naturally occurring cell death, and survive in the absence of *Trk* receptors and neurotrophic support.

We next analyzed whether changes in the expression of proteins known to be involved in the regulation of neuronal survival or cell death could be detected in DRG of *Tau*$^{EWS\text{-}Pea3/+}$ *Isl1*$^{Cre/+}$ embryos. We found no significant quantitative changes in the level of Akt/p-Akt or CREB/p-CREB in DRG (Figure 6O, P) both of which have been shown to be key regulators of neuronal survival (Huang and Reichardt, 2003). Moreover, the level of the pro-apoptotic Bcl-2 family member Bax was not significantly reduced (Figure 6O, P). In contrast, the expression level of the anti-apoptotic Bcl-2 family members Bcl-xl and Bcl-2 was significantly increased when compared to wild-type levels (Bcl-2: 157%, Bcl-xl: 259%, mean average of n=3 independent experiments, Figure 6O, P), providing a potential molecular explanation for the enhanced neuronal survival of DRG neurons of *Tau*$^{EWS\text{-}Pea3/+}$ *Isl1*$^{Cre/+}$ embryos in the absence of *Trk* receptor expression (Pettmann and Henderson, 1998).

Only precocious but not isochronic ETS signaling in DRG neurons interferes with neuronal fate acquisition

The observed changes in neuronal survival and neurite outgrowth between precocious and isochronic expression of EWS-Pea3 prompted us to perform a direct comparative analysis in gene expression between mice with precocious EWS-Pea3 expression and mice in which the expression of *EWS-Pea3* is initiated in DRG sensory neurons from the time of normal onset of Er81 expression. Moreover, to rule out the possibility that a differential effect may be due to the different genetic strategies by which expression of *EWS-Pea3* in proprioceptive afferents is achieved, we performed this analysis both in *Er81*$^{EWS\text{-}Pea3/-}$ and *Tau*$^{EWS\text{-}Pea3/+}$ *PV*$^{Cre/+}$ embryos.

We first analyzed expression of *TrkC*, a gene downregulated in DRG neurons of $Tau^{EWS\text{-}Pea3/+}$ $Isl1^{Cre/+}$ embryos (Figure 7A, B). In contrast, the level of expression of *TrkC* was indistinguishable from wild-type in DRG neurons of $Er81^{EWS\text{-}Pea3/-}$ and $Tau^{EWS\text{-}Pea3/+}$ $PV^{Cre/+}$ embryos (Figure 7A, C, D). Moreover, PV was not expressed in DRG neurons of $Tau^{EWS\text{-}Pea3/+}$ $Isl1^{Cre/+}$ embryos (Supplemental Figure 5) but was expressed by proprioceptive afferents in both wild-type and $Er81^{EWS\text{-}Pea3/-}$ embryos (Figure 1, Supplemental Figure 5) (Arber et al., 2000a). We also found several genes which were ectopically upregulated in DRG neurons of $Tau^{EWS\text{-}Pea3/+}$ $Isl1^{Cre/+}$ embryos. Calretinin and Calbindin, two different calcium binding proteins expressed by subpopulations of DRG neurons in wild-type, $Er81^{EWS\text{-}Pea3/-}$ and $Tau^{EWS\text{-}Pea3/+}$ $PV^{Cre/+}$ embryos (Figure 7E, G, H; data not shown) (Ichikawa et al., 1994; Zhang et al., 1990), were induced in >95% of all DRG neurons of $Tau^{EWS\text{-}Pea3/+}$ $Isl1^{Cre/+}$ embryos (Figure 7F, Supplemental Figure 5). These findings suggest that DRG neurons in $Tau^{EWS\text{-}Pea3/+}$ $Isl1^{Cre/+}$ embryos fail to differentiate to a normal fate and instead acquire an aberrant identity distinct from any subpopulation of wild-type DRG neurons. Finally, to assess whether EWS-Pea3 expressed precociously acts exclusively cell-autonomously or may also influence neighboring DRG neurons, we activated expression of EWS-Pea3 using $Hb9^{Cre}$ mice (Yang et al., 2001). Due to a transient and rostro-caudally graded expression of *Hb9* at neural plate stages, very few DRG neurons at brachial levels and increasingly more neurons progressing caudally undergo recombination in $Tau^{EWS\text{-}Pea3/+}$ $Hb9^{Cre/+}$ and $Tau^{mGFP/+}$ $Hb9^{Cre/+}$ embryos (Figure 8). Nevertheless, downregulation of Trk receptor expression or upregulation of Calretinin is restricted exclusively to neurons which have undergone recombination and cannot be observed in $Tau^{mGFP/+}$ $Hb9^{Cre/+}$ embryos (Figure 8). Together, these results and the findings obtained from *in vitro* culture experiments (Figures 4, 5) demonstrate that precocious or isochronic expression of *EWS-Pea3* in the same neurons leads to significantly different cell-autonomous cellular responses with respect to gene expression, neuronal survival and neurite outgrowth (Figure 9).

Discussion

Target-derived signals exhibit a conserved role in the induction of defined programs of transcription factor expression late in post-mitotic neuronal differentiation (Hippenmeyer et al., 2004). This study provides evidence that the late onset of transcription factors is essential for many later aspects of neuronal differentiation and circuit formation. Our data indicate that DRG neurons undergo a temporal change in their competence to respond to ETS transcription factor signaling, as assessed by changes in gene expression and axonal target invasion (Figure 9). Our findings argue for the necessity of target-induced, and therefore temporally-controlled upregulation of ETS transcription factor signaling. More generally, they suggest that temporally-regulated activation of transcriptional programs coupled to a particular fate induced in neurons at early developmental stages represents an important mechanism of neuronal maturation.

One striking observation of this study is that precocious induction of ETS signaling promotes neuronal survival without a requirement for neurotrophic support and in complete absence of Trk receptor expression. In contrast, ETS signaling at the normal time of onset of *Er81* expression does not result in enhanced neuronal survival in the absence of neurotrophins and also does not lead to downregulation of TrkC expression in proprioceptive afferents. These findings demonstrate very distinct activities of one transcriptional regulator at different developmental steps within a committed post-mitotic neuronal lineage. The absence of Trk receptor expression upon precocious induction of ETS signaling can only partially explain the observed phenotype in axonal projections. Elimination of TrkA receptor signaling in *Bax* mutant mice perturbs establishment of peripheral projections of cutaneous afferents whereas establishment of central projections does not appear to be affected (Patel et al., 2000). In the absence of NT-3 signaling, development of central as well as peripheral proprioceptive afferent projections is perturbed (Patel et al., 2003). In contrast, upon precocious induction of ETS signaling, we found more pronounced defects in the establishment of central rather than peripheral projections for all DRG neurons.

Induction of Er81 expression in proprioceptive afferents is controlled by peripheral NT-3 as axons reach the vicinity of target muscles and thus occurs only approximately three days after proprioceptive neurons become post-mitotic (Arber et al., 2000a; Patel et al., 2003). This temporally delayed and target-induced upregulation of ETS transcription factor expression several days after a neuronal lineage of a specific identity first emerges is not restricted to DRG sensory neurons, but is also found in motor neuron pools (Lin et al., 1998a). Target-derived factors have also been implicated in controlling neuronal maturation of predetermined neurons in Drosophila where expression of members of the BMP family in the target region is essential for the induction of mature peptidergic properties in a subpopulation of neurons marked by the coordinate expression of the two transcription factors apterous and squeeze (Allan et al., 2003; Marques et al., 2003). Thus, both in Drosophila and vertebrates, target-derived factors appear to act permissively to induce the expression of transcriptional programs involved in terminal neuronal maturation.

Our findings are compatible with a model in which DRG neurons acquire their mature fate by sequential and temporally-controlled addition of lineage-specific features (Figure 9). Target-derived factors act on pre-determined neuronal lineages to switch their developmental programs to become compatible with processes such as target invasion and branching. Such a transition state in the acquisition of a defined neuronal fate would be accompanied by the induction of appropriate transcriptional programs through the expression of specific transcription factors. Mechanisms such as chromosomal remodeling that restrict or expand access to certain target genes (Kouzarides, 2002) or activation by cofactors responsible to change the action of particular transcription factors (Verger and Duterque-Coquillaud, 2002) could represent possible mechanisms by which the downstream transcriptional profile of a transcription factor could be temporally shifted towards the selection and control of distinct target genes. Interestingly, several ETS transcription factors are activated through release of autoinhibition upon interaction with cofactors and/or by post-translational modifications (Greenall et al., 2001; Pufall and Graves, 2002; Verger and Duterque-Coquillaud, 2002). The fusion of EWS with Pea3 could circumvent a need for activation through specific cofactors while still

maintaining ETS-site dependence, thus rendering EWS-Pea3 less sensitive to the cellular context than endogenous ETS transcription factors. Using this fusion protein, our experiments demonstrate a profound change in the action of ETS signaling at the level of transcriptional regulation within post-mitotic DRG neurons over time. Moreover, the observed transcriptional shift in ETS signaling is paired with the onset of appropriate regulation of neuronal subtype specification and establishment of axonal projections into the target area.

Recent experiments addressing the temporal requirement of transcription factor action in proliferating neural progenitor cells adds to the idea that defined temporal windows during which transcription factors act to control distinct downstream target genes are of key importance to neuronal fate acquisition. During *Drosophila* neuroblast generation, the transcription factor hunchback controls specification and differentiation of early born neuroblasts (Isshiki et al., 2001). Over time, however, neuroblasts progressively lose their competence to generate cells of an early fate in response to hunchback expression (Pearson and Doe, 2003). These findings thus also argue for a change in cellular competence to respond to a specific transcription factor over time albeit in an early precursor context. More generally, during the differentiation of haematopoietic lineages, several transcription factors have also been shown to exhibit distinct functions at progressive steps of lineage specification (Orkin, 2000). Analysis of the mechanisms by which transcription factor programs can be shifted over time to control different complements of downstream genes and thus aspects of neuronal and cellular fates in progenitor cells or post-mitotic neurons may provide further insight into the way in which transcription factors act to control the assembly of neuronal circuits.

Experimental Procedures

generation of transgenic mice and mouse genetics

Er81$^{EWS\text{-}Pea3}$ mice were generated following a similar strategy as described for the generation of *Er81*^{NLZ} mice (Arber et al., 2000a). In brief, a targeting vector with a cDNA coding for *EWS-Pea3* was inserted in frame with the endogenous start ATG into exon 2

of the *Er81* genomic locus and used for homologous recombination in W95 ES cells. *EWS-Pea3* represents a fusion gene between the amino terminal of EWS and the ETS domain of Pea3 (Urano et al., 1996). Primer pairs to specifically detect the $Er81^{EWS\text{-}Pea3}$ allele were as follows: (5'): CAGCCACTGCACCTACAAGAC; (3'): CTTCCTGCTTGATGTCTCCTTC. Generation of Tau^{mGFP} and $Tau^{EWS\text{-}Pea3}$ mice: *lox-STOP-lox-mGFP-IRES-NLS-LacZ-pA* and *lox-STOP-lox-EWS-Pea3-IRES-NLS-LacZ-pA* targeting cassettes were integrated into exon 2 of the *Tau* genomic locus (the endogenous start ATG was removed in the targeting vectors; details available upon request). Membrane-targeted GFP (mGFP) was provided by P. Caroni (De Paola et al., 2003). ES cell recombinants were screened by Southern blot analysis using the probe in the 5' region as described previously (Tucker et al., 2001). Frequency of recombination in 129/Ola ES cells was ~1:3 for both *Tau* constructs. For the generation of PV^{Cre} mice, mouse genomic clones were obtained by screening a 129SV/J genomic library (Incyte Genomics). For details on the genomic structure of the mouse *Parvalbumin* locus see (Schwaller et al., 1999). An *IRES-Cre-pA* targeting cassette (Yang et al., 2001) was integrated into the 3' UTR of exon 5 and ES cell recombinants were screened with a 5' probe (oligos: (5')GAGATGACCCAGCCAGGATGCCTC and (3')CTGACCACTCTCGCTCCGGTGTCC ; genomic DNA: HindIII digest). The frequency of recombination in 129/OLA ES cells was ~1:20. Recombinant clones were aggregated with blastocysts to generate chimeric founder mice that transmitted the mutant alleles. In all experiments performed in this study, animals were of mixed genetic background (129/Ola and C57Bl6). $Thy\text{-}1^{spGFP}$ transgenic mice were generated in analogy to De Paola et al., 2003 and for these experiments a strain of mice with early embryonic expression was selected. $Isl1^{Cre}$ and $Hb9^{Cre}$ mouse strains have been described (Srinivas et al., 2001; Yang et al., 2001) and $Bax^{+/-}$ animals were from Jackson Laboratories (White et al., 1998). Timed pregnancies were set up to generate embryos of different developmental stages with all genotypes described throughout the study.

Transcriptional transactivation assays

The following plasmids were used for transcriptional transactivation assays: pRc/RSV (Invitrogen), pRc/RSV-Er81, pRc/RSV-EWS-Pea3, pTP-5xETS, pTP-5xETSmut. pRc/RSV-Er81 and pRc/RSV-EWS-Pea3 were obtained by insertion of the cDNAs for Er81 or EWS-Pea3 (gift from J. A. Hassell) into pRc/RSV. pTP-5xETS was constructed by inserting a cassette of five repetitive copies of high affinity Pea3 binding sites (5'-GCCGGAAGC -3') (Bojovic and Hassell, 2001; Mo et al., 1998) into a modified version of pTK-Luc. pTP-5xETSmut was generated as pTP-5xETS but using a mutated complement of the Pea3 binding sites (5'- GCCTATGGC-3'). A control plasmid to normalize for transfection efficiency (placZ) and pTK-Luc were a gift from D. Kressler. COS-7 cells were co-transfected with 1-1.2μg of total DNA including one of the effector plasmids pRc/RSV-empty, pRc/RSV-Er81, or pRc/RSV-EWS-Pea3, respectively; one of the reporter plasmids pTP-5xETS or pTP-5xETSmut and placZ. Cells were harvested after 25h and processed for assays to determine luciferase and LacZ activity as described previously (Kressler et al., 2002). Luciferase values normalized to LacZ activity are referred to as luciferase units.

***In Situ* hybridization and immunohistochemistry**

For *in situ* hybridization analysis, cryostat sections were hybridized using digoxigenin-labeled probes (Schaeren-Wiemers and Gerfin-Moser, 1993) directed against mouse *TrkA*, *TrkB*, and rat *TrkC*, respectively (gift from L.F. Parada). Antibodies used in this study were: rabbit anti-Er81 (c-term), rabbit anti-Pea3 (c-term), rabbit anti-PV (Arber et al., 2000a), rabbit anti-eGFP (Molecular Probes), rabbit anti-Calbindin, rabbit anti-Calretinin (SWANT), rabbit anti-CGRP (Chemicon), rabbit anti-vGlut1 (Synaptic System), rabbit anti-Brn3a (gift from E. Turner), rabbit anti-TrkA and -p75 (gift from L.F. Reichardt), rabbit anti-Runx3 (Kramer and Arber, unpublished reagent), rabbit anti-Rhodamine (Molecular Probes), mouse anti-neurofilament (3A10), sheep anti-eGFP (Biogenesis Ltd), goat anti-LacZ, goat anti-TrkC (gift from L.F. Reichardt), guinea pig anti-Isl1 (Arber et al., 2000a). Terminal deoxynucleotidyl transferase-mediated biotinylated UTP nick end labeling (TUNEL) to detect apoptotic cells in E13.5 DRG on

cryostat sections was performed as described by the manufacturer (Roche). Quantitative analysis of TUNEL$^+$ DRG cells was performed essentially as described (White et al., 1998). BrdU pulse-chase experiments and LacZ wholemount stainings were performed as previously described (Arber et al., 1999). For anterograde tracing experiments to visualize projections of sensory neurons, rhodamine-conjugated dextran (Molecular Probes) was injected into single lumbar (L3) DRG at E13.5 or applied to whole lumbar dorsal roots (L3) at P5 using glass capillaries. After injection, animals were incubated for 2-3h (E13.5) or over night (P5). Cryostat sections were processed for immunohistochemistry as described (Arber et al., 2000a) using fluorophore-conjugated secondary antibodies (1:1000, Molecular Probes). Images were collected on an Olympus confocal microscope. Images from *in situ* hybridization experiments were collected with an RT-SPOT camera, and Corel Photo Paint 10.0 was used for digital processing of images.

In Vitro cultures of dorsal root ganglia

Individual lumbar DRG were dissected from E13.5 or E14.5 embryos and placed on Matrigel (BD Biosciences) coated coverslips in DMEM/F12 (Gibco), 2mM L-Gln (Gibco), N2 (Gibco), 1mg/ml BSA (Sigma) without neurotrophins or supplemented with either NGF (100ng/ml, Gibco) or NT-3 (20ng/ml, Sigma). DRG explants ($n \geq 20$ for each condition) were cultured for 48h, processed for immunocytochemistry and analyzed using confocal microscopy.

Western blot analysis

Lumbar DRG from E16.5 embryos were isolated, mechanically disrupted, homogenized using glass beads (Sigma) and lysed in standard lysis buffer supplemented with protease and phosphatase inhibitors as described (Markus et al., 2002b). Protein extracts were resolved by SDS-PAGE, and immunoblotting was performed using antibodies against Akt, p-Akt (Ser473), CREB, p-CREB (Ser133), Bax, Bcl-xl (Cell Signaling Technology),

and Bcl-2 (BD PharMingen). For quantification, films (X-OMAT AR, Kodak) were scanned and densitometry was performed using IMAGE QUANT 5.2.

Electrophysiology

Electrophysiological analysis was performed as previously described (Mears and Frank, 1997). Briefly, intracellular recordings from identified quadriceps motor neurons were made using sharp electrodes (75-120MΩ, 3M KCl). Average responses (10-20 trials) from suprathreshold nerve stimulation (1.5x strength that evokes maximal monosynaptic response) of the quadriceps nerve were acquired with LTP software (Anderson and Collingridge, 2001). Only cells with stable resting potentials more negative than -50mV were considered for analysis. Monosynaptic amplitudes were determined offline using custom routines in the Matlab environment as previously described (Mears and Frank, 1997).

Figures and Supplemental Figures

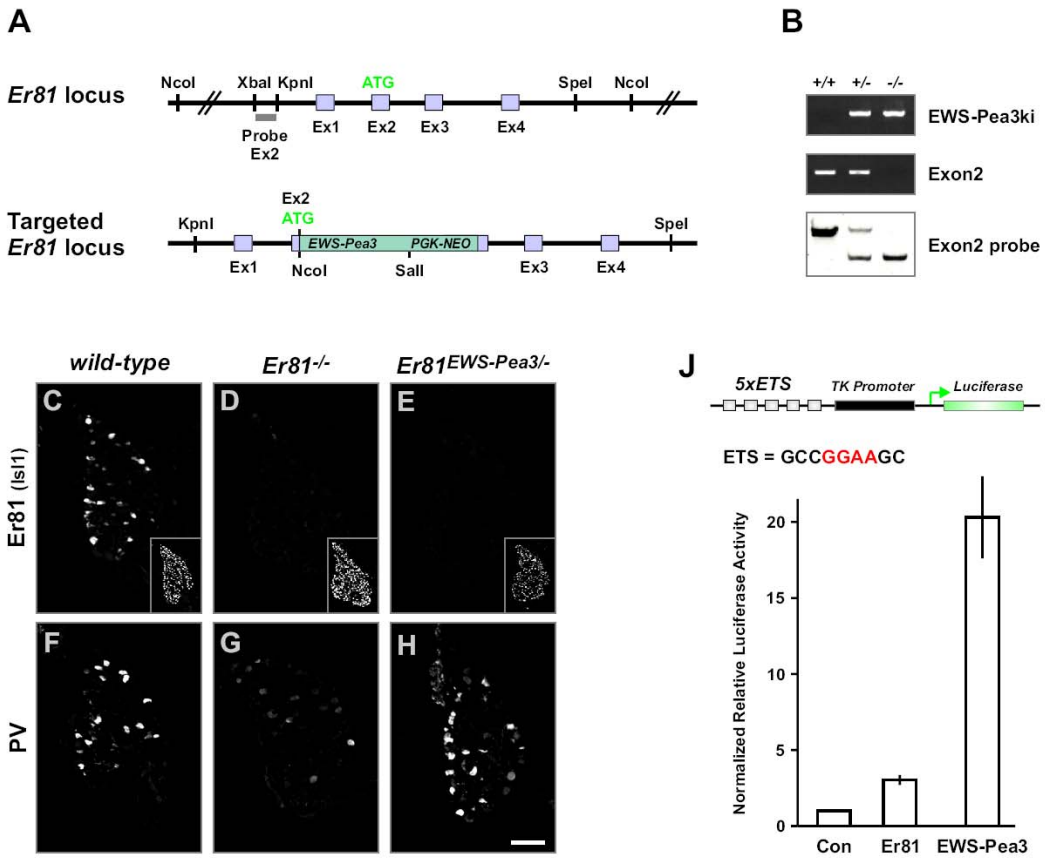

Figure 1. Replacement of *Er81* by *EWS-Pea3*

(A) Generation of $Er81^{EWS\text{-}Pea3}$ mutant mice. (Top panel) Organization of the *Er81* genomic locus in the region targeted by homologous recombination in analogy to Arber et al. 2000. Exons 1-4 are shown as light blue boxes and the *Er81* start codon in exon 2 is indicated as ATG. The probe used to detect homologous recombination is shown as a grey box. (Bottom panel) Replacement of *Er81* by *EWS-Pea3* through the integration of *EWS-Pea3* in frame with the endogenous start codon of the *Er81* locus in exon 2 (in analogy to Arber et al. 2000).

(B) PCR and Southern blot analysis of $Er81^{EWS\text{-}Pea3}$ wild-type (+/+), heterozygous (+/-) and homozygous (-/-) genomic DNA to detect the mutant allele. PCR primer pairs (EWS-Pea3ki) were used to detect specifically the recombined allele and a primer pair in exon2 was used to detect the presence of the wild-type allele (Arber et al., 2000a).

(C-E) Analysis of Er81 expression in lumbar DRG neurons of E16.5 wild-type (C), $Er81^{-/-}$ (D), $Er81^{EWS\text{-}Pea3/-}$ (E) mutant embryos. Inset in lower right corner of each panel shows Islet1 (Isl1) expression in the respective DRG.

(F-H) PV expression in lumbar DRG of E16.5 wild-type (F), *Er81*$^{-/-}$ (G), *Er81*$^{EWS\text{-}Pea3/-}$ (H) embryos. Confocal scans were performed with equal gain intensity.

(J) Transcriptional transactivation of luciferase expression from a minimal reporter construct containing five consensus ETS DNA binding sites (GCCGGAAGC; (Bojovic and Hassell, 2001; Mo et al., 1998) and a minimal TK promoter upon transient transfection of Er81 ($n \geq 7$; 3.03 ± 0.66) or EWS-Pea3 ($n \geq 7$; 20.3 ± 2.7), relative luciferase activity normalized to control.

Scale bar = 80μm.

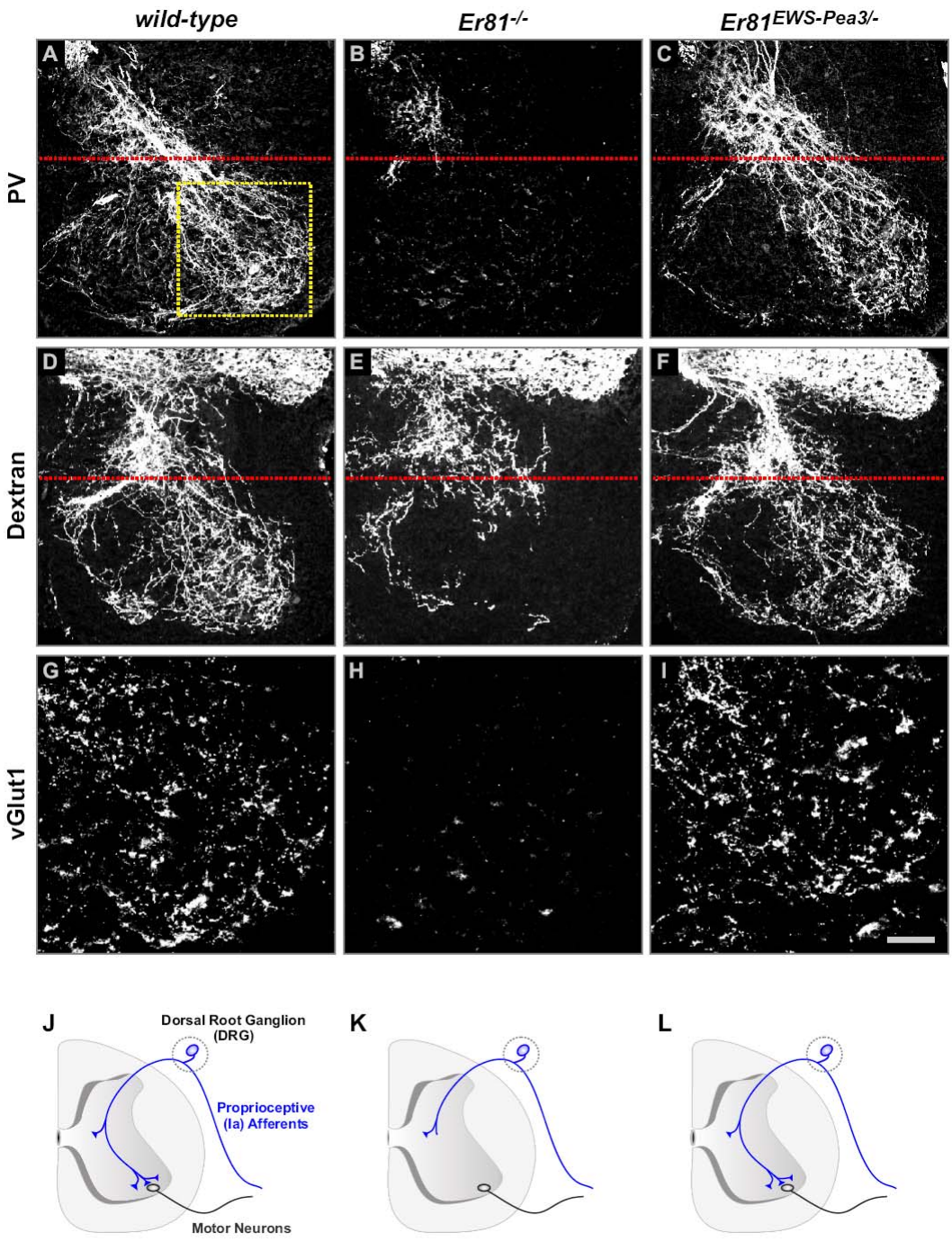

Figure 2. Rescue of Ia proprioceptive afferent projections into the ventral spinal cord in *Er81*$^{EWS\text{-}Pea3}$ mutants

(A-F) Morphological analysis of central projections at lumbar level L3 of PV^{+} DRG neurons (A-C) or all DRG sensory afferents after application of fluorescently labeled dextran to individual dorsal roots (D-F) in P0.5 (A-C) or P5 (D-F) wild-type (A, D), *Er81*$^{-/-}$ (B, E), *Er81*$^{EWS\text{-}Pea3/-}$ (C, F) mice. Red dotted line indicates intermediate level of spinal cord.

(G-I) Analysis of vGlut1 immunocytochemistry in the ventral horn of P0.5 wild-type (G), *Er81*$^{-/-}$ (H), *Er81*$^{EWS\text{-}Pea3/-}$ (I) mice. Yellow dotted box in (A) indicates size of images shown in (G-I).

(J-L) Schematic summary diagrams of the morphological rescue of Ia proprioceptive afferent projections (blue) into the ventral spinal cord observed in wild-type (J), *Er81*$^{-/-}$ (K), *Er81*$^{EWS\text{-}Pea3/-}$ (L) mice. DRG are illustrated as dotted line, motor neurons are shown in black.

Scale bar: (A-C) = 150μm; (D-F) = 160μm; (G-I) = 70μm.

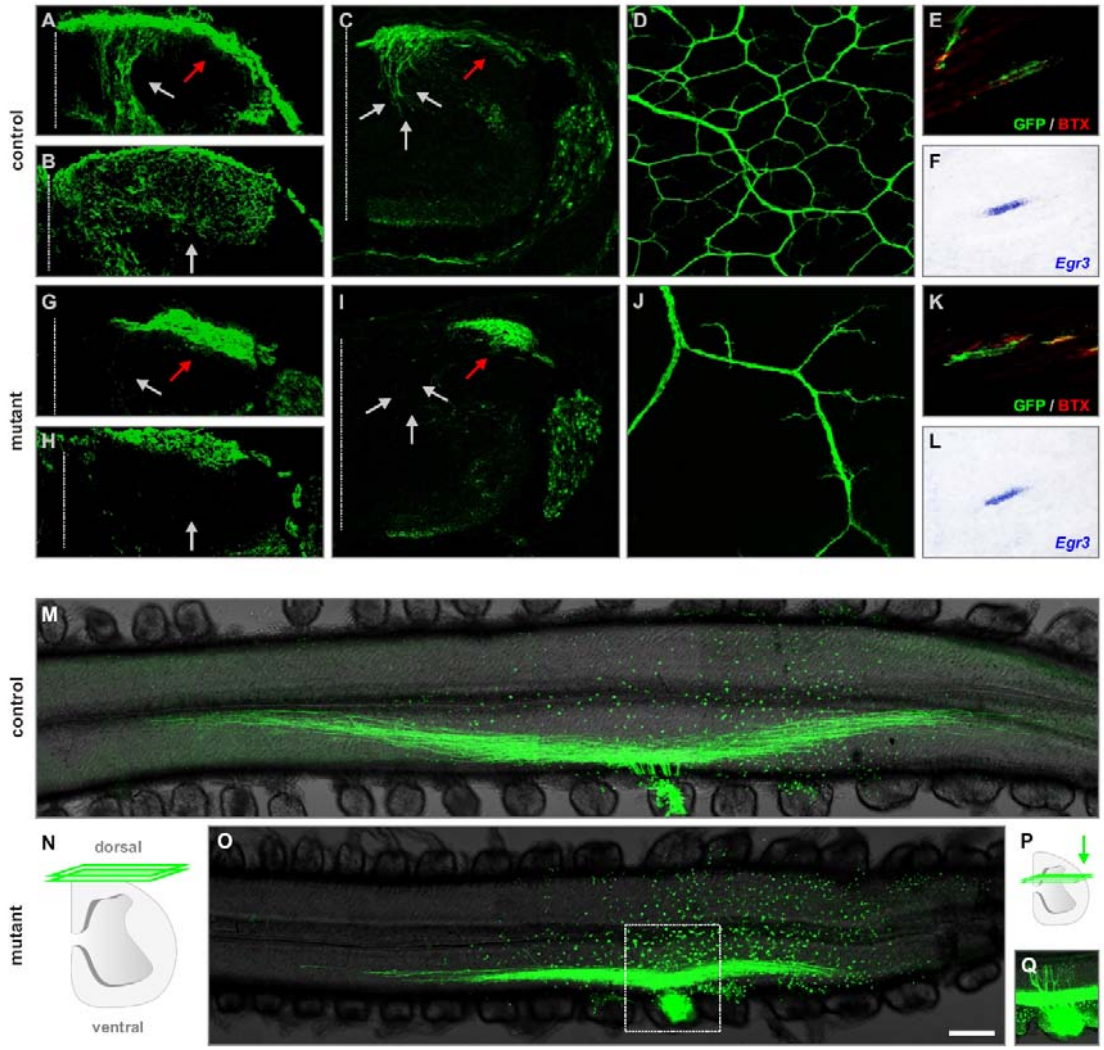

Figure 3. Defects in the establishment of sensory afferent projections upon precocious expression of *EWS-Pea3* in DRG neurons

(A-C, G-I) Visualization of sensory afferent projections (green) into the spinal cord of wild-type (A-C) and $Tau^{EWS\text{-}Pea3/+}$ $Isl1^{Cre/+}$ (G-I) embryos at E13.5 (A, C, G, I) and E16.5 (B, H) by Cre recombinase mediated activation of mGFP expression from the *Tau* locus (A, B, G, H) or by a $Thy\text{-}1^{spGFP}$ transgene (C, I; (De Paola et al., 2003)). White arrows indicate normal pattern of afferent projections into the spinal cord whereas red arrows show aberrant accumulation of sensory afferents at the lateral edge of the spinal cord in $Tau^{EWS\text{-}Pea3/+}$ $Isl1^{Cre/+}$ embryos.

(D-F, J-L) Analysis of sensory afferent projections (green) into the skin (D, J) or muscle (E, K; red: α-Bungarotoxin, BTX) of wild-type (D-F) and $Tau^{EWS\text{-}Pea3/+}$ $Isl1^{Cre/+}$ (J-L) embryos at E16.5 by Cre recombinase mediated activation of mGFP (D, E, J, K) expression from the *Tau* locus. (F,

L) *Egr3* expression in intrafusal muscle fibers using *in situ* hybridization (consecutive sections to E, K are shown).

(M-Q) Analysis of bifurcation of sensory afferent projections towards the spinal cord in E13.5 wild-type (M) and $Tau^{EWS\text{-}Pea3/+}$ $Isl1^{Cre/+}$ (O, Q) embryos after injection of fluorescently labeled dextran (green) into one DRG (lumbar level L3). Confocal scanning plane for (M, O) is schematically illustrated in (N). Inset in (O) is also shown at a deeper confocal scanning plane (P, Q) to visualize aberrant axonal projections.

Scale bar: (A, G) = 60μm; (B, H) = 80μm; (C, I) = 100μm; (D, J) = 160μm; (E, F, K, L) = 70μm; (M, O, Q) = 240μm.

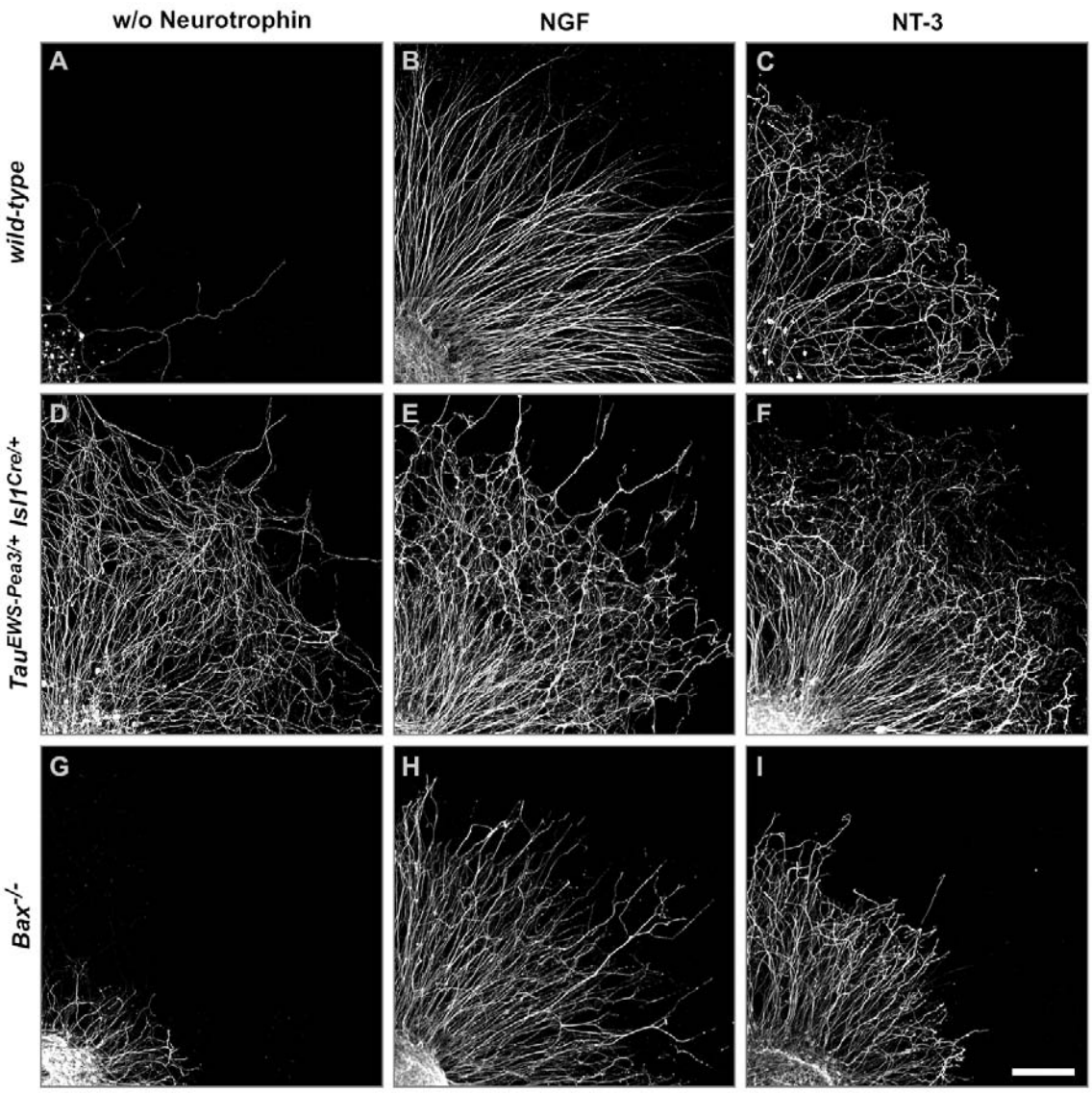

Figure 4. Neurotrophin-independent neurite outgrowth *in vitro* of DRG neurons expressing EWS-Pea3 precociously

E13.5 lumbar DRG from wild-type (A, B, C), *Tau*$^{EWS\text{-}Pea3/+}$ *Isl1*$^{Cre/+}$ (D, E, F) or *Bax*$^{-/-}$ (G, H, I) embryos cultured for 48 hours without neurotrophic support (A, D, G) or in the presence of NGF (B, E, H) or NT-3 (C, F, I) were stained for expression of neurofilament to visualize axonal extensions.

Scale bar = 130 μm.

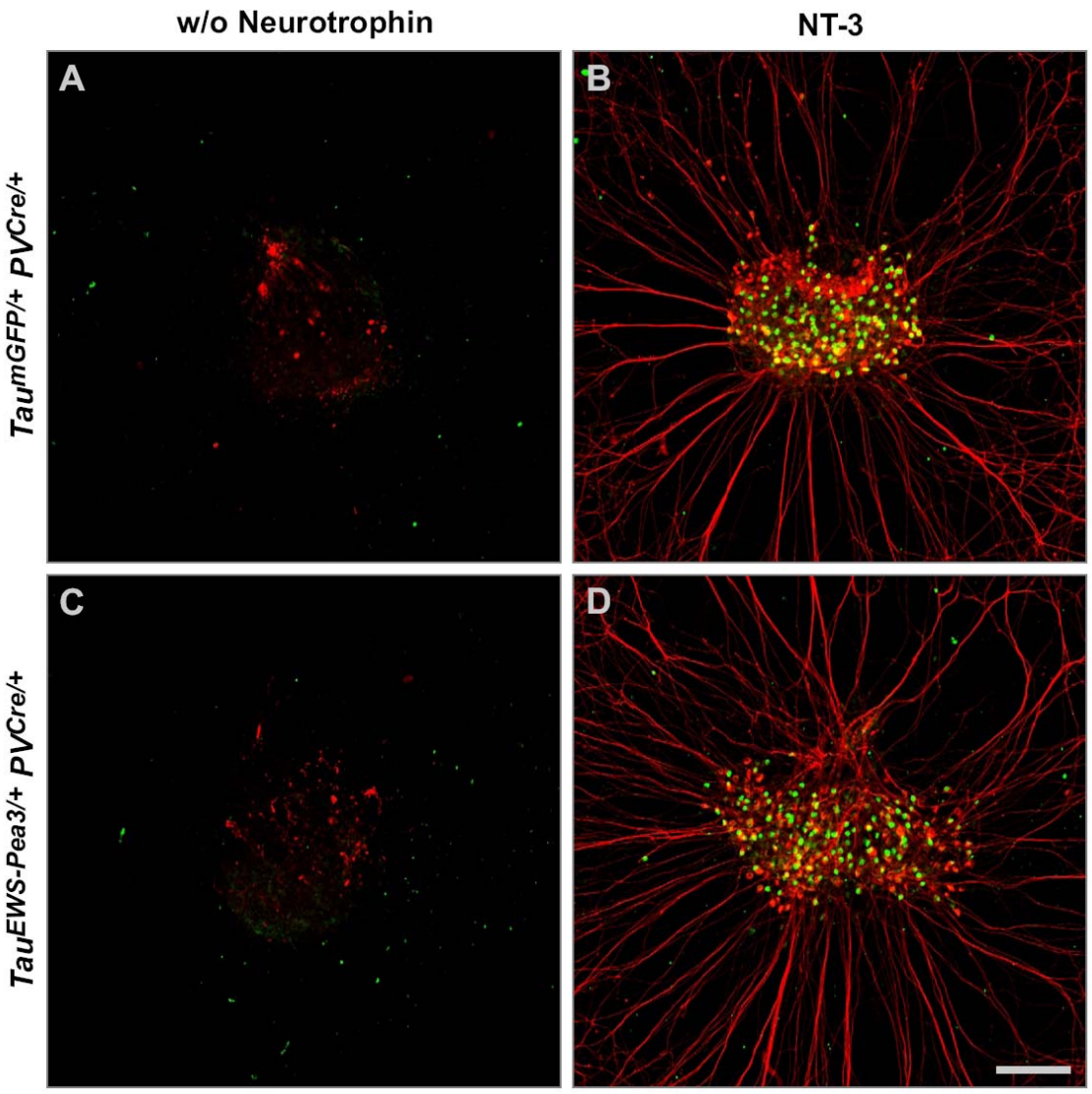

Figure 5. DRG neurons expressing EWS-Pea3 isochronically depend on neurotrophins for survival

E14.5 lumbar DRG from $Tau^{mGFP/+}$ $PV^{Cre/+}$ (A, B) and $Tau^{EWS\text{-}Pea3/+}$ $PV^{Cre/+}$ (C, D) embryos cultured for 48 hours without neurotrophic support (A, C) or in the presence of NT-3 (B, D) were stained for expression of neurofilament (red) and LacZ (green) to visualize axonal extensions and survival of PV expressing proprioceptive afferents.

Scale bar = 150μm.

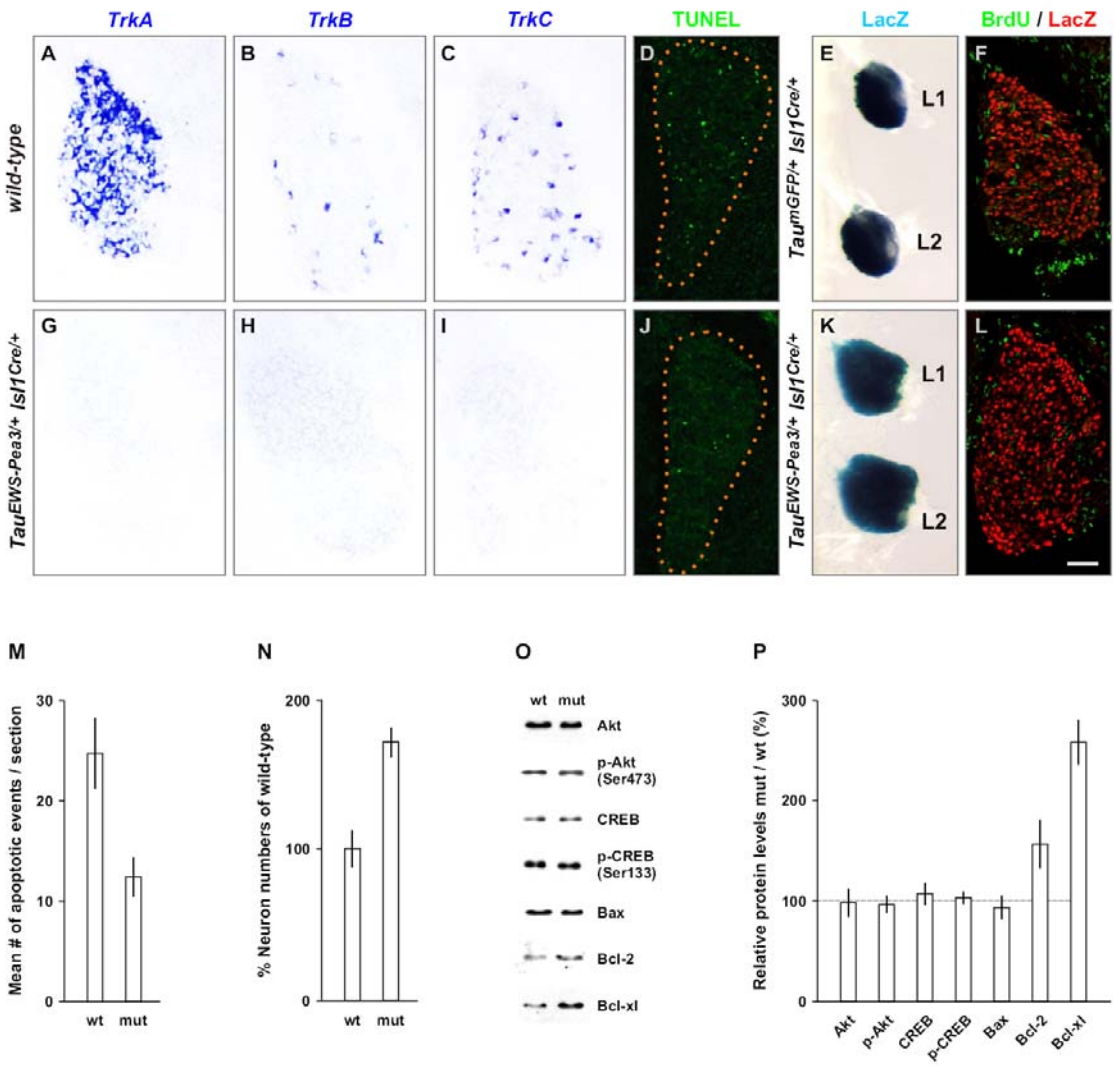

Figure 6. Loss of Trk receptor expression and increased survival in DRG neurons upon precocious ETS signaling

(A-C, G-I) *In situ* hybridization analysis of *TrkA* (A, G), *TrkB* (B, H) and *TrkC* (C, I) expression in E16.5 lumbar DRG of wild-type (A-C) and $Tau^{EWS\text{-}Pea3/+}$ $Isl1^{Cre/+}$ (G-I) embryos.

(D-F, J-L) Analysis of lumbar DRG of wild-type (D), $Tau^{mGFP/+}$ $Isl^{Cre/+}$ (E, F) and $Tau^{EWS\text{-}Pea3/+}$ $Isl1^{Cre/+}$ (J, K, L) embryos for neuronal cell death at E13.5 by TUNEL (green; D, J), cell survival and proliferation at E16.5 by LacZ (blue) wholemount staining (E, K; lumbar levels L1 and L2 are shown), and BrdU (green)/LacZ (red) double labelling (F, L) respectively. Quantitative analysis ($n \geq 3$ independent experiments) of the mean number of apoptotic events relative to wild-type levels is shown in (M) and neuronal survival in (N) as percent of wild-type of DRG at lumbar levels L1 to L5 as quantified on serial sections.

(O) Western blot analysis of protein extracts isolated from lumbar DRG isolated from E16.5 wild-type (wt) and $Tau^{EWS\text{-}Pea3/+}$ $Isl1^{Cre/+}$ (mut) embryos using the following antibodies: Akt, p-Akt (Ser473), CREB, p-CREB (Ser133), Bax, Bcl-2 and Bcl-xl.

(P) Quantitative analysis of protein levels relative to wild-type in % is shown on the right (n=3 independent experiments).

Scale bar: (A-C, G-I) = 35μm; (D, J) = 40μm; (E, K) = 200μm; (F, L) = 50μm.

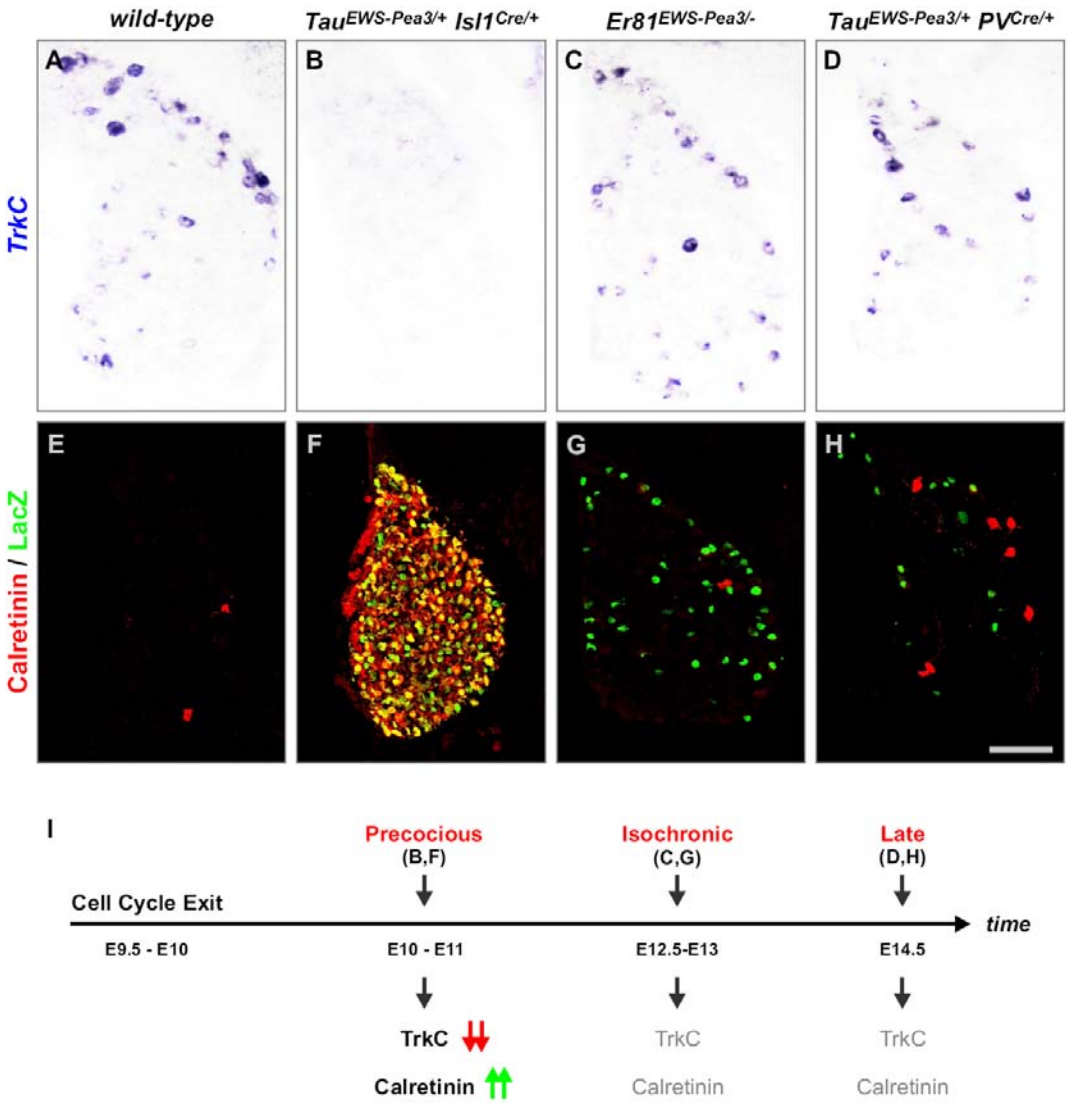

Figure 7. Gene expression analysis upon induction of precocious or isochronic ETS signaling (A-H) Analysis of *TrkC* expression by *in situ* hybridization (A-D) or Calretinin (red) and LacZ (green) expression by immunohistochemistry (E-H) on E16.5 lumbar DRG of wild-type (A, E), $Tau^{EWS\text{-}Pea3/+}$ $Isl1^{Cre/+}$ (B, F), $Er81^{EWS\text{-}Pea3/-}$ (C, G) and $Tau^{EWS\text{-}Pea3/+}$ $PV^{Cre/+}$ (D, H) embryos. (I) Summary diagram illustrating deregulation of TrkC (red arrows, downregulation) and Calretinin (green arrows, upregulation) expression upon precocious (B, F) induction of EWS-Pea3 expression in DRG neurons (B, F; E10-E11, i.e. shortly after cell cycle exit, E9.5-10). In contrast, activation of EWS-Pea3 from the endogenous *Er81* locus (C, G; E12.5-13) or via Cre recombinase expression from the *PV* locus activating expression from the *Tau* locus late (D, H; E14.5) does not interfere with the normal expression of *TrkC* and Calretinin (shown in grey). Scale bar: (A-D) = 65µm; (E-H) = 80µm.

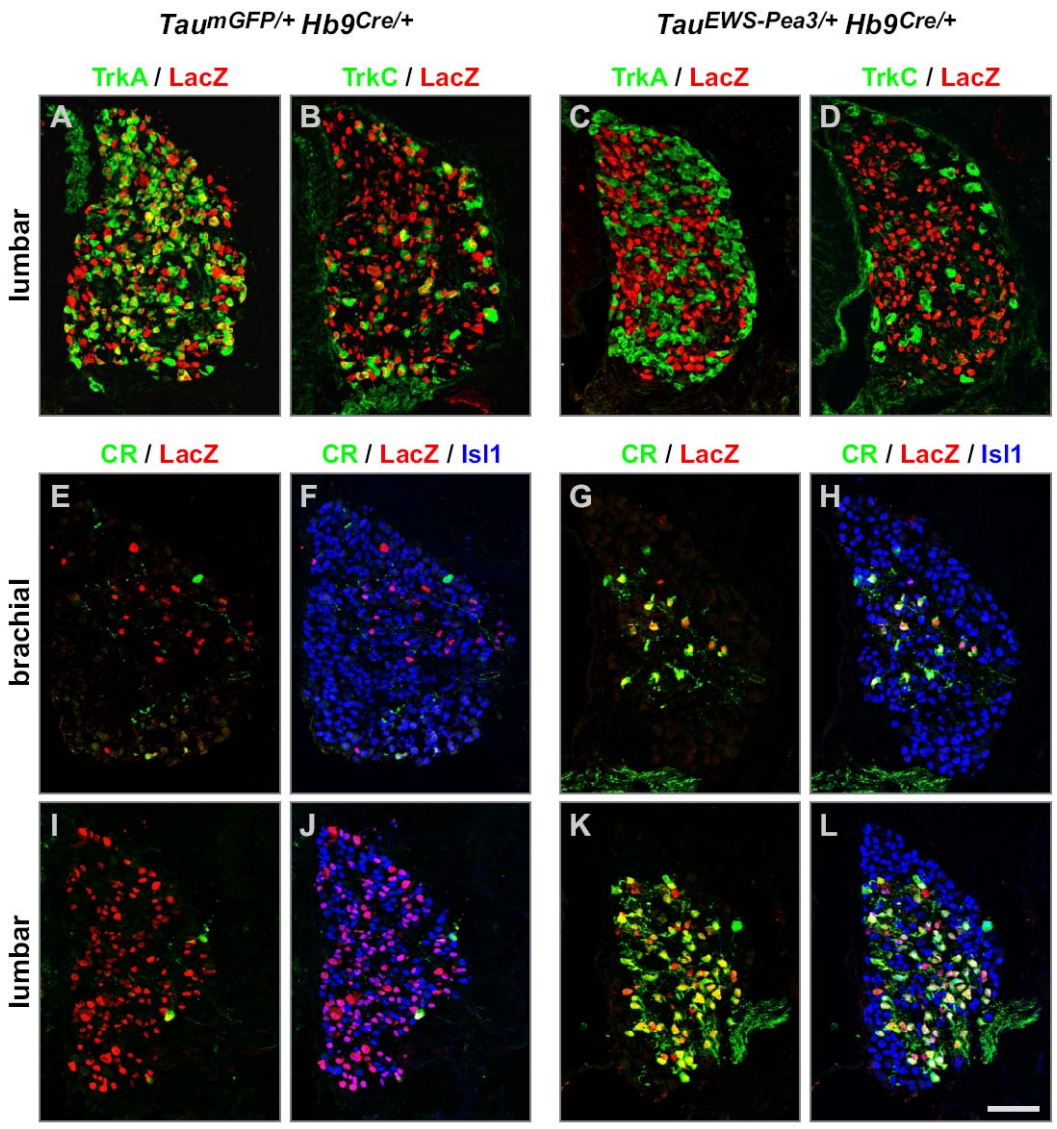

Figure 8. Precocious ETS signaling induces gene expression changes cell-autonomously

(A-D) Expression of TrkA (A, C; green), TrkC (B, D; green) and LacZ (red) in E16.5 lumbar DRG of *Tau*$^{mGFP/+}$ *Hb9*$^{Cre/+}$ (A, B) and *Tau*$^{EWS\text{-}Pea3/+}$ *Hb9*$^{Cre/+}$ (C, D) embryos.

(E-L) Expression of Calretinin (green), LacZ (red) and Isl1(F, J, H, L; blue) in E16.5 brachial (E-H) and lumbar (I-L) DRG of *Tau*$^{mGFP/+}$ *Hb9*$^{Cre/+}$ (E, F, I, J) and *Tau*$^{EWS\text{-}Pea3/+}$ *Hb9*$^{Cre/+}$ (G, H, K, L) embryos.

Scale bar: (A-D) = 80μm; (E-L) = 70μm.

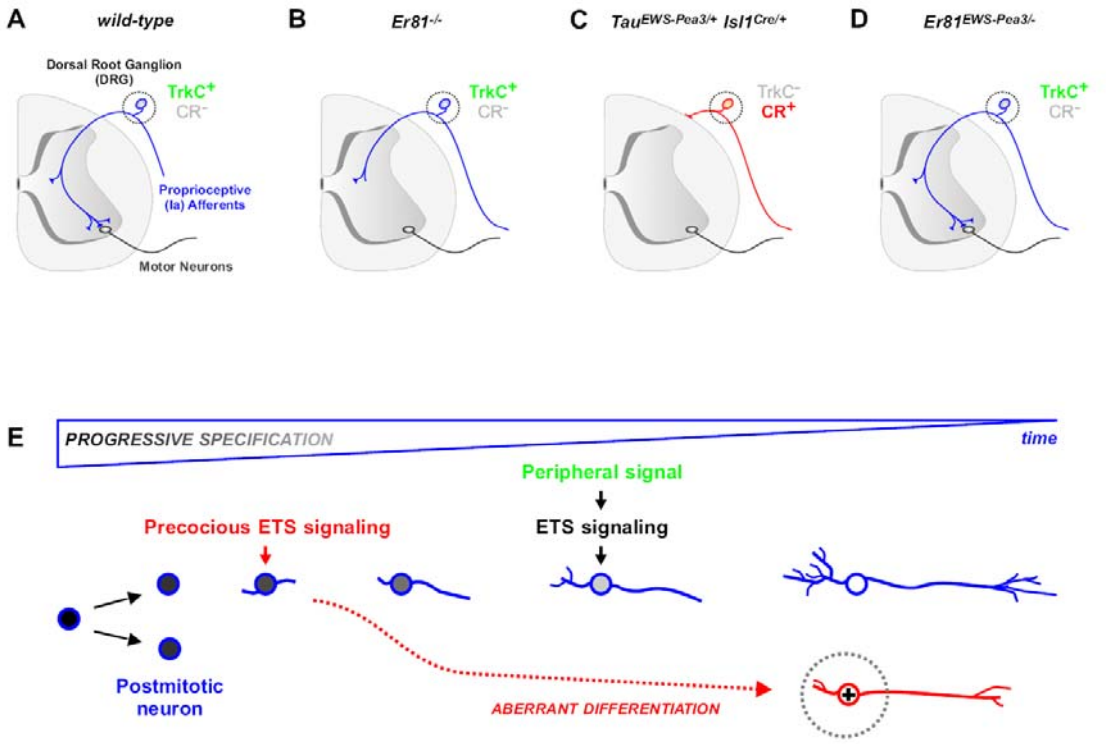

Figure 9. Progressive neuronal specification is paralleled by a developmental shift in response to ETS transcription factor signaling

Schematic summary diagram illustrating the importance of temporally appropriate upregulation of transcription factor expression during specification of DRG neurons for late aspects of neuronal differentiation and circuit assembly.

(A-D) Expression of *EWS-Pea3* from the endogenous *Er81* locus can rescue anatomical defects observed in *Er81*$^{-/-}$ mice and no change in expression of TrkC (green) or Calretinin (CR; grey) is observed in proprioceptive afferents (A, B, D). In contrast, precocious ETS signaling leads to severe defects in the establishment of DRG neuronal projections accompanied by inappropriate gene expression changes (C; upregulation of CR (red) and downregulation of TrkC (grey)).

(E) Precocious ETS signaling (red) during progressive specification of proprioceptive sensory neurons leads to aberrant neuronal differentiation (red dashed line). In contrast, the isochronic, target-induced (green; peripheral signal) onset of ETS transcription factor signaling (black) induces appropriate terminal neuronal differentiation (blue).

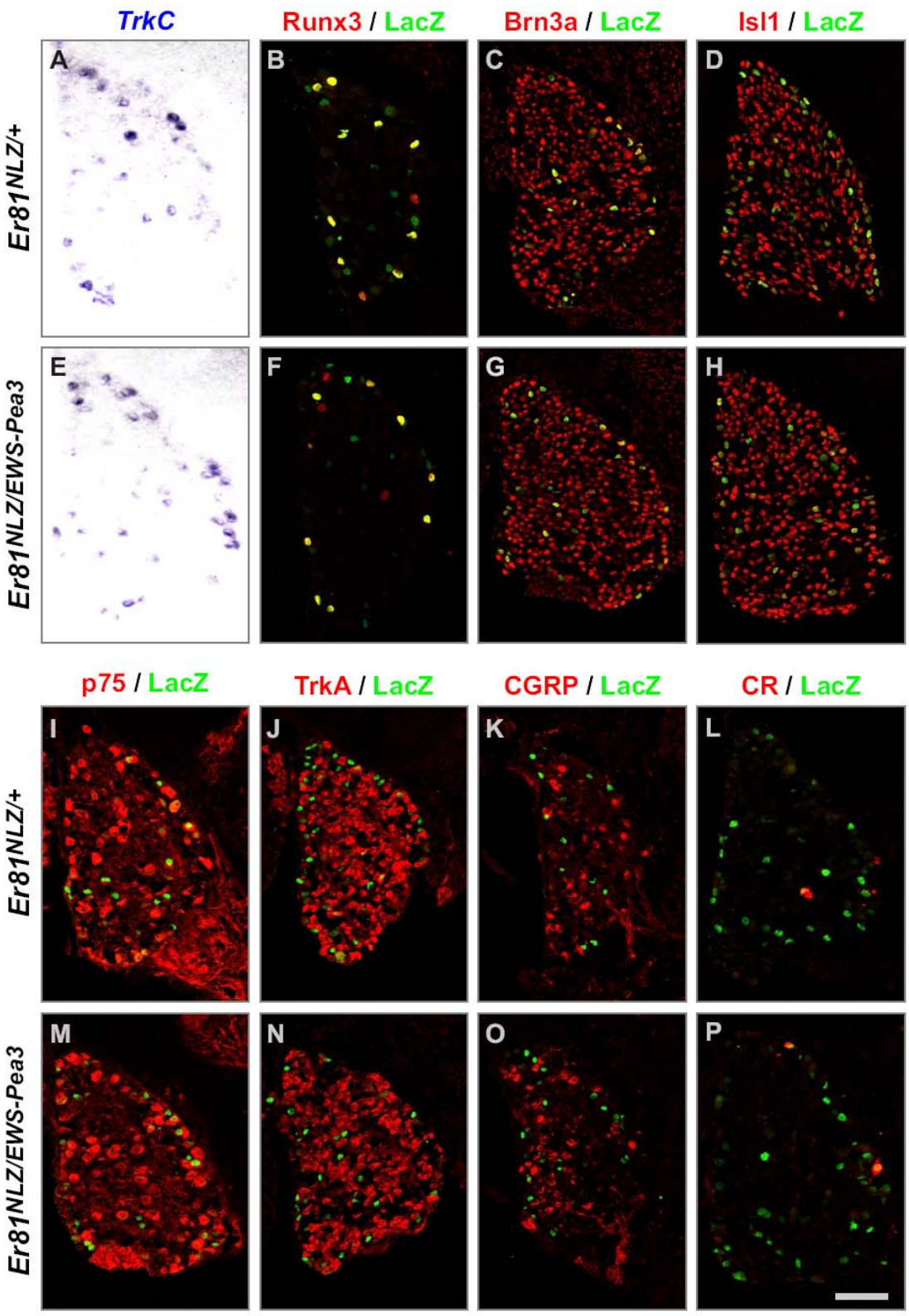
TrkC
Runx3 / LacZ
Brn3a / LacZ
Isl1 / LacZ
Er81NLZ/+
Er81NLZ/EWS-Pea3
A
B
C
D
E
F
G
H
p75 / LacZ
TrkA / LacZ
CGRP / LacZ
CR / LacZ
I
J
K
L
M
N
O
P

Supplemental Figure 1. Gene expression analysis in DRG neurons of *Er81*$^{EWS\text{-}Pea3}$ mice

Analysis of *TrkC* expression by *in situ* hybridization (A, E), Runx3 (red; B, F), Brn3a (red; C, G), Isl1 (red; D, H), p75 (red; I, M), TrkA (red; J, N), CGRP (red; K, O), Calretinin (CR; red; L, P) and LacZ (green; B-D, F-P) by immunohistochemistry on E16.5 lumbar DRG of *Er81*$^{NLZ/+}$ (A-D, I-L) and *Er81*$^{EWS\text{-}Pea3/-}$ (E-H, M-P) embryos.

Scale bar: (A, B, E, F, L, P) = 70μm; (C, D, G, H, I-K, M-O) = 75μm.

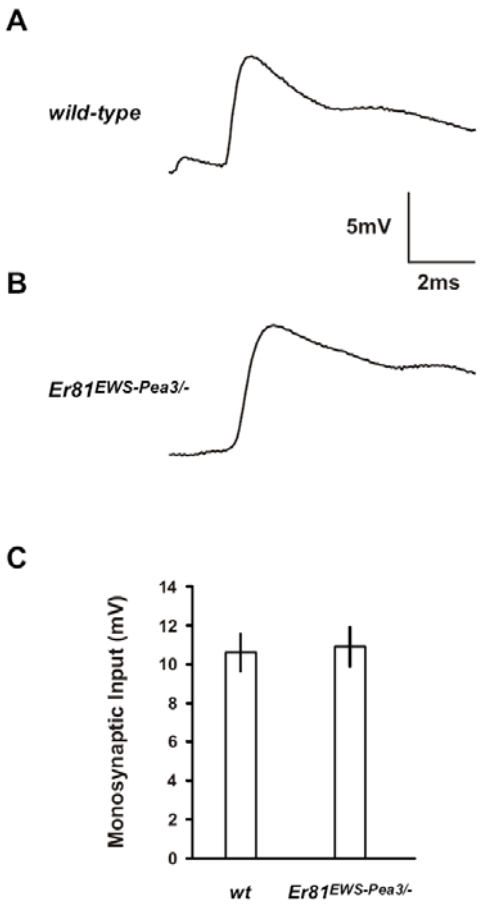

Supplemental Figure 2. Ia proprioceptive afferents make functional connections with motor neurons in *Er81*$^{EWS\text{-}Pea3}$ mutants

Representative traces from intracellular recordings measuring Ia afferent monosynaptic input to quadriceps motor neurons evoked by suprathreshold stimulation of the quadriceps nerve in wild-type (A) and *Er81*$^{EWS\text{-}Pea3/-}$ mutant (B) animals. (C) Average monosynaptic amplitudes (± SEM) from all recorded cells (wt: n=11; mutant: n=8).

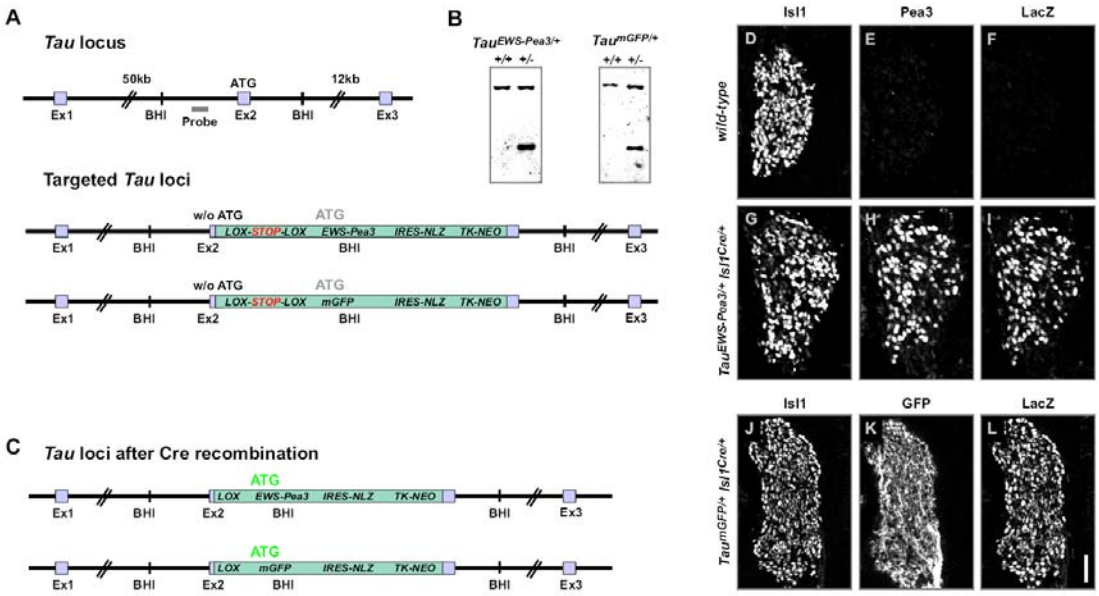

Supplemental Figure 3. Generation of mice expressing *EWS-Pea3* or *mGFP* in early postmitotic DRG neurons

(A) (Top panel) Organization of the *Tau* genomic locus in the region targeted by homologous recombination in analogy to Tucker et al. 2001. Exons 1-3 are shown as light blue boxes and the *Tau* start codon in exon 2 is indicated as ATG. The probe used to detect homologous recombination is shown as a grey box. (Middle; bottom panels) *Tau* locus after homologous recombination integrating targeting cassettes (green) into exon 2 with coincident elimination the endogenous *Tau* start codon. The integrated targeting cassettes allow for conditional expression of *EWS-Pea3* (middle) or membrane linked *eGFP* (*mGFP*;bottom) and *NLS-LacZ* (*NLZ*) upon Cre recombinase-mediated activation. In the absence of Cre recombinase, a transcriptional stop sequence flanked by *loxP* sites inhibits expression of the respective transgenes from their start codons (ATG in grey). (B) Southern blot analysis of $Tau^{EWS\text{-}Pea3/+}$ and $Tau^{mGFP/+}$ genomic DNA to detect the mutant allele. (C) In the presence of Cre recombinase, the transcriptional stop sequence in the cassettes integrated into the *Tau* locus is removed. Expression of *EWS-Pea3* (top) or *mGFP* (bottom) and *NLS-LacZ* (*NLZ*) can now occur in neurons coincidently expressing Cre recombinase and *Tau* (indicated as ATG in green).

(D-L) Expression of Isl1 (D, G, J), EWS-Pea3 (E, H) or GFP (K), and LacZ (F, I, L), in E12 (D-I) or E13.5 (J-L) DRG neurons of wild-type (D, E, F), $Tau^{EWS\text{-}Pea3/+}$ $Isl1^{Cre/+}$ (G, H, I) and $Tau^{mGFP/+}$ $Isl1^{Cre/+}$ (J, K, L) embryos. Scale bar: (D-F) = 40µm; (G-I) = 35µm; (J-K) = 50µm.

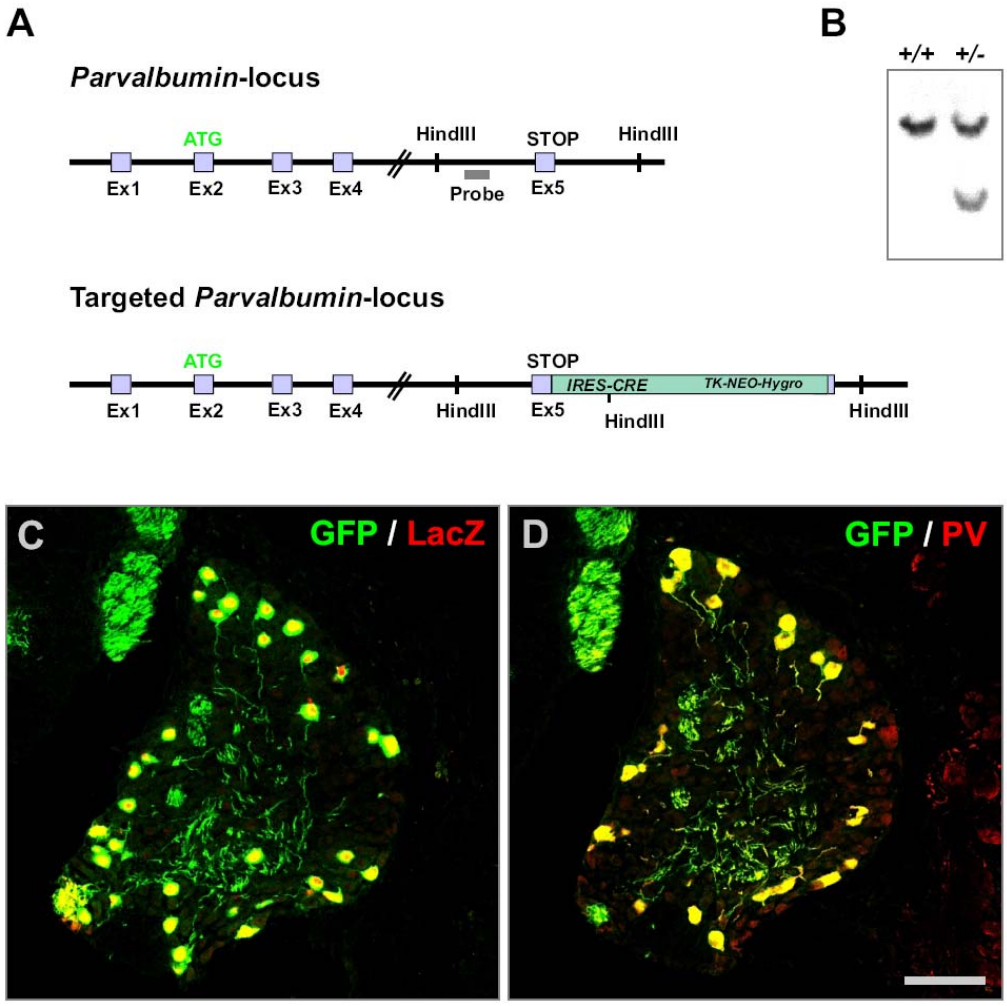

Supplemental Figure 4. Generation of *PV*^{Cre} mice

(A) (Top) Organization of the *Parvalbumin* (*PV*) genomic locus. Exons are schematically illustrated as light blue boxes, where exon 2 contains the start codon (ATG) and exon 5 contains the stop codon (STOP). Probe to screen for homologous recombination is shown as grey box. (Bottom) Schematic diagram to show the *PV* locus after the integration of an *IRES-Cre* cassette (green) 3' to the translational stop codon of *PV* using homologous recombination in ES cells. (B) Southern blot analysis of *PV*^{Cre} wild-type (+/+) and heterozygous (+/-) genomic DNA using the probe indicated in (A). (C, D) Expression of GFP (green) and LacZ (red: C) or PV (red: D) in P0 *Tau*$^{mGFP/+}$ *PV*$^{Cre/+}$ mice. Note that >90% of PV^{+} neurons coexpress GFP (D, data not shown). Scale bar: (C, D) = 50μm.

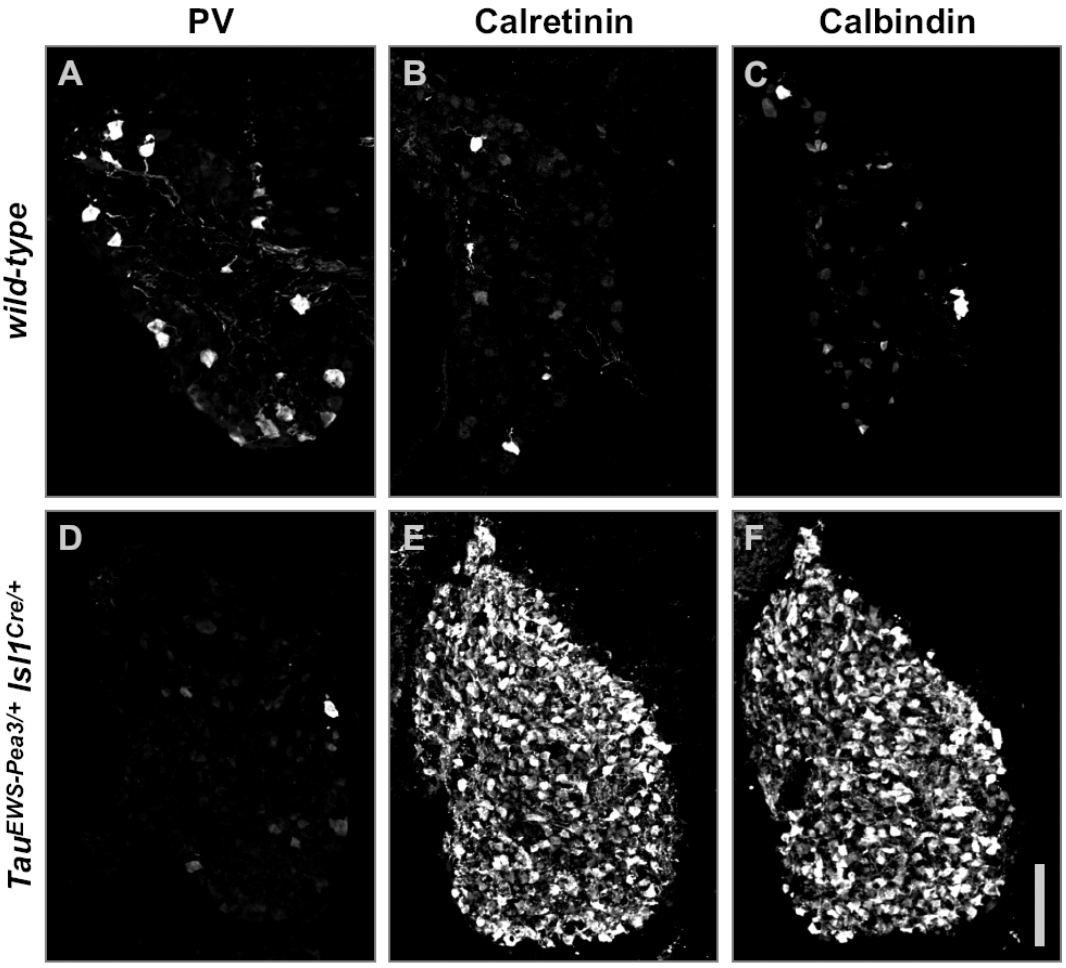

Supplemental Figure 5. Gene expression analysis upon precocious induction of EWS-Pea3 in DRG neurons

Immunohistochemical analysis of PV (A, D), Calretinin (B, E) and Calbindin (C, F) expression on E16.5 lumbar DRG of wild-type (A-C) and *Tau*$^{EWS\text{-}Pea3/+}$ *Isl1*$^{Cre/+}$ (D-F) embryos.

Scale bar = 80μm.

Abbreviations:

DRG	Dorsal root ganglion
E	Embryonic day
ETS	E twenty-six or E26 transformation specific
EWS	Ewing sarcoma
mGFP	Membrane-targeted green fluorescent protein
IRES	Internal ribosomal entry site
NGF	Nerve growth factor
NLS	Nuclear localization signal
NT-3	Neurotrophin 3
PV	Parvalbumin

Chapter 4

General Discussion and Perspectives

Previous work has shown that the formation of monosynaptic connections between IaPA and MNs within the spinal cord is occurring with a high level of specificity, but so far only very limited data was available on the mechanisms directing the assembly of such precise neuronal connectivity. To begin to get insight into the cellular and molecular pathways directing the formation of selective interactions between IaPAs and MNs in the spinal monosynaptic stretch reflex circuit, a careful comparison between dendrite pattern and IaPA-MN connectivity in both wild-type and *Pea3*$^{-/-}$ mice represented the major focus of my thesis. The findings and implications obtained throughout this work are discussed here within the broader context of neural network formation in the CNS.

Dendrite patterns as determinants for neuronal connectivity

The general function of a neuron is to connect spatially separated areas with each other, thereby allowing communication between these areas to ultimately control proper functioning of the organism. To achieve this challenging task, a neuron has to receive information from the area(s) from which it has to transmit information to the target structure. What would we do to receive information and communicate it specifically to somebody else? Indeed, we would need to form the accurate contact in order to be able to perform our task. In much the same way, a neuron depends on its appropriate connections. The result of no connections is no communication, but the result of wrong connections is misleading communication, which might be even worse than no communication at all. The mechanisms by which neurons form their connections are only partially understood. While there is quite some knowledge about axonal pathfinding towards the target area and the selection of the appropriate target areas, the mechanisms that directing dendrite growth and patterning are much less understood. This might be partially due to generally higher degree of complexity of dendritic trees when compared to axons. Dendritic trees mostly receive input and integrate information derived from multiple areas. For example, MNs in the spinal cord receive information from peripheral targets, spinal neural networks and from the brain and these inputs have to be integrated to produce the final motor output response in MNs. Most of the presynaptic inputs are

known to converge on dendrites of the postsynaptic neuron. Assuming that the presynaptic partners coming from different areas are located in stereotyped positions, the neuron has to form a selective spatial dendritic pattern in order to collect all its inputs. This is reflected by the huge variety of neuronal dendritic morphologies found in the vertebrate CNS, each belonging to a specific neuronal type (Mell B, 1994). Moreover, subgroups of neurons belonging to one type, as for the amacrine cells in the retina (MacNeil and Masland, 1998) and MNs in the spinal cord (Szekely et al., 1980) can be even further subdivided on the basis of the morphology of their dendritic tree. However, in these studies, a direct link between function and dendritic morphology has not been made. Pyramidal neurons in each layer of the cortex can also be subdivided on the basis of their specific dendritic patterns (McAllister et al., 1995) and by their lamina-specific dendritic termination zones. For example, pyramidal neurons in layer 6 of the visual cortex projecting to the lateral geniculate nucleus have an apical dendrite terminating in layer 3 and side branches in layer 4 and 5, while claustrum-projecting neurons have an apical dendrite that extends to layer 1 of the cerebral cortex with side branches in layer 5 (Katz, 1987). Another example of such a lamina specific dendritic projection pattern is found in the retina. Retinal ganglion cells (RGCs) receiving input from either the 'ON' or 'OFF' bipolar cells show a non-overlapping dendritic termination within the 'ON' or 'OFF' sublamina of the inner plexiform layer, respectively. Such a selective spatial dendritic termination zone correlating with the axonal innervation of a selective target (and most likely also with selective presynaptic connectivity) as shown for the cortex or the type of presynaptic inputs the cells receive as found in the retina is also nicely reflected in our study on the dendritic arborization patterns of subpopulations of spinal MNs. We could show a strong correlation between MN pool dendrite projection pattern and the presynaptic IaPA connectivity to a particular MN pool. Thus indeed it seems that neurons throughout the CNS acquire specific dendritic arborization patterns allowing them to sample input from those areas where their presynaptic terminations are located. Our study on CM and LD MN pools in addition suggests that dendrites might actively avoid areas in which axons terminate which are not required to make input to their dendrites.

However, the function of a neuron is not only determined by the pattern of presynaptic inputs it receives. Dendrites themselves are also actively involved in integration and processing of synaptic inputs contributing to the function that can be carried out by an individual neuron within the network it is implemented (Hausser et al., 2000). The dendritic arborization pattern thus contributes in different ways to the function of the neuron. The dendritic termination zone determines the initial presynaptic input pattern the neuron receives by the area it samples, and the complexity of dendritic arborization contributes to the shaping of the final activity pattern received by the soma.

Molecular mechanisms underlying dendrite patterning

What are the mechanisms through which neurons acquire their type and even subtype-specific dendrite morphologies? This is an important issue to resolve since factors that control dendrite patterning directly affect neuronal circuit connectivity and thus the functional output of this circuit. Genetic screens in Drosophila have identified numerous transcription factors regulating dendrite morphology, mainly controlling the length and complexity of the dendritic tree ((Grueber et al., 2003; Moore et al., 2002). We also found that a transcription factor controls dendrite morphology of a subgroup of spinal MNs. However in contrast to the above mentioned studies where it was found that the transcription factors *hamlet* and *cut* mainly regulate dendrite elaboration and branching, we found that *Pea3* in CM and LD MNs has an important role in directing the spatial organization of dendrites. These findings suggest that there might be specific transcriptional pathways responsible for controlling different aspects of dendrite patterning and maturation.

Our data also suggests that there is an important interplay between intrinsic and extrinsic factors during dendrite patterning, because the expression of Pea3 is induced by the target-derived factor GDNF. This idea is further supported by the finding that not only CM and LD but also other MNs express the GDNF receptors RET and Gfrα1, but they do not induce the expression of Pea3 when cultured *in vitro* (Haase et al., 2002).

These findings suggest that the signaling pathway described here is rather a permissive than an instructive one. They implicate the molecular identity and predetermination of the neurons, most likely through the expression of a defined set of Hox and LIM-HD transcription factors, in endowing the CM and LD MNs with the capacity to respond to GDNF by the induction of Pea3. Our findings thus support the idea that a target-derived factor regulates dendrite patterning of spinal MNs. This in contrast to a study in Drosophila where the authors have specifically eliminated muscle founder cells, using the UAS/GAL4 system to misexpress Notch in the developing mesoderm, thereby creating a muscle-less fly. These flies developed normal MN dendrite patterns (Landgraf et al., 2003) and therefore the authors suggested that interaction with the peripheral target muscle is not important for proper dendrite patterning in Drosophila. However, by selective elimination of all muscles, muscle mesenchyme is still present and it has been shown that GDNF is expressed at high levels in mesenchymal tissue (Brophy et al., 2001; Haase et al., 2002). Thus, we believe that the GDNF signal required for the induction of *Pea3* in MNs is not coming from the muscle itself, but instead from the mesenchyme surrounding the muscle. In addition to our finding that the target does communicate with MNs through the activation of a retrograde signal, in another study in Drosophila it has been also shown that interaction between neuron and target is critical for the induction of a specific molecular identity (Allan et al., 2003). In this study it was shown that the expression of the neuropeptide gene *FMRFamide* in neuropeptidergic cells depends on a combination of intrinsic expression of *squeeze* and *apterous* transcription factors, and that this expression represents a prerequisite for these neurons to be able to respond to the retrograde BMP signal from the target.

In support of our findings that GDNF controls dendrite morphology, other studies also have found that neurotrophic factors can control dendrite patterning. In organotypic slice cultures of the developing ferret cortex, it was shown that neurotrophins promote growth and branching of cortical pyramidal cells in a very specific manner. Specifically, different neurotrophins displayed differential effects on basal versus apical dendrite elaboration (McAllister et al., 1997; McAllister et al., 1995). Interestingly, these authors also showed that brain derived neurotrophic factor (BDNF) and neurotrophin 3 (NT-3) had opposing

effects on layer 4 and layer 6 pyramidal cells. In layer 4, NT-3 inhibited the dendritic growth stimulated by BDNF and visa versa for layer 6. An *in vivo* study in mice lacking tyrosine receptor kinase B (TrkB) from cortical pyramidal cells supported these *in vitro* studies by showing that these mice exhibited a reduction in the complexity of dendrites (Xu et al., 2000).

The mechanisms by which neurotrophins and their receptors induce these effects still have to be resolved. At least two studies have shown that neurotrophins can regulate the expression of transcription factors required for neuronal patterning. The expression of peripheral NT-3 results in the induction of the ETS transcription factor Er81, a family member of Pea3, in PAs, and *Er81* expression in turn is required for the elaboration of a proper termination of IaPAs in the ventral horn of the spinal cord (Arber et al., 2000b). In addition, our findings that GDNF induces the expression of the transcription factor *Pea3* required for MN dendrite patterning. An idea which would be interesting to pursue further is that neurotrophins might mediate their effect through cross-talk with a family of axon guidance molecules, the semaphorins. A recent study has demonstrated that co-expression of BDNF with semaphorin3E (Sema3E) in RGC explant cultures of E6 chickens counteracts the collapsing activity of Sema3E on RGC axon growth cones. This cross-talk between semaphorins and neurotrophins was suggested, because both semaphorins and neurotrophins partially mediate their signaling via changes in intracellular cyclic nucleotide levels (Steffensky et al., 2006). Interestingly in this context, in *Pea3*$^{-/-}$ mice, the expression of *Sema3E* in CM MNs is absent (Livet et al., 2002), thus showing that *Sema3E*, either directly or indirectly, is controlled by the activity of Pea3.

An increasing amount of data seems to suggest that molecules initially described as axon guidance molecules play also crucial roles in dendrite patterning. Among these molecules are Slits and their receptors roundabout (Robos), Netrin and its receptor DCC/Frazzled/UNC-40 as well as semaphorins (Furrer et al., 2003; Godenschwege et al., 2002; Polleux et al., 2000; Whitford et al., 2002). For example, analyses of the roles of Slit/Robo, Commisureless (a regulator of Robo expression), and Netrin/Frazzled in both

axonal and dendritic guidance of three individually identifiable MNs in Drosophila embryonic CNS showed that mutations of these genes led to both axonal and dendritic guidance defects at the CNS midline (Furrer et al., 2003). Interestingly, these genes can affect axon and dendrite patterning of a single neuron independently of each other. Another axon guidance molecule that can regulate both axon and dendrite growth of the same neuronal type is Sema3A (Polleux et al., 2000). In *Sema3A*$^{-/-}$ mice, many cortical pyramidal neurons show misoriented cortical dendrites (Polleux et al., 1998; Polleux et al., 2000). Moreover, in a slice overlay assay in which dissociated mouse cortical neurons were grown on top of cultured rat brain slices exposed to Sema3A-expressing 293T cell aggregates, the apical dendrites specifically extended towards the Sema3A source (Polleux et al., 2000). In contrast, the axons of these neurons were repelled by Sema3A (He and Tessier-Lavigne, 1997; Kolodkin et al., 1997; Polleux et al., 1998). This differential response of axons and dendrites to Sema3A appears to be mediated by the asymmetric localization of soluble guanylate cyclase (SGC) to developing apical dendrites (Polleux et al., 2000). As a third example, Slit/Robo signaling also mediates dendritic growth and branching in mammalian cortical neurons. Slit/Robo mutant mice have not yet been analyzed in the context of dendrite development, but *in vitro* experiments performed using primary cell culture assays with developing rat cortex have demonstrated that Slit1 promotes dendrite growth and branching through the interaction with Robo1 and Robo2 (Whitford et al., 2002).

Developing MNs at overlapping levels of the brachial spinal cord in mice were found to express besides Sema3E, also Semaphorins Sema3A, Sema3C and Sema3F (Cohen et al., 2005). Studies on axon guidance have shown that Sema3A and Sema3F expression in brachial LMC MNs is required for proper axon guidance to the limb, by signaling through NP-1 and NP-2, respectively (Huber et al., 2005). Relating these findings to our observation that Sema3E expression is absent in CM MNs of *Pea3* mutant mice, it would be interesting to assess whether the expression of the different class 3 Semaphorins at overlapping segmental levels of the spinal cord play also a role in regulating the precise patterns with which IaPA-MN connections are formed within the monosynaptic reflex circuit.

Activity-dependent mechanisms underlying dendrite patterning

In addition to molecular signals, several observations suggest a role for neuronal activity in regulating dendrite morphology. Many regions of the CNS, including the retina, hippocampus and cortex, show spontaneous calcium transients before sensory experience (Benari et al., 1997; Feller et al., 1996; Garaschuk et al., 2000; Yuste et al., 1995). For example TTX sensitive calcium waves were observed in the developing cortex, traveling across the anterior-posterior axis (Garaschuk et al., 2000). This period of spontaneous network activity correlates with the period of rapid dendritic growth (Konur and Ghosh, 2005). Calcium influx is mediated mainly by voltage-sensitive calcium channels (VSCC) and NMDA receptors. Calcium transients in developing neurons can activate a variety of intracellular signaling pathways. The major signaling targets of calcium influx are calcium/calmodulin-dependent protein kinases (CaMKs) and mitogen-activated kinase (MAPK) (Ghosh and Greenberg, 1995). Interference with a variety of signaling pathways induced by these factors effect various aspects of early dendritic development (Konur and Ghosh, 2005). Thus, CaMKs and MAPKs appear to be regulators of initial dendritic growth, before sensory input is present.

Time-lapse imaging of dendritic arbor growth in the intact animal has revealed that dendrite growth and branching of retinal tectal neurons in Xenopus tadpoles and MNs in zebrafish, is a highly dynamic process (Jontes et al., 2000; Rajan and Cline, 1998). Young neurons contain mainly ‘silent’ synapses, which have a low AMPA/NMDA ratio. Upon activity, AMPA receptors become inserted into the postsynaptic membrane, correlating with a decrease in the dynamics and an increase in the stabilization of the dendritic arbor. This might reflect the necessity of dendrites to probe their environment for appropriate presynaptic contacts. Once they have encountered an appropriate presynaptic partner, synaptic activity is increased. This induces an increase in the number of AMPA receptors inserted into the postsynaptic membrane, in concert with the activation of other downstream pathways induced by a change in calcium influx. Together, this mechanism creates a ‘stop-signal’ for dendritic

growth and leads to the stabilization of the dendritic arbor (Cline, 2001). Whether dendritic growth of MNs in the spinal cord of mice is also a dynamic process is still an open question. However, since spinal cord tissue is deeply embedded and dense tissue, live imaging is very difficult to achieve and not technically feasible at present. Moreover, in order to trace MNs in the spinal cord, we depend on axons growing already out into the periphery. This time point might already be too late to observe the initial outgrowth of dendrites. In order to visualize MN dendrites at the time point of initial dendritic outgrowth we depend on genetic tools to label these cells. For this approach it would be of high value to find MN pool-specific molecular markers allowing us to MN pool specifically express GFP and compare not only the initial outgrowth and patterning of a MN dendritic tree, but also to compare the initial patterning of different MN pools. This would allow us to answer the question whether initially, all MNs exhibit the same 'baseline' dendritic pattern. For example all MNs would exhibit a radial dendritic morphology as observed for the MNs analyzed in our study in the *Pea3* mutant, and subsequently the dendrite patterns would be remodeled upon contact with extrinsic factors, to sub-serve the specific function that has to be carried out by a particular MN pool.

We can rule out the possibility that ingrowth and activity of PAs play a major role in shaping the initial spatial pattern of MN dendrites, since tissue specific ablation of these afferents during development did not have an obvious effect on spatial dendrite morphology. However, we have not focused our studies on determining the precise dendritic length and number of branches. For this reason, we cannot exclude the possibility that PAs are involved in regulating refinement of MN dendritic morphology. Moreover, we have analyzed the morphology of the dendritic tree only during the 1st postnatal week. Studies in rat have demonstrated that from the 1st till the 3rd postnatal week, MN dendrites exhibit an extensive growth and increase in the number of dendritic bifurcations, followed by a week of dendritic regression till the mature state is reached (Kalb, 1994). Blocking NMDA receptors using either the NMDA receptor antagonist MK-801 or aminophosphonovaleric acid (APV), during this postnatal period in rodents, resulted in a decrease in the number of dendritic branches but did not affect the radial

length of the longest dendrite of spinal MNs. These findings thus suggest that activation of the NMDA receptor promotes elaboration of new dendritic branches (Inglis et al., 1998; Kalb, 1994). An activity-dependent molecular pathway, which is likely to underlie these developmental changes, involves the activity-dependent expression of the neuronal nitric oxide synthase (nNOS) upon activation of the NMDA receptor. Activation of the NMDA receptor leads to an influx of Ca^{2+} through the NMDA receptor channel. This increase in intracellular Ca^{2+} might induce expression of the Ca^{2+}-dependent effector molecule nNOS which is physically linked and functionally coupled to the NMDA receptor ((Brenman et al., 1996; Garthwaite et al., 1988). This in turn leads to a local production of the growth promoting substance, nitric oxide (NO) in the ventral horn. nNOS mutant mice exhibit a very similar MN dendrite phenotype as mice treated with MK-801 or APV (reduction in total dendritic surface, due to lower number of dendritic bifurcations; (Inglis et al., 1998). A further observation that supports the idea that NMDA-dependent release of NO is involved in promoting the growth of the dendritic tree during the first 3 weeks of postnatal development is on the expression pattern of nNOS, NMDA receptors and NO in the ventral horn of the spinal cord. nNOS in the INs that surround the MNs, NMDA and non-NMDA subtypes of glutamate receptors and NO are only transiently expressed during the first few weeks of postnatal development (Jakowec et al., 1995; Kalb and Agostini, 1993; Kalb et al., 1992). Whether NO effects MN dendrite growth directly or indirectly via a postulated effect on ingrowing afferents is not known. A described function for NO is the induction of growth cone collapse (Hess et al., 1993). This led to the suggestion that NO serves as a 'Stop Signal' for ingrowing axons to maintain the initial contact between axons and their postsynaptic targets. The absence of NO due to blocking NMDA receptor activity in the spinal cord or through the elimination of nNOS in *nNOS* mutant mice, may lead to a reduction in the number of presynaptic contacts onto MN dendrites. The synaptotropic hypothesis of Vaughn (Vaughn et al., 1988), that synapses give tropic support to MN dendrites, together with the *in vitro* observation that branching of MN dendrites is promoted by co-culture with INs that form synapses on MN soma and dendrites, would suggest that the loss of presynaptic input leads to reduced growth of MN dendrites (Inglis et al., 1998). From these findings we can thus conclude that, although we do not see an effect on the spatial

dendritic organization of the dendritic tree in the absence of PAs in the 1st week of postnatal development, we might see an effect on dendrite remodeling after the end this critical time period of NMDA receptor sensitive MN dendrite growth. It would therefore be interesting to compare the spatial organization from dendritic arbors of for example CM and Tri MN pools in the 1st postnatal week with those in the 3rd postnatal week. This would reveal whether NMDA receptor-dependent activity is also required for the fine tuning of the final spatial dendritic organization or whether direction of main dendritic projections is determined earlier during development and that NMDA receptor-dependent activity in the first 3 postnatal weeks is solely required for dendrite growth and branching, in order to cope with the overall growth of the organism and the increase in presynaptic inputs from in growing descending pathways during the first 3 postnatal weeks. Interestingly, visual experience in the early postnatal life of cats can modify the orientation of cortical layer III pyramidal cell dendrites, which may determine receptive field properties (Tieman and Hirsch, 1982). Afferents also seem to play important roles in shaping dendrites in several other areas of the brain, in which it has been found that a loss or increase of sensory input alters dendritic development of the target neurons ((Coleman and Riesen, 1968; Greenough and Volkmar, 1973; Holloway, 1966; Sin et al., 2002; Volkmar and Greenough, 1972; Wiesel and Hubel, 1963).

The stabilization of the dendritic morphology after this early postnatal period of rapid dendrite growth in rodents might also underlie the eventual strengthening of synapses. As discussed above, studies on the dendritic structure of retinal tectal neurons in Xenopus and MNs in zebrafish have demonstrated that the dendritic arbor becomes stabilized upon an activity-dependent increase of the AMPA receptor content inserted into the postsynaptic membrane, reflecting a strengthening of synapses ((Jontes et al., 2000; Rajan et al., 1998; Rajan and Cline, 1998). In the first 3 postnatal weeks in rodents, LTP can be induced in spinal MNs (Pockett and Figurov, 1993), which reflects strengthening of synapses. Furthermore, a developmental change in glutamate receptor (GluR) subunit composition of AMPA receptors is also likely to underlie dendrite arbor stabilization, since it has been shown that the GluR1 subunit of the AMPA receptor,

expressed highly in only neonatal MNs, can induce remodeling of the mature dendritic arbor when reintroduced into mature MNs (Inglis et al., 2002).

The precise development of MN dendrites is most likely due to an interaction between cell autonomous intrinsic factors regulating the number and orientation of primary dendrites, and extrinsic factors controlling branching and number of terminal dendrites (Kalb, 1994). Cross-linking intrinsic and extrinsic factors produces an effective way to establish the enormous variety of dendrite patterns and most likely also precise synaptic connectivity, contributing to the formation of precise neuronal circuits found within the CNS.

Neuronal information processing in dendrites

After having received the presynaptic input the second major function of the dendrite is to compute this input. Cajal was the first one to describe that the information flow in a neuron is going from synapse -> dendrite -> soma -> axon -> synapse. In that early time, it was generally thought that dendrites were passive structures which simply conducted a current from the site of initiation to the soma. The idea was that distal synapses would not have any significance since the current would have shunted till it would have reached the soma, due to the conductive properties of the membrane. However, Rall was the first one to show that dendrites were critical to signal processing due to their structural and electrical properties. Surprisingly, it became apparent that distal synapses are in fact effective in activating the soma. Thanks to an improvement in sharp electrode and patch clamp recording techniques our knowledge about synaptic integration and processing by dendrites has enormously increased (Hausser et al., 2000). We know now that dendrites do not have just passive properties, but are highly specialized structures actively involved in generating responses.

Dendritic recordings from cerebellar Purkinje and dendritic hippocampal neurons provided evidence that dendrites were highly excitable structures containing voltage-

gaited ion-channels used for the generation of spikes (Fujita, 1968; Llinas et al., 1968; Llinas and Sugimori, 1980a; Llinas and Sugimori, 1980b). Sophisticated patch-clamp recording techniques have made it possible to record from different sites of a neuron in a brain slice under visual control (Stuart et al., 1993), including distal dendritic sites. This together with immunohistochemical techniques has revealed that voltage-gated ion channels are widely distributed across the dendritic tree. The distribution of the channels across the dendritic arbor differs between neuronal types and probably even neuronal subtypes. It seems that each neuronal type has a highly regulated set of dendritic voltage gated channels, the pattern of which might change during development and is modulated by neurotransmitters (Hausser et al., 2000). The dendrites can, partially through a non-equal distribution of voltage-gated ion channels and through specific dendritic morphologies, be divided into compartments, which can function as isolated units. The importance of dendritic morphology in determining the outcome of a particular signal was shown by modeling experiments in a neocortical layer V neuron versus a cerebellar Purkinje cell, two neurons with a different morphology. They were provided with the same uniform density of voltage-gated Na+ and K+ channels. The efficacy of a backpropagating spike (action potential initiated in axon and subsequently innervates soma and dendrites) or dendritic spike was assessed. Showing that the morphology clearly influences the degree to which the spike is transmitted into and through the dendritic tree (Vetter et al., 2001).

Thus the development of a dendritic tree which can sub-serve its specific function does not only require the formation of a highly complex structure, but in addition also has to regulate the precise expression of electrical and chemical properties. This, together with the finding that many aspects of dendrite formation are developmentally regulated, reveal that dendrite patterning, as simple as the word may sound, is a highly complicated developmental process.

References

Allan, D. W., St Pierre, S. E., Miguel-Aliaga, I., and Thor, S. (2003). Specification of neuropeptide cell identity by the integration of retrograde BMP signaling and a combinatorial transcription factor code. Cell *113*, 73-86.

Anderson, D. J., Groves, A., Lo, L., Ma, Q., Rao, M., Shah, N. M., and Sommer, L. (1997). Cell lineage determination and the control of neuronal identity in the neural crest. Cold Spring Harb Symp Quant Biol *62*, 493-504.

Anderson, W. W., and Collingridge, G. L. (2001). The LTP Program: a data acquisition program for on-line analysis of long-term potentiation and other synaptic events. J Neurosci Methods *108*, 71-83.

Arber, S., Han, B., Mendelsohn, M., Smith, M., Jessell, T. M., and Sockanathan, S. (1999). Requirement for the homeobox gene Hb9 in the consolidation of motor neuron identity. Neuron *23*, 659-674.

Arber, S., Ladle, D. R., Lin, J. H., Frank, E., and Jessell, T. M. (2000a). ETS gene Er81 controls the formation of functional connections between group Ia sensory afferents and motor neurons. Cell *101*, 485-498.

Arvand, A., and Denny, C. T. (2001). Biology of EWS/ETS fusions in Ewing's family tumors. Oncogene *20*, 5747-5754.

Baldissera, F., Hultbron, H., and Llert, M. (1981). Handbook of Physiology: Integration in spinal neuronal systems (Bethesda, MD, USA: American Physiological Society).

Baulac, M., and Meininger, V. (1981). [Organization of pectoral muscle motor neurons in the rat. Contribution to the study of the axillary arch (Achselbogen)]. Acta Anat (Basel) *109*, 209-217.

Benari, B., Erel, J., Allen, H. N., Friedman, J., Kiat, H., Silverman, J. M., Trento, A., and Berman, D. (1997). Aneurysm of saphenous vein bypass graft detected by first-pass radionuclide ventriculography. Am Heart J *133*, 133-136.

Bibel, M., and Barde, Y. A. (2000). Neurotrophins: key regulators of cell fate and cell shape in the vertebrate nervous system. Genes Dev *14*, 2919-2937.

Blaser, P. F., Catsicas, S., and Clarke, P. G. (1990). Retrograde modulation of dendritic geometry in the vertebrate brain during development. Brain Res Dev Brain Res *57*, 139-142.

Bojovic, B. B., and Hassell, J. A. (2001). The PEA3 Ets transcription factor comprises multiple domains that regulate transactivation and DNA binding. J Biol Chem *276*, 4509-4521.

Brenman, J. E., Christopherson, K. S., Craven, S. E., McGee, A. W., and Bredt, D. S. (1996). Cloning and characterization of postsynaptic density 93, a nitric oxide synthase interacting protein. J Neurosci *16*, 7407-7415.

Brophy, P. D., Ostrom, L., Lang, K. M., and Dressler, G. R. (2001). Regulation of ureteric bud outgrowth by Pax2-dependent activation of the glial derived neurotrophic factor gene. Development *128*, 4747-4756.

Brown, A. (1981a). Organization in the spinal cord (New York: Springer).

Brown, A. G. (1981b). Organization in the spinal cord: the anatomy and physiology of identified neurones (Berlin: Springer-Verlag).

Brown, A. G., and Fyffe, R. E. (1978). The morphology of group Ia afferent fibre collaterals in the spinal cord of the cat. J Physiol *274*, 111-127.

Butt, S. J., and Kiehn, O. (2003). Functional identification of interneurons responsible for left-right coordination of hindlimbs in mammals. Neuron *38*, 953-963.
Clandinin, T. R., and Zipursky, S. L. (2002). Making connections in the fly visual system. Neuron *35*, 827-841.

Cline, H. T. (2001). Dendritic arbor development and synaptogenesis. Curr Opin Neurobiol *11*, 118-126.

Cohen, S., Funkelstein, L., Livet, J., Rougon, G., Henderson, C. E., Castellani, V., and Mann, F. (2005). A semaphorin code defines subpopulations of spinal motor neurons during mouse development. Eur J Neurosci *21*, 1767-1776.

Coleman, P. D., and Riesen, A. H. (1968). Evironmental effects on cortical dendritic fields. I. Rearing in the dark. J Anat *102*, 363-374.

Dasen, J. S., Liu, J. P., and Jessell, T. M. (2003). Motor neuron columnar fate imposed by sequential phases of Hox-c activity. Nature *425*, 926-933.

Dasen, J. S., Tice, B. C., Brenner-Morton, S., and Jessell, T. M. (2005). A Hox regulatory network establishes motor neuron pool identity and target-muscle connectivity. Cell *123*, 477-491.

de Alava, E., and Gerald, W. L. (2000). Molecular biology of the Ewing's sarcoma/primitive neuroectodermal tumor family. J Clin Oncol *18*, 204-213.

de Launoit, Y., Baert, J. L., Chotteau, A., Monte, D., Defossez, P. A., Coutte, L., Pelczar, H., and Leenders, F. (1997). Structure-function relationships of the PEA3 group of Ets-related transcription factors. Biochem Mol Med *61*, 127-135.

De Paola, V., Arber, S., and Caroni, P. (2003). AMPA receptors regulate dynamic equilibrium of presynaptic terminals in mature hippocampal networks. Nat Neurosci *6*, 491-500.

Doyle, M. W., and Andresen, M. C. (2001). Reliability of monosynaptic sensory transmission in brain stem neurons in vitro. J Neurophysiol *85*, 2213-2223.

Eccles, J. C., Eccles, R. M., and Lundberg, A. (1957). The convergence of monosynaptic excitatory afferents on to many different species of alpha motoneurones. J Physiol (Lond) *137*, 22-50.

Edlund, T., and Jessell, T. M. (1999). Progression from extrinsic to intrinsic signaling in cell fate specification: a view from the nervous system. Cell *96*, 211-224.

Feller, M. B., Delaney, K. R., and Tank, D. W. (1996). Presynaptic calcium dynamics at the frog retinotectal synapse. J Neurophysiol *76*, 381-400.

Ferguson, B. A. (1983). Development of motor innervation of the chick following dorsal-ventral limb bud rotations. J Neurosci *3*, 1760-1772.

Frank, C. B., and Jackson, D. W. (1997). The science of reconstruction of the anterior cruciate ligament. J Bone Joint Surg Am *79*, 1556-1576.

Frank, E., Smith, C., and Mendelson, B. (1988). Strategies for selective synapse formation between muscle sensory and motor neurons in the spinal cord (Sunderland, MA: Sinauer Associates Ind.).

Frank, E., and Wenner, P. (1993). Environmental specification of neuronal connectivity. Neuron *10*, 779-785.

Frank, E., and Westerfield, M. (1982). Synaptic organization of sensory and motor neurones innervating triceps brachii muscles in the bullfrog. J Physiol *324*, 479-494.

Frank, E., and Westerfield, M. (1983). Development of sensory-motor synapses in the spinal cord of the frog. J Physiol *343*, 593-610.

Fujita, Y. (1968). Activity of dendrites of single Purkinje cells and its relationship to so-called inactivation response in rabbit cerebellum. J Neurophysiol *31*, 131-141.

Furrer, M. P., Kim, S., Wolf, B., and Chiba, A. (2003). Robo and Frazzled/DCC mediate dendritic guidance at the CNS midline. Nat Neurosci *6*, 223-230.

Garaschuk, O., Linn, J., Eilers, J., and Konnerth, A. (2000). Large-scale oscillatory calcium waves in the immature cortex. Nat Neurosci *3*, 452-459.

Garthwaite, J., Charles, S. L., and Chess-Williams, R. (1988). Endothelium-derived relaxing factor release on activation of NMDA receptors suggests role as intercellular messenger in the brain. Nature *336*, 385-388.

Ghosh, A., and Greenberg, M. E. (1995). Calcium signaling in neurons: molecular mechanisms and cellular consequences. Science *268*, 239-247.

Godenschwege, T. A., Simpson, J. H., Shan, X., Bashaw, G. J., Goodman, C. S., and Murphey, R. K. (2002). Ectopic expression in the giant fiber system of Drosophila reveals distinct roles for roundabout (Robo), Robo2, and Robo3 in dendritic guidance and synaptic connectivity. J Neurosci *22*, 3117-3129.

Gosgnach, S., Lanuza, G. M., Butt, S. J., Saueressig, H., Zhang, Y., Velasquez, T., Riethmacher, D., Callaway, E. M., Kiehn, O., and Goulding, M. (2006). V1 spinal neurons regulate the speed of vertebrate locomotor outputs. Nature *440*, 215-219.

Goulding, M., and Pfaff, S. L. (2005). Development of circuits that generate simple rhythmic behaviors in vertebrates. Curr Opin Neurobiol *15*, 14-20.

Greenall, A., Willingham, N., Cheung, E., Boam, D. S., and Sharrocks, A. D. (2001). DNA binding by the ETS-domain transcription factor PEA3 is regulated by intramolecular and intermolecular protein.protein interactions. J Biol Chem *276*, 16207-16215.

Greene, E. C. (1935). Anatomy of the rat (New York: Hafner Press).
Greenough, W. T., and Volkmar, F. R. (1973). Pattern of dendritic branching in occipital cortex of rats reared in complex environments. Exp Neurol *40*, 491-504.

Grueber, W. B., Jan, L. Y., and Jan, Y. N. (2003). Different levels of the homeodomain protein cut regulate distinct dendrite branching patterns of Drosophila multidendritic neurons. Cell *112*, 805-818.

Gurdon, J. B., and Bourillot, P. Y. (2001). Morphogen gradient interpretation. Nature *413*, 797-803.

Haase, G., Dessaud, E., Garces, A., de Bovis, B., Birling, M., Filippi, P., Schmalbruch, H., Arber, S., and deLapeyriere, O. (2002). GDNF acts through PEA3 to regulate cell body positioning and muscle innervation of specific motor neuron pools. Neuron *35*, 893-905.

Hanson, M. G., and Landmesser, L. T. (2004). Normal patterns of spontaneous activity are required for correct motor axon guidance and the expression of specific guidance molecules. Neuron *43*, 687-701.

Hausser, M., Spruston, N., and Stuart, G. J. (2000). Diversity and dynamics of dendritic signaling. Science *290*, 739-744.

He, Z., and Tessier-Lavigne, M. (1997). Neuropilin is a receptor for the axonal chemorepellent Semaphorin III. Cell *90*, 739-751.

Hess, D. T., Patterson, S. I., Smith, D. S., and Skene, J. H. (1993). Neuronal growth cone collapse and inhibition of protein fatty acylation by nitric oxide. Nature *366*, 562-565.

Hippenmeyer, S., Kramer, I., and Arber, S. (2004). Control of neuronal phenotype: what targets tell the cell bodies. Trends Neurosci *27*, 482-488.

Hippenmeyer, S., Shneider, N. A., Birchmeier, C., Burden, S. J., Jessell, T. M., and Arber, S. (2002). A role for neuregulin1 signaling in muscle spindle differentiation. Neuron *36*, 1035-1049.

Hippenmeyer, S., Vrieseling, E., Sigrist, M., Portmann, T., Laengle, C., Ladle, D. R., and Arber, S. (2005). A developmental switch in the response of DRG neurons to ETS transcription factor signaling. PLoS Biol *3*, e159.

Holloway, R. L., Jr. (1966). Dendritic branching: some preliminary results of training and complexity in rat visual cortex. Brain Res *2*, 393-396.

Huang, E. J., and Reichardt, L. F. (2001). Neurotrophins: roles in neuronal development and function. Annu Rev Neurosci *24*, 677-736.

Huang, E. J., and Reichardt, L. F. (2003). Trk receptors: roles in neuronal signal transduction. Annu Rev Biochem *72*, 609-642.

Hubel, D. H., Wiesel, T. N., and LeVay, S. (1977). Plasticity of ocular dominance columns in monkey striate cortex. Philos Trans R Soc Lond B Biol Sci *278*, 377-409.

Huber, A. B., Kania, A., Tran, T. S., Gu, C., De Marco Garcia, N., Lieberam, I., Johnson, D., Jessell, T. M., Ginty, D. D., and Kolodkin, A. L. (2005). Distinct roles for secreted semaphorin signaling in spinal motor axon guidance. Neuron *48*, 949-964.

Ichikawa, H., Deguchi, T., Nakago, T., Jacobowitz, D. M., and Sugimoto, T. (1994). Parvalbumin, calretinin and carbonic anhydrase in the trigeminal and spinal primary neurons of the rat. Brain Res *655*, 241-245.

Inglis, F. M., Crockett, R., Korada, S., Abraham, W. C., Hollmann, M., and Kalb, R. G. (2002). The AMPA receptor subunit GluR1 regulates dendritic architecture of motor neurons. J Neurosci *22*, 8042-8051.

Inglis, F. M., Furia, F., Zuckerman, K. E., Strittmatter, S. M., and Kalb, R. G. (1998). The role of nitric oxide and NMDA receptors in the development of motor neuron dendrites. J Neurosci *18*, 10493-10501.

Isshiki, T., Pearson, B., Holbrook, S., and Doe, C. Q. (2001). Drosophila neuroblasts sequentially express transcription factors which specify the temporal identity of their neuronal progeny. Cell *106*, 511-521.

Jack, J. J., Miller, S., Porter, R., and Redman, S. J. (1971). The time course of minimal excitory post-synaptic potentials evoked in spinal motoneurones by group Ia afferent fibres. J Physiol *215*, 353-380.

Jakowec, M. W., Yen, L., and Kalb, R. G. (1995). In situ hybridization analysis of AMPA receptor subunit gene expression in the developing rat spinal cord. Neuroscience *67*, 909-920.

Jan, Y. N., and Jan, L. Y. (2003). The control of dendrite development. Neuron *40*, 229-242.

Jessell, T. M. (2000). Neuronal specification in the spinal cord: inductive signals and transcriptional codes. Nat Rev Genet *1*, 20-29.

Jontes, J. D., Buchanan, J., and Smith, S. J. (2000). Growth cone and dendrite dynamics in zebrafish embryos: early events in synaptogenesis imaged in vivo. Nat Neurosci *3*, 231-237.

Kalb, R. G. (1994). Regulation of motor neuron dendrite growth by NMDA receptor activation. Development *120*, 3063-3071.

Kalb, R. G., and Agostini, J. (1993). Molecular evidence for nitric oxide-mediated motor neuron development. Neuroscience *57*, 1-8.

Kalb, R. G., Lidow, M. S., Halsted, M. J., and Hockfield, S. (1992). N-methyl-D-aspartate receptors are transiently expressed in the developing spinal cord ventral horn. Proc Natl Acad Sci U S A *89*, 8502-8506.

Katz, L. C. (1987). Local circuitry of identified projection neurons in cat visual cortex brain slices. J Neurosci *7*, 1223-1249.

Kiehn, O., and Butt, S. J. (2003). Physiological, anatomical and genetic identification of CPG neurons in the developing mammalian spinal cord. Prog Neurobiol *70*, 347-361.

Knecht, A. K., and Bronner-Fraser, M. (2002). Induction of the neural crest: a multigene process. Nat Rev Genet *3*, 453-461.

Kolodkin, A. L., Levengood, D. V., Rowe, E. G., Tai, Y. T., Giger, R. J., and Ginty, D. D. (1997). Neuropilin is a semaphorin III receptor. Cell *90*, 753-762.

Konur, S., and Ghosh, A. (2005). Calcium signaling and the control of dendritic development. Neuron *46*, 401-405.

Kouzarides, T. (2002). Histone methylation in transcriptional control. Curr Opin Genet Dev *12*, 198-209.

Kressler, D., Schreiber, S. N., Knutti, D., and Kralli, A. (2002). The PGC-1-related protein PERC is a selective coactivator of estrogen receptor alpha. J Biol Chem *277*, 13918-13925.

Kullander, K., Butt, S. J., Lebret, J. M., Lundfald, L., Restrepo, C. E., Rydstrom, A., Klein, R., and Kiehn, O. (2003). Role of EphA4 and EphrinB3 in local neuronal circuits that control walking. Science *299*, 1889-1892.

Laget, M. P., Defossez, P. A., Albagli, O., Baert, J. L., Dewitte, F., Stehelin, D., and de Launoit, Y. (1996). Two functionally distinct domains responsible for transactivation by the Ets family member ERM. Oncogene *12*, 1325-1336.

Lance-Jones, C., and Landmesser, L. (1980). Motoneurone projection patterns in the chick hind limb following early partial reversals of the spinal cord. J Physiol *302*, 581-602.

Lance-Jones, C., and Landmesser, L. (1981a). Pathway selection by chick lumbosacral motoneurons during normal development. Proc R Soc Lond B Biol Sci *214*, 1-18.

Lance-Jones, C., and Landmesser, L. (1981b). Pathway selection by embryonic chick motoneurons in an experimentally altered environment. Proc R Soc Lond B Biol Sci *214*, 19-52.

Landgraf, M., Jeffrey, V., Fujioka, M., Jaynes, J. B., and Bate, M. (2003). Embryonic origins of a motor system: motor dendrites form a myotopic map in Drosophila. PLoS Biol *1*, E41.

Landmesser, L. (1978a). The development of motor projection patterns in the chick hind limb. J Physiol *284*, 391-414.

Landmesser, L. (1978b). The distribution of motoneurones supplying chick hind limb muscles. J Physiol *284*, 371-389.

Lanuza, G. M., Gosgnach, S., Pierani, A., Jessell, T. M., and Goulding, M. (2004). Genetic identification of spinal interneurons that coordinate left-right locomotor activity necessary for walking movements. Neuron *42*, 375-386.

Lee, K. J., and Jessell, T. M. (1999). The specification of dorsal cell fates in the vertebrate central nervous system. Annu Rev Neurosci *22*, 261-294.

Lee, M. T., and O'Donovan, M. J. (1991). Organization of hindlimb muscle afferent projections to lumbosacral motoneurons in the chick embryo. J Neurosci *11*, 2564-2573.

Lentz, S. I., Knudson, C. M., Korsmeyer, S. J., and Snider, W. D. (1999). Neurotrophins support the development of diverse sensory axon morphologies. J Neurosci *19*, 1038-1048.

Li, W. C., Higashijima, S., Parry, D. M., Roberts, A., and Soffe, S. R. (2004). Primitive roles for inhibitory interneurons in developing frog spinal cord. J Neurosci *24*, 5840-5848.

Lichtman, J. W., and Frank, E. (1984). Physiological evidence for specificity of synaptic connections between individual sensory and motor neurons in the brachial spinal cord of the bullfrog. J Neurosci *4*, 1745-1753.

Lichtman, J. W., Jhaveri, S., and Frank, E. (1984). Anatomical basis of specific connections between sensory axons and motor neurons in the brachial spinal cord of the bullfrog. J Neurosci *4*, 1754-1763.

Liebl, D. J., Tessarollo, L., Palko, M. E., and Parada, L. F. (1997). Absence of sensory neurons before target innervation in brain-derived neurotrophic factor-, neurotrophin 3-, and TrkC-deficient embryonic mice. J Neurosci *17*, 9113-9121.

Lin, J. H., Saito, T., Anderson, D. J., Lance-Jones, C., Jessell, T. M., and Arber, S. (1998a). Functionally related motor neuron pool and muscle sensory afferent subtypes defined by coordinate ETS gene expression. Cell *95*, 393-407.

Livet, J., Sigrist, M., Stroebel, S., De Paola, V., Price, S. R., Henderson, C. E., Jessell, T. M., and Arber, S. (2002). ETS gene Pea3 controls the central position and terminal arborization of specific motor neuron pools. Neuron *35*, 877-892.

Llinas, R., Nicholson, C., Freeman, J. A., and Hillman, D. E. (1968). Dendritic spikes and their inhibition in alligator Purkinje cells. Science *160*, 1132-1135.

Llinas, R., and Sugimori, M. (1980a). Electrophysiological properties of in vitro Purkinje cell dendrites in mammalian cerebellar slices. J Physiol *305*, 197-213.

Llinas, R., and Sugimori, M. (1980b). Electrophysiological properties of in vitro Purkinje cell somata in mammalian cerebellar slices. J Physiol *305*, 171-195.

MacNeil, M. A., and Masland, R. H. (1998). Extreme diversity among amacrine cells: implications for function. Neuron *20*, 971-982.

Markus, A., Patel, T. D., and Snider, W. D. (2002a). Neurotrophic factors and axonal growth. Curr Opin Neurobiol *12*, 523-531.

Markus, A., Zhong, J., and Snider, W. D. (2002b). Raf and akt mediate distinct aspects of sensory axon growth. Neuron *35*, 65-76.

Marques, G., Haerry, T. E., Crotty, M. L., Xue, M., Zhang, B., and O'Connor, M. B. (2003). Retrograde Gbb signaling through the Bmp type 2 receptor wishful thinking regulates systemic FMRFa expression in Drosophila. Development *130*, 5457-5470.

May, W. A., Lessnick, S. L., Braun, B. S., Klemsz, M., Lewis, B. C., Lunsford, L. B., Hromas, R., and Denny, C. T. (1993). The Ewing's sarcoma EWS/FLI-1 fusion gene encodes a more potent transcriptional activator and is a more powerful transforming gene than FLI-1. Mol Cell Biol *13*, 7393-7398.

McAllister, A. K., Katz, L. C., and Lo, D. C. (1997). Opposing roles for endogenous BDNF and NT-3 in regulating cortical dendritic growth. Neuron *18*, 767-778.

McAllister, A. K., Lo, D. C., and Katz, L. C. (1995). Neurotrophins regulate dendritic growth in developing visual cortex. Neuron *15*, 791-803.

McConnell, S. K. (1995). Strategies for the generation of neuronal diversity in the developing central nervous system. J Neurosci *15*, 6987-6998.

Mears, S. C., and Frank, E. (1997). Formation of specific monosynaptic connections between muscle spindle afferents and motoneurons in the mouse. J Neurosci *17*, 3128-3135.

Mel, B. W. (1994). Information processing in dendritic trees. Neural Computation *6*, 1031-1085.

Mendell, L. M., and Henneman, E. (1971). Terminals of single Ia fibers: location, density, and distribution within a pool of 300 homonymous motoneurons. J Neurophysiol *34*, 171-187.

Mendell, L. M., Munson, J. B., and Arvanian, V. L. (2001). Neurotrophins and synaptic plasticity in the mammalian spinal cord. J Physiol *533*, 91-97.

Mendelson, B., and Frank, E. (1991). Specific monosynaptic sensory-motor connections form in the absence of patterned neural activity and motoneuronal cell death. J Neurosci *11*, 1390-1403.

Mo, Y., Vaessen, B., Johnston, K., and Marmorstein, R. (1998). Structures of SAP-1 bound to DNA targets from the E74 and c-fos promoters: insights into DNA sequence discrimination by Ets proteins. Mol Cell *2*, 201-212.

Moore, A. W., Jan, L. Y., and Jan, Y. N. (2002). hamlet, a binary genetic switch between single- and multiple- dendrite neuron morphology. Science *297*, 1355-1358.

Moore, M. W., Klein, R. D., Farinas, I., Sauer, H., Armanini, M., Phillips, H., Reichardt, L. F., Ryan, A. M., Carver-Moore, K., and Rosenthal, A. (1996). Renal and neuronal abnormalities in mice lacking GDNF. Nature *382*, 76-79.

Moran-Rivard, L., Kagawa, T., Saueressig, H., Gross, M. K., Burrill, J., and Goulding, M. (2001). Evx1 is a postmitotic determinant of v0 interneuron identity in the spinal cord. Neuron *29*, 385-399.

Mountcastle, V. B. (1997). The columnar organization of the neocortex. Brain *120 (Pt 4)*, 701-722.

Niederreither, K., McCaffery, P., Drager, U. C., Chambon, P., and Dolle, P. (1997). Restricted expression and retinoic acid-induced downregulation of the retinaldehyde dehydrogenase type 2 (RALDH-2) gene during mouse development. Mech Dev *62*, 67-78.

Ohno, T., Rao, V. N., and Reddy, E. S. (1993). EWS/Fli-1 chimeric protein is a transcriptional activator. Cancer Res *53*, 5859-5863.

Okado, N., Homma, S., Ishihara, R., and Kohno, K. (1990). Distribution patterns of dendrites in motor neuron pools of lumbosacral spinal cord of the chicken. Anat Embryol (Berl) *182*, 113-121.

Oliveira, A. L., Hydling, F., Olsson, E., Shi, T., Edwards, R. H., Fujiyama, F., Kaneko, T., Hokfelt, T., Cullheim, S., and Meister, B. (2003). Cellular localization of three vesicular glutamate transporter mRNAs and proteins in rat spinal cord and dorsal root ganglia. Synapse *50*, 117-129.

Orkin, S. H. (2000). Diversification of haematopoietic stem cells to specific lineages. Nat Rev Genet *1*, 57-64.

Patel, T. D., Jackman, A., Rice, F. L., Kucera, J., and Snider, W. D. (2000). Development of sensory neurons in the absence of NGF/TrkA signaling in vivo. Neuron *25*, 345-357.

Patel, T. D., Kramer, I., Kucera, J., Niederkofler, V., Jessell, T. M., Arber, S., and Snider, W. D. (2003). Peripheral NT3 signaling is required for ETS protein expression and central patterning of proprioceptive sensory afferents. Neuron *38*, 403-416.

Pearson, B. J., and Doe, C. Q. (2003). Regulation of neuroblast competence in Drosophila. Nature *425*, 624-628.

Pettmann, B., and Henderson, C. E. (1998). Neuronal cell death. Neuron *20*, 633-647.
Pierani, A., Moran-Rivard, L., Sunshine, M. J., Littman, D. R., Goulding, M., and Jessell, T. M. (2001). Control of interneuron fate in the developing spinal cord by the progenitor homeodomain protein Dbx1. Neuron *29*, 367-384.

Pockett, S., and Figurov, A. (1993). Long-term potentiation and depression in the ventral horn of rat spinal cord in vitro. Neuroreport *4*, 97-99.

Polleux, F., Giger, R. J., Ginty, D. D., Kolodkin, A. L., and Ghosh, A. (1998). Patterning of cortical efferent projections by semaphorin-neuropilin interactions. Science *282*, 1904-1906.

Polleux, F., Morrow, T., and Ghosh, A. (2000). Semaphorin 3A is a chemoattractant for cortical apical dendrites. Nature *404*, 567-573.

Pufall, M. A., and Graves, B. J. (2002). Autoinhibitory domains: modular effectors of cellular regulation. Annu Rev Cell Dev Biol *18*, 421-462.

Rajan, D. K., Croteau, D. L., Sturza, S. G., Harvill, M. L., and Mehall, C. J. (1998). Translumbar placement of inferior vena caval catheters: a solution for challenging hemodialysis access. Radiographics *18*, 1155-1167; discussion 1167-1170.

Rajan, I., and Cline, H. T. (1998). Glutamate receptor activity is required for normal development of tectal cell dendrites in vivo. J Neurosci *18*, 7836-7846.

Rall, W. (1962). Theory of physiological properties of dendrites. Ann N Y Acad Sci *96*, 1071-1092.

Rall, W., Burke, R. E., Smith, T. G., Nelson, P. G., and Frank, K. (1967). Dendritic location of synapses and possible mechanisms for the monosynaptic EPSP in motoneurons. J Neurophysiol *30*, 1169-1193.

Romanes, G. J. (1951). The motor cell columns of the lumbo-sacral spinal cord of the cat. J Comp Neurol *94*, 313-363.

Romanes, G. J. (1964). The Motor Pools Of The Spinal Cord. Prog Brain Res *11*, 93-119.

Rose, H. J., and Metherate, R. (2005). Auditory thalamocortical transmission is reliable and temporally precise. J Neurophysiol *94*, 2019-2030.

Ryan, J. M., Cushman, J., Jordan, B., Samuels, A., Frazer, H., and Baier, C. (1998). Topographic position of forelimb motoneuron pools is conserved in vertebrate evolution. Brain Behav Evol *51*, 90-99.

Sagne, C., El Mestikawy, S., Isambert, M. F., Hamon, M., Henry, J. P., Giros, B., and Gasnier, B. (1997). Cloning of a functional vesicular GABA and glycine transporter by screening of genome databases. FEBS Lett *417*, 177-183.

Salie, R., Niederkofler, V., and Arber, S. (2005). Patterning molecules; multitasking in the nervous system. Neuron *45*, 189-192.

Sanes, J. R., and Yamagata, M. (1999). Formation of lamina-specific synaptic connections. Curr Opin Neurobiol *9*, 79-87.

Schaeren-Wiemers, N., and Gerfin-Moser, A. (1993). A single protocol to detect transcripts of various types and expression levels in neural tissue and cultured cells: in situ hybridization using digoxigenin-labelled cRNA probes. Histochemistry *100*, 431-440.

Scheibel, M. E., and Scheibel, A. B. (1969). Terminal patterns in cat spinal cord. 3. Primary afferent collaterals. Brain Res *13*, 417-443.

Schwaller, B., Dick, J., Dhoot, G., Carroll, S., Vrbova, G., Nicotera, P., Pette, D., Wyss, A., Bluethmann, H., Hunziker, W., and Celio, M. R. (1999). Prolonged contraction-relaxation cycle of fast-twitch muscles in parvalbumin knockout mice. Am J Physiol *276*, C395-403.

Shirasaki, R., and Pfaff, S. L. (2002). Transcriptional codes and the control of neuronal identity. Annu Rev Neurosci *25*, 251-281.

Sin, W. C., Haas, K., Ruthazer, E. S., and Cline, H. T. (2002). Dendrite growth increased by visual activity requires NMDA receptor and Rho GTPases. Nature *419*, 475-480.

Smith, C. L., and Frank, E. (1987). Peripheral specification of sensory neurons transplanted to novel locations along the neuraxis. J Neurosci *7*, 1537-1549.

Smith, C. L., and Frank, E. (1988). Specificity of sensory projections to the spinal cord during development in bullfrogs. J Comp Neurol *269*, 96-108.

Sockanathan, S., and Jessell, T. M. (1998). Motor neuron-derived retinoid signaling specifies the subtype identity of spinal motor neurons. Cell *94*, 503-514.

Srinivas, S., Watanabe, T., Lin, C. S., William, C. M., Tanabe, Y., Jessell, T. M., and Costantini, F. (2001). Cre reporter strains produced by targeted insertion of EYFP and ECFP into the ROSA26 locus. BMC Dev Biol *1*, 4.

Steffensky, M., Steinbach, K., Schwarz, U., and Schlosshauer, B. (2006). Differential impact of semaphorin 3E and 3A on CNS axons. Int J Dev Neurosci *24*, 65-72.

Sterling, P., and Kuypers, H. G. (1967). Anatomical organization of the brachial spinal cord of the cat. II. The motoneuron plexus. Brain Res *4*, 16-32.

Stuart, G. J., Dodt, H. U., and Sakmann, B. (1993). Patch-clamp recordings from the soma and dendrites of neurons in brain slices using infrared video microscopy. Pflugers Arch *423*, 511-518.

Szekely, G., Matesz, C., and Antal, M. (1980). Different dendritic arborization patterns of motoneurons in various places of the rat's lumbosacral spinal cord. Acta Biol Acad Sci Hung *31*, 305-319.

Tang, J., Rutishauser, U., and Landmesser, L. (1994). Polysialic acid regulates growth cone behavior during sorting of motor axons in the plexus region. Neuron *13*, 405-414.

Tessier-Lavigne, M., and Goodman, C. S. (1996). The molecular biology of axon guidance. Science *274*, 1123-1133.

Thaler, J., Harrison, K., Sharma, K., Lettieri, K., Kehrl, J., and Pfaff, S. L. (1999). Active suppression of interneuron programs within developing motor neurons revealed by analysis of homeodomain factor HB9. Neuron *23*, 675-687.

Tieman, S. B., and Hirsch, H. V. (1982). Exposure to lines of only one orientation modifies dendritic morphology of cells in the visual cortex of the cat. J Comp Neurol *211*, 353-362.

Tsuchida, T., Ensini, M., Morton, S. B., Baldassare, M., Edlund, T., Jessell, T. M., and Pfaff, S. L. (1994). Topographic organization of embryonic motor neurons defined by expression of LIM homeobox genes. Cell *79*, 957-970.

Tucker, K. L., Meyer, M., and Barde, Y. A. (2001). Neurotrophins are required for nerve growth during development. Nat Neurosci *4*, 29-37.
Urano, F., Umezawa, A., Hong, W., Kikuchi, H., and Hata, J. (1996). A novel chimera gene between EWS and E1A-F, encoding the adenovirus E1A enhancer-binding protein, in extraosseous Ewing's sarcoma. Biochem Biophys Res Commun *219*, 608-612.

Vaughn, J. E., Barber, R. P., and Sims, T. J. (1988). Dendritic development and preferential growth into synaptogenic fields: a quantitative study of Golgi-impregnated spinal motor neurons. Synapse *2*, 69-78.

Verger, A., and Duterque-Coquillaud, M. (2002). When Ets transcription factors meet their partners. Bioessays *24*, 362-370.

Vetter, P., Roth, A., and Hausser, M. (2001). Propagation of action potentials in dendrites depends on dendritic morphology. J Neurophysiol *85*, 926-937.

Volkmar, F. R., and Greenough, W. T. (1972). Rearing complexity affects branching of dendrites in the visual cortex of the rat. Science *176*, 1445-1447.

Wenner, P., and Frank, E. (1995). Peripheral target specification of synaptic connectivity of muscle spindle sensory neurons with spinal motoneurons. J Neurosci *15*, 8191-8198.
White, F. A., Keller-Peck, C. R., Knudson, C. M., Korsmeyer, S. J., and Snider, W. D. (1998). Widespread elimination of naturally occurring neuronal death in Bax-deficient mice. J Neurosci *18*, 1428-1439.

Whitford, K. L., Marillat, V., Stein, E., Goodman, C. S., Tessier-Lavigne, M., Chedotal, A., and Ghosh, A. (2002). Regulation of cortical dendrite development by Slit-Robo interactions. Neuron *33*, 47-61.

Wiesel, T. N., and Hubel, D. H. (1963). Effects Of Visual Deprivation On Morphology And Physiology Of Cells In The Cats Lateral Geniculate Body. J Neurophysiol *26*, 978-993.

Wong, R. O., and Ghosh, A. (2002). Activity-dependent regulation of dendritic growth and patterning. Nat Rev Neurosci *3*, 803-812.

Xu, B., Zang, K., Ruff, N. L., Zhang, Y. A., McConnell, S. K., Stryker, M. P., and Reichardt, L. F. (2000). Cortical degeneration in the absence of neurotrophin signaling: dendritic retraction and neuronal loss after removal of the receptor TrkB. Neuron *26*, 233-245.

Yang, X., Arber, S., William, C., Li, L., Tanabe, Y., Jessell, T. M., Birchmeier, C., and Burden, S. J. (2001). Patterning of muscle acetylcholine receptor gene expression in the absence of motor innervation. Neuron *30*, 399-410.

Yu, T. W., and Bargmann, C. I. (2001). Dynamic regulation of axon guidance. Nat Neurosci *4 Suppl*, 1169-1176.

Yuste, R., Nelson, D. A., Rubin, W. W., and Katz, L. C. (1995). Neuronal domains in developing neocortex: mechanisms of coactivation. Neuron *14*, 7-17.
Zhang, J. H., Morita, Y., Hironaka, T., Emson, P. C., and Tohyama, M. (1990). Ontological study of calbindin-D28k-like and parvalbumin-like immunoreactivities in rat spinal cord and dorsal root ganglia. J Comp Neurol *302*, 715-728.

Appendix

Acknowledgments

During my PhD I had the opportunity to work in a highly stimulating and excellent scientific environment. This has made my PhD to a successful and inspiring experience, which has motivated me only more to continue working in science. Many people have contributed over the past years to this great working environment and to all of them I want to say a big thank you, but to a few with who I have worked closely together I would like to say a few extra words.

First of all my supervisor Prof. Dr. Silvia Arber. When I started in her lab I had the challenge to establish electrophysiological recording techniques. This was for me a great learning experience which has been throughout my PhD very helpful. She not only has given me very good working possibilities within her lab, but also has supported me in visiting numerous scientific meetings, at some of which I had the opportunity to present my work. This gave me the change to discuss my work with other great researchers and introduce myself into the scientific world, which are invaluable experiences for my future career. Together, working in her lab has given me an excellent overview of what it means being a scientist, up, and till today I enjoy it a lot. I would like to thank her for all her support, enthusiasm and valuable scientific input throughout my PhD, and for the great working possibilities within her lab.

I also would like to thank Prof. Dr. Andreas Lüthi for his help during the period that I was setting up the electrophysiology. Whenever I had a question I could just walk in his office and he would be always willing to help and answer my questions.

Another person within the lab to who I would like to say a special thank you is Dr. David Ladle. He brought a lot of knowledge about the electrophysiology and I am very thankful to him that he shared this knowledge with me and that he has teached me the ‘ins and outs’ of this method. Our enthusiasm for science let to many stimulating discussions which have helped me a lot to think about my project and science in general. He has been throughout my PhD a fantastic colleague.

Further I would like to thank all the colleagues which have in the mean time left the lab and those which are still in the lab for there discussions, support and friendship. In particular I would like to thank Ina Kramer which became a good friend of me during my PhD. With her broad scientific knowledge she gave always very honest comments on my project and she gave me always very helpful feedback on my presentations, this together I appreciate a lot.

Not only the people in my working environment have made my PhD successful, also my mother, father, sister, Richard and grandparents have supported and motivated me throughout my whole PhD. My mother is as curious as I am and likes to learn about new things all the time. Therefore, she always enjoyed it to listen to my scientific stories. Even my grandparents were always interested to hear about my work. In the last month when I had to write this thesis and prepare for the defense my mother was over at our place and was doing the cooking, cleaning, shopping for me and whenever I needed a moment to relax, we did some fun stuff. This was great.

A special thank you also deserves my boyfriend Juraj. I feel really honored having a boyfriend like him. He always took it with a smile when I again had to excuse myself for being late or having to spend the weekend in the lab. He encourages me in doing what I really like to do and making the best out of it.

Curriculum Vitae

Name:	Eline Vrieseling
Date of Birth:	16 November 1977
Sex:	Female
Nationality:	Dutch
Home address:	Krummeneichstrasse 2, 4133 Pratteln, Switzerland ++41-(0)61 461 1026, Eline.Vrieseling@unibas.ch
Present Occupation:	PhD-Student. Group of Prof. Dr. S. Arber Dep. Cell Biology, Biozentrum and Friedrich Miescher Institute, Basel, Switzerland

Education:

2000 – 2002:	Master of Science in Biology with Biomolecular Sciences Swammerdam Institute for Life Sciences, University of Amsterdam (UvA), the Netherlands
1996 – 2000:	Bachelor of Science in Biotechnology University of applied science (NHL), Leeuwarden, the Netherlands
1990 – 1996:	High school with Matura, specialization in science and mathematics, Leeuwarden, the Netherlands

Publications:

1. **Vrieseling E.** and Arber, S. A Target-regulated induction of ETS transcription factor *Pea3* in specific motor neuron pools controls dendrite patterning and sensory-motor connectivity. **Cell,** 2006, Dec.29; 127(7):1439-52.
2. Hippenmeyer S., **Vrieseling E.**, Sigrist M., Portmann T., Laengle C., Ladle, D.R. and Arber, S. A developmental switch in the response of DRG neurons to ETS transcription factor signaling. **PLoS Biol** 3: e159, 2005.

Meetings attended (with poster and/or oral presentations):

2006:	**Gordon Research Conference on Neuronal Development**, Salve Regina University, Rhode Island, USA.
2004, 2005, 2006:	**Society for Neuroscience 34th, 35th and 36th Annual Meeting**, USA.
2003, 2005:	**EMBO Workshop:** Formation and Function of Neuronal Circuits, Ascona, Switzerland.

Prizes:

08/2006:	Poster prize at the Gordon Research Conference on Neuronal Development, Salve Regina University, Rhode Island, USA.